

ABSTRACT

Periphyton-Nutrient Dynamics in a Gradient-Dominated Freshwater Marsh Ecosystem

J. Thad Scott, M.S.

Mentor: Robert D. Doyle, Ph.D.

In this study, the factors influencing the development of a nutrient availability gradient in a wetland ecosystem and the subsequent controls to, and feedbacks from, the structure and function of the periphyton community were investigated. Field surveys, field experiments, and a laboratory experiments were conducted over a three year period in the Lake Waco Wetlands, a created wetland system near Waco, Texas. Results of these studies indicated that nitrogen (N) retention/removal always exceeded phosphorus (P) retention/removal along the flow path of water. Over 90% of nitrate (NO_3^-) entering the wetland was generally retained by the system and 50% of that retention was a result of influx into sediments. Intact sediment core experiments revealed that virtually all available NO_3^- in the sediments was denitrified. Inorganic P entering the wetland was less well retained (up to 50%), but the wetland was sometimes a source of P as well. The disproportionate loss of inorganic N resulted in a distinct gradient of nutrient availability where N was relatively more abundant near the inflow, but became decreasingly less abundant than P as distance from the inflow increased. Experimental N and Penrichments at the inflow often resulted in an increase in periphyton biomass accumulation. However,

only N alone stimulated biomass accumulation in downstream areas. Floating periphyton mats, or “metaphyton”, appeared to overcome N deficiency on a seasonal basis by fixing, and efficiently retaining, large quantities of atmospheric N₂. In fact, average N-specific metaphyton production throughout the entire wetland was inversely correlated with average metaphyton phosphatase activity ($r^2 = 0.78$; $p = 0.0015$). These results suggest that fixed N₂ may supply a sufficient quantity of N to offset periphyton N limitation and initiate P limitation. The response to inorganic N additions is maintained because use of NO₃⁻-N is less energetically expensive to utilize than N₂. Furthermore, results of laboratory experiments suggest that some mechanisms may exist by which bacteria and photoautotrophs compensate the supply of P and fixed N₂, respectively, to one another within the community.


Periphyton-Nutrient Dynamics in a Gradient-Dominated Freshwater Marsh Ecosystem

by

J. Thad Scott, M.S.

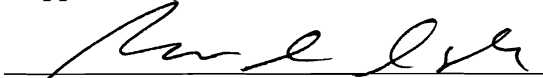
A Dissertation

Approved by the Department of Biology

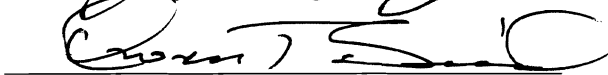

Robert D. Doyle, Ph.D., Chairperson

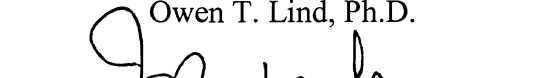
Submitted to the Graduate Faculty of
Baylor University in Partial Fulfillment of the
Requirements for the Degree
of
Doctor of Philosophy

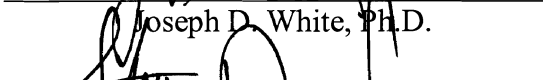
Approved by the Dissertation Committee


Robert D. Doyle, Ph.D., Chairperson


Ryan S. King, Ph.D.

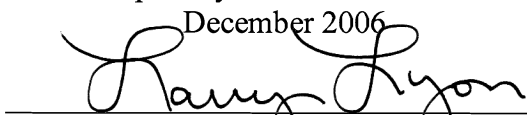

Owen T. Lind, Ph.D.


Joseph D. White, Ph.D.


Stephen I. Dworkin, Ph.D.

Accepted by the Graduate School

December 2006


J. Larry Lyon, Ph.D., Dean

Copyright © 2006 by J. Thad Scott

All rights reserved

TABLE OF CONTENTS

LIST OF FIGURES	vi
LIST OF TABLES	viii
ACKNOWLEDGMENTS	ix
DEDICATION	xi
CHAPTER ONE	1
Introduction and Background	1
Periphyton, Nutrients and their Interaction in Wetland Ecosystems	1
Statement of Problem	5
Objectives of Study	6
Study Area	6
Summary of Chapter Contents	7
CHAPTER TWO	9
Alteration of Inorganic N:P Supply in a Shallow Marsh by Ecosystem Retention and Nitrogen Transformations	9
Introduction	9
Materials and Methods	12
Sediment Nutrient Flux and N Transformations	12
Hydraulic and Nutrient Loading Estimates	13
Contribution of Sediments to Ecosystem Nutrient Dynamics	15
Results	16
Physical and Chemical Data at Sediment Coring Stations	16
Sediment Nutrient Flux and N Transformations	17
Hydraulic and Nutrient Loading Estimates	20
Contribution of Sediments to Ecosystem Nutrient Dynamics	21
Discussion	25
Are Sediments a Net Source or Sink of Dissolved N and P?	25

What are the Rates of Sediment N Transformations such as N ₂ Fixation, Denitrification, and DNRA?	26
To What Extent are Sediment Nutrient Fluxes, and Associated Biogeochemical Transformations, Correlated with Ecosystem Nutrient Fluxes?	28
Do Sediment Nutrient Dynamics Impact Inorganic N and P Supply?	29
Conclusions	31
CHAPTER THREE	33
Periphyton Nutrient Limitation and Nitrogen Fixation Potential Along the Wetland Nutrient-Depletion Gradient	33
Introduction	33
Materials and Methods	35
Nutrient Limitation Status	35
Water Quality and Nitrogen Fixation	38
Periphyton Assemblage Composition	40
Results	40
Nutrient Limitation Status	40
Water Quality and Nitrogen Fixation	41
Periphyton Assemblage Composition	46
Discussion	46
Conclusions	50
CHAPTER FOUR	52
Elemental, Isotopic, and Enzymatic Evidence for Seasonally-Evolving Phosphorus Limitation in a Nitrogen-Fixing Periphyton Community	52
Introduction	52
Materials and Methods	56
Primary Production	56
N ₂ Fixation	58
Phosphatase Activity	59
Periphyton Elemental and Isotopic Composition	60
Contribution of N ₂ fixation to Total N Uptake	60
Water Chemistry	62
Results	63

Water Chemistry	63
Periphyton Primary Production and Enzyme Activity	64
Periphyton Elemental and Isotopic Composition	66
Contribution of N ₂ fixation to Total N Uptake	68
Correlates of Periphyton Primary Production	72
Discussion	72
Conclusions	77
CHAPTER FIVE	78
Coupled Photosynthesis and Heterotrophic Bacterial Biomass Production in a Nutrient-Limited Wetland Periphyton Mat	78
Introduction	78
Materials and Methods	80
Dual-Labeled Radioassay	81
Effect of TCA Precipitation on Autotrophic ¹⁴ C Retention	83
Light Saturation of PS and Relationship of PS to BBP	84
Effect of Nutrient Enrichment on PS and BBP	84
Results	86
Effect of TCA Precipitation on Autotrophic ¹⁴ C Retention	86
Light Saturation of PS and Relationship of PS to BBP	86
Effect of Nutrient Enrichment on PS and BBP	89
Discussion	92
Conclusions	98
CHAPTER SIX	100
Summary and Conclusions	100
Synthesis of Chapter Contents	100
Future Directions	102
APPENDIX	104
Peer-Reviewed Publications Derived from this Research	104
BIBLIOGRAPHY	105

LIST OF FIGURES

Figure 1.1 Lake Waco Wetlands (LWW), near Waco, Texas, USA. Arrows indicate the flow path of water. Sampling areas 1A, 1B, 2A, and 2B, and sampling stations B, C, D, and E were intentionally positioned along the flow path of water. Details concerning sampling are provided in subsequent chapters.	8
Figure 2.1. Relationship between sediment NO_3^- flux and sediment N_2 flux for all sampling events.	20
Figure 2.2. Hydraulic loading, water loss, and relative contribution of evapotranspiration (ET) and infiltration to water loss.	21
Figure 2.3. Relationship between sediment nutrient flux and ecosystem nutrient flux.	24
Figure 2.4. Relationship between DIN supply rate and sediment net N_2 flux.	25
Figure 3.1. Ecosystem trophic status index at areas 1A and 1B for all nutrient enrichment bioassays ($F_{5,26} = 27.92$, $p < 0.0001$).	43
Figure 3.2 Mean dissolved inorganic nitrogen (DIN), soluble reactive phosphorus (SRP), and turbidity for summer 2003 at each station in cell 1 (error bars represent SE).	44
Figure 4.1. N_2 fixation measured by acetylene reduction (expressed in hourly units) at each incubation light level for the entire study. Bars indicate mean rate determined at each site for the entire summer (\pm SE).	66
Figure 4.2. Enzymatic activity versus nutrient concentrations for each sampling event. A) Daily N_2 fixation, measured by acetylene reduction, versus mean DIN concentration in the water column. B) Phosphatase activity versus mean SRP concentration in the water column.	67
Figure 4.3. Elemental ratios of periphyton for each sampling event (mean \pm SD; $n = 7-8$, see Table 2 for details on number of samples). Black bars represent samples collected in May 2004, light gray bars represent samples collected in July 2004, and medium gray represent samples collected in September 2004. Insufficient sample was collected during May 2004 for phosphorus determination (IS*), therefore, C:P and N:P values are not available for that sampling event.	69
Figure 4.4. Measured versus modeled percentage of N uptake derived from N_2 fixation. Measured values determined by dividing acetylene reduction estimates of N_2 fixation by estimates of gross N uptake. Modeled values determined from	

isotope mixing model. Black circles represent samples from area 1A, white circles represent samples from area 1B, and black triangles represent samples from 2B. The mixing model estimates generally agreed with empirical estimates from acetylene reduction in May only. In July and September, modeling with $\delta^{15}\text{N}$ tended to overestimate the instantaneous contribution of N_2 fixation to total N uptake. 70

Figure 4.5. Relationship between percent contribution of N_2 fixation to total N uptake, and periphyton N content. In both plots, black circles represent samples collected in May 2004, white circles represent samples from July 2004, and black triangles represent samples from September 2004. A) Percent contribution of N_2 fixation derived from acetylene reduction and gross N assimilation estimates. B) Percent contribution of N_2 fixation derived from isotope ($\delta^{15}\text{N}$) mixing model. Regression line derived for data collected in area 2B and area 1B in May 2004. See discussion for details of these groupings. 71

Figure 4.6. Relationship between mean phosphatase activity and mean nitrogen-specific primary production from all sampling events. 73

Figure 5.1. Response of photosynthesis (PS) and bacterial biomass production (BBP) to varying light. A) Ratio of PS:BBP observed with increasing irradiance; B) Response of mean PS to increasing irradiance; C) Response of BBP to increasing irradiance. Error bars in all panels indicate standard deviation (SD). 87

Figure 5.2. Scatterplot of periphyton photosynthetic production and bacterial biomass production in light saturation experiment; samples incubated across a range of photon flux density. The following symbols represent each respective light level: $\blacktriangle = 0 \mu\text{mol m}^{-2} \text{s}^{-1}$; $\bullet = 19 \mu\text{mol m}^{-2} \text{s}^{-1}$; $\blacksquare = 44 \mu\text{mol m}^{-2} \text{s}^{-1}$; $\triangle = 94 \mu\text{mol m}^{-2} \text{s}^{-1}$; $\circ = 202 \mu\text{mol m}^{-2} \text{s}^{-1}$; $\square = 484 \mu\text{mol m}^{-2} \text{s}^{-1}$. 88

Figure 5.3. Scatterplots of periphyton photosynthetic production and bacterial biomass production across each nutrient enrichment where all samples were incubated under equal photon flux density ($250 \mu\text{mol m}^{-2} \text{s}^{-1}$): A) phosphorus enrichment, B) nitrogen enrichment, C) control (inset in panel C shows the relationship of data when jar 5 is excluded). Numbers represent jars (nesting factor in PERMANOVA and PERMDISP) from which triplicate measures were made. 91

Figure 5.4. Bacterial biomass production rates for samples incubated under dark conditions in the nutrient enrichment experiment (mean \pm SD; $n=3$). 92

LIST OF TABLES

Table 2.1. Physical and chemical characteristics of water for each sampling station in all events.	17
Table 2.2. Nutrient flux and nitrogen transformation rates; NF, nitrogen fixation; DNF, potential denitrification; DNRA, dissimilatory NO_3^- reduction to NH_4^+ ; % Coupled, percent of denitrification coupled with nitrification. Positive values indicate flux out of sediments and negative values indicate flux into sediments. All rates expressed as $\mu\text{mol N m}^{-2} \text{h}^{-1}$ except PO_4^{3-} flux ($\mu\text{mol P m}^{-2} \text{h}^{-1}$) and % coupled.	18
Table 2.3. Average monthly water column nutrient concentrations, estimated flow rates, nutrient supply rates from water column and sediments, and total nutrient supply rates at each station in the confined flow path. SWL, surface water load; SDL, sediment load. All values \pm SD.	22
Table 3.1. Mean responses of periphyton to nutrient enrichment and results of REGWQ multiple comparison procedure conducted on log transformed values using REGWQ in SAS 8e. Means with same grouping letter are not significantly different at $\alpha_{\text{FW}}=.05$. Differences among means at this significance level were interpreted as response to nutrient limitation.	42
Table 3.2. Water column nutrient content and periphyton N_2 fixation potential for each bioassay period (mean \pm SE [n]).	45
Table 4.1. Water chemistry values for sites on each sampling date (mean \pm SD; n=2 for all events).	63
Table 4.2. Primary production, enzyme activities, elemental composition, and isotopic composition of periphyton community for sites on each sampling date. All values are mean \pm SD. For all values, n=8 except where indicated parenthetically.	65
Table 5.1. ANOVA tables for bivariate test of location (PERMANOVA) and the bivariate test of dispersion (PERMDISP), and the results of post-hoc multiple comparisons for both statistical tests. Mean photosynthesis (PS) and bacterial biomass production (BBP) rates and the average ratio of PS:BBP in the nutrient enrichment experiment are reported with the results of the post-hoc comparisons. SE represents standard error of mean.	90
Table 5.2. The ratio of photosynthesis to bacterial biomass production (PS:BBP) observed in this study and others.	96

ACKNOWLEDGMENTS

I cannot express my gratitude to the countless number of individuals that have provided unending support and guidance throughout my academic and professional career. However, several deserve special thanks for their assistance and support in my completion of this dissertation. First, I am genuinely indebted to Dr. Robert Doyle for his steadfast leadership throughout my Ph.D. program, for the partial financial support of my research, and for the unwavering example he has provided both professionally and personally. I can say without reservation that Robert exceeded all my expectations for a mentor and has taught me that great scientists can be truly humble. My hope is that I may exemplify these characteristics in my own professional career. I am also grateful to the other members of my graduate committee: Dr. Owen Lind, Dr. Joseph White, Dr. Ryan King, and Dr. Steve Dworkin. Thank you for your willingness to serve and your guidance and support throughout this endeavor. Because this work did not exist in a vacuum, I also thank my co-authors and collaborators: Christopher Filstrup, Jeffrey Back, and Brad Christian. I am particularly indebted to Mark McCarthy and Dr. Wayne Gardner for enabling me to create a more detailed account of nutrient chemistry dynamics in Chapter Two. I also thank lab technicians Sarah Williams, Erin Martin, and James Newman who dedicated their own time to assist me with sample collection and analyses. I would also like to thank the Texas Water Resources Institute and the Department of Biology at Baylor for providing partial funding for my project. I thank my fellow graduate students for always lending a helping hand and support when necessary. I also appreciate the effort of countless other faculty and staff at Baylor University for guiding me through the

minefield of advanced studies and dissertation preparation. I would also like to recognize City of Waco staff: Tom Conry, John McMillan, and Nora Schell were instrumental in providing logistical assistance at the Lake Waco Wetlands.

I wish to acknowledge those who guided my early career, and helped pave the way for this achievement. Dr. Jack Stanford, Dr. Ed Roth, Dr. Linda Schultz, Dr. Carol Thompson, Mark Murphy, Dr. Anne McFarland, and Dr. Larry Hauck, each of you opened doors for me along the way, thank you.

I would like to thank my family and friends for years of support, in all my endeavors. To my parents, brother and sisters, in-laws, and all of our extended family, thanks for being a friend when I needed one, and a kick in the pants when I needed one of those.

DEDICATION

To Stephanie and Timber,
without you, accomplishments are meaningless.
Thank you for your sacrifice and unconditional love

CHAPTER ONE

Introduction and Background

Periphyton, Nutrients and their Interaction in Wetland Ecosystems

Wetlands are unique ecosystems that provide substantial environmental, economic, and social benefits throughout the world. The geology, chemistry, and biology of wetland systems have been studied for many years, resulting in the publication of large texts such as Mitsch and Gosselink (2000) and Keddy (2002). Because wetlands form the transition between terrestrial and aquatic systems, wetland ecology has generally been approached from two primary perspectives: 1) the terrestrial perspective focusing on plant community dynamics and soil physics and chemistry, and 2) the aquatic perspective focusing on planktonic communities and related environmental factors. A number of issues concerning the ecological functioning of wetlands have been left unresolved in both approaches. However, the functioning of benthic microbial communities in wetland ecosystems remains conspicuously absent from either perspective.

The term “benthic” generally refers to organisms that live in association with various substrata in aquatic habitats. These organisms may include, but are not necessarily limited to, fish, invertebrates, fungi, algae, and bacteria. The term “periphyton” is often used to describe microorganisms such as algae and bacteria growing in association with substrata (Stevenson 1996). Periphyton is generally used synonymously with the German word “aufwuchs”, which means “to grow upon”. Periphyton assemblages are also often named by the structure of the substrata they inhabit (Stevenson 1996). For example, periphyton substrata may include submersed

plants or plant parts, rocks, and sediments, and their attached microbiota are referred to as epiphyton, epilithon, and epipelon, respectively. One of the most important habitat types for benthic microbial communities in wetlands is the floating microbial mat, often termed metaphyton. Metaphyton are loosely associated epiphyton, epilithon, or epipelon assemblages that separate from substrata and float to (or near) the waters surface (Goldsborough and Robinson 1996). Throughout this document the terms epiphyton, epilithon, epipelon, and metaphyton will be used to identify benthic microbial groups according to their physical location. The term periphyton will be used hereafter to describe the collection of all benthic microbial groups or when a measurement does not distinguish between particular habitat types (e.g. accumulation of cells on an artificial substrate).

Wetlands provide unique structural environments that often allow the proliferation of various periphyton assemblages. In simple terms, wetlands provide suitable habitat where sufficient light reaches substrate for periphyton attachment. The occurrence of particular periphyton assemblages in wetlands may be predicted with a conceptual model of periphyton structure (Goldsborough and Robinson 1996). The model aids in the prediction of dominant periphyton assemblages based on a variety of physical factors that determine one of four wetland stable states: dry, open, sheltered, or lake (Goldsborough and Robinson 1996).

Dry State – Periods of drawdown or drought result in the wetland dry state. Though standing water may be intermittent, continuous soil saturation can lead to the proliferation of the epipelon assemblage. Production and biomass accumulation of epipelon is then dependent on changes of environmental conditions due to alterations in the macrophyte community or a shift to another wetland stable state. Long term exposure of wetland sediments may shift the macrophyte community to a prairie meadow, thereby decreasing habitat availability for epipelon assemblages.

Open State – Seasonal flooding of wetlands in the dry state, or biogeochemical alterations to wetlands in the lake state, may result in a shift to wetland open state. The open state is characterized by a relatively turbulent water column where emergent macrophytes grow in shallow areas and submersed macrophytes develop in deeper water. The proliferation of macrophytes in standing water provide suitable habitat for epiphyton growth. Epiphyton are reduced due to shading and phytoplankton are reduced by nutrient competition. The wetland open state is maintained unless turbulent energy in the water column is reduced to a point where epiphyton become too dominant and begin to negatively affect submersed macrophyte production through shading. In time, such an occurrence may lead to a shift from open state to sheltered or lake state.

Sheltered State – The wetland sheltered state is characterized by a highly stable water column protected by fringing vegetation. Increased nutrient loading may further stimulate the development of sheltered state conditions by providing resources for highly productive metaphyton assemblages. Metaphyton mats in sheltered wetlands often carpet the water surface, reducing light available to submersed algal assemblages and macrophytes.

Lake State – Wetlands exhibiting high water column nutrient and turbidity levels often result in the stable lake state and subsequent phytoplankton dominance. Reduction of submersed vegetation, and subsequently epiphyton, occurs due to reduced water column irradiance. Phytoplankton dominance is generally maintained unless light availability increases to a point where submersed macrophytes, epiphyton, or metaphyton may outcompete phytoplankton for nutrient resources.

In addition to the unique structural environment that contributes to establishing and maintaining the four wetland stable states, wetland ecosystems often demonstrate high biogeochemical activity that result in unique N and P availability signatures in the water column (Bowden 1987, Reddy et al. 1999). Nutrient control of periphyton has been confirmed in both temperate and subtropical wetlands (McDougal et al. 1997, McCormick et al. 2001). Wu and Mitsch (1998) observed that periphyton biomass was generally greatest near the inflow of a newly constructed wetland where available nutrient concentrations were greatest, and then decreased along with available nutrients as distance from inflow increased. A similar trend was observed between decreasing

algal growth potential and nutrient concentrations in the Florida Everglades (McCormick et al. 1996) due to point discharge of P enriched waters.

Nutrient availability gradients develop in freshwater wetlands as water column N and P are depleted along the flow path of water in natural (Johnston et al. 2001, Doyle and Fisher 1994), hydrologically modified (Vaithyanathan and Richardson 1997), and created (Nairn and Mitsch 2000, Spieles and Mitsch 2000) wetland ecosystems. Studies of biological responses to such gradients have focused mostly on aquatic macrophytes (Vaithyanathan and Richardson 1999, Olde Venterink et al. 2001). Goldsborough and Robinson (1996) reviewed a number of studies that have demonstrated short periods of N and P limitation of periphyton in wetlands. However, these studies have not focused on within-wetland changes on the intensity of nutrient limitation or to the nutrient limiting periphyton growth. An exception to this gap in knowledge is the work conducted in the Florida Everglades. In that ecosystem, metaphyton P limitation is exacerbated by depletion of water column N and P and a concurrent increase in N:P ratio with increasing distance from source waters (Vymazal and Richardson 1995, McCormick et al. 1996, 1998).

Although this trend has been widely demonstrated in the Everglades, it may not be a general pattern amongst wetland ecosystems given the general knowledge on N and P retention and cycling. In fact, much of the literature on wetland nutrient cycling points toward a greater affinity for N retention and removal rather than P. Greater N removal efficiency may be explained to a certain degree by the potential for a maximum P assimilative capacity in wetlands (Richardson and Qian 1999) and the possibility for sustained and permanent N removal via sediment denitrification and/or coupled sediment

nitrification and denitrification. Richardson and Qian (1999) demonstrated that natural and constructed wetlands throughout the United States receiving P loadings at a rate less $1 \text{ g P m}^{-2} \text{ y}^{-1}$ had significantly lower effluent P concentrations than did wetlands where P loadings exceeded this marker. Decreased P assimilation in wetlands indicates increased P availability, simply due to loading rate. Nitrogen retention however, may not be as substantially impacted by variability in loading rates. In fact, Reddy et al. (1999) found that denitrifying enzyme activity was greatest in areas of high N and P loading in the Florida Everglades, and that denitrification in areas of reduced nutrient availability increased after experimental nutrient additions.

Several studies have demonstrated sediment denitrification to be the major mechanism of N removal in wetlands (Bachand and Horne 2000, Casey et al. 2001, Poe et al. 2003, Whitmire and Hamilton 2005). As previously mentioned, substrate availability (i.e. nitrate availability) is often the factor limiting denitrification in wetland sediments. This limitation is apparent from trends associated with seasonal nitrate loading (Davidsson and Leardson 1998) or coupled nitrification-denitrification (Risgaard-Petersen and Jensen 1997) patterns in wetlands. Spatial patterns in wetland nitrate depletion, denitrifying enzyme activity, and denitrification rates, similar to the nutrient availability gradient previously described, have also been reported (White and Reddy 1999, Poe et al. 2003).

Statement of Problem

Given the evidence for a maximum P assimilative capacity of freshwater wetlands (Richardson and Qian 1999), and because sustainable and permanent N removal may occur via sediment denitrification (Saunders and Kalff 2001), N limitation of wetland

periphyton assemblages may be under-reported. If unequal N and P removal efficiencies impact ecosystem function (i.e. via differential nutrient limitation of periphyton), it is imperative to assess the relative importance of mechanisms for permanent nutrient loss from these systems and to identify how periphyton communities are limited by and respond to insufficient nutrient resources.

Objectives of Study

The following research objectives are proposed. 1) Characterize spatial and temporal trends in water column N and P concentrations in a constructed, flow-through, freshwater wetland, and quantify rates of sediment N and P flux, denitrification, and other N transformation processes regulating the availability of inorganic N and P within the ecosystem. 2) Experimentally quantify nutrient limitation status of periphyton assemblages along a wetland nutrient gradient. 3) Quantify the functional response of periphyton assemblages to nutrient limitation by characterizing relationships, if any, between wetland periphyton productivity, molecular nitrogen (N₂) fixation, alkaline phosphatase activity (APA), N isotopic composition, and C:N:P stoichiometry. 4) Examine the response of periphyton primary production and bacterial production to experimental N and P additions.

Study Area

The Lake Waco Wetland is located near the inflow of the North Bosque River into Lake Waco, Texas, USA (Figure 2.1). The wetland is an 80 ha created marsh that receives water pumped from the North Bosque River. Inflowing water meanders through five cascading wetland cells before flowing back to the North Bosque River and into

Lake Waco. The North Bosque River and its receiving waters, Lake Waco, are currently experiencing accelerated eutrophication as a result of nutrient enrichment from point and non-point anthropogenic sources in the watershed (McFarland and Hauck 1999). The wetlands were constructed as habitat mitigation to replace fringing wetlands destroyed by the 2 m conservation pool rise of Lake Waco. However, ancillary benefits such as reductions of nutrient concentrations in water moving through the wetlands were anticipated.

Average daily inflow into the wetland ranges between 20,000 and 40,000 cubic meters. Cells 1 and 2 were originally flooded in January 2003 and the remainder of the wetland was flooded in November 2003. Aquatic vegetation began dispersing in spring 2003 and was well established by August 2004. The aquatic habitat within the wetland is primarily emergent marsh dominated by the macrophytes *Typha* sp., *Schoenoplectus* sp., *Pontederia* sp., and *Sagittaria* sp. Deep areas (> 1 m) of the marsh contain a variety of submerged and floating aquatic vegetation such as *Najas* sp., the macroalgae *Chara* sp., *Nuphar* sp., and *Nymphaea* sp. A large proportion of both shallow and relatively deep open water area is inhabited by floating and submerged microbial mats.

Summary of Chapter Contents

This document is divided into six chapters, including the current chapter with introductory and background material. Chapter two details a study conducted to identify spatial trends in inorganic nutrient (nitrogen and phosphorus) availability in the LWW and the factors controlling changes to nutrient supply along the flow path of water in this wetland. Chapter three describes a series of in-situ nutrient enrichment experiments used

to identify which nutrient(s), if any, were limiting and how strongly they limited periphyton production along the along the flow path of water in the LWW. Chapter four

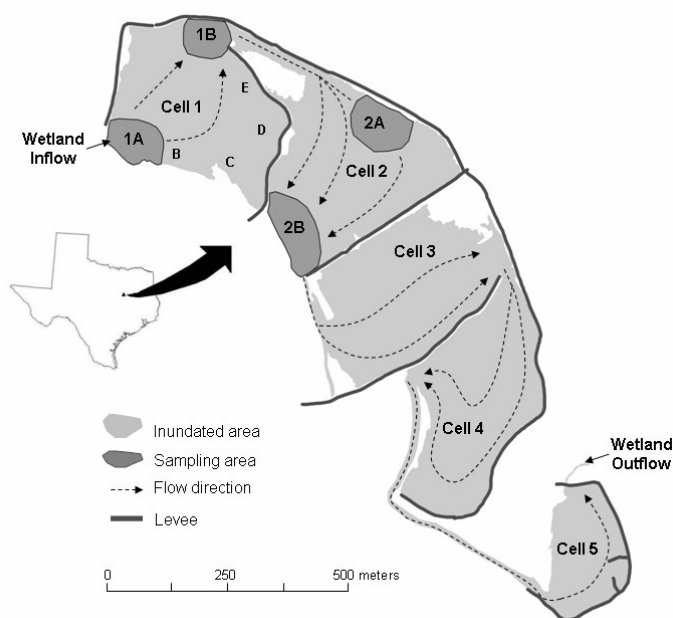


Figure 1.1 Lake Waco Wetlands (LWW), near Waco, Texas, USA. Arrows indicate the flow path of water. Sampling areas 1A, 1B, 2A, and 2B, and sampling stations B, C, D, and E were intentionally positioned along the flow path of water. Details concerning sampling are provided in subsequent chapters.

provides details on a study assessing how periphyton respond to the unique nutrient availability signature throughout the LWW and modify specific biological functions in response to the environmental gradient. Chapter five describes a series of experiments exploring how photoautotrophs and bacteria in the periphyton community respond specifically to nutrient enrichment and how changes in nutrient availability may act to couple or decouple their functioning. Finally, chapter six provides a synthesis of each of the individual projects (chapters 2-5) and discusses some of the general themes and interconnections from each.

CHAPTER TWO

Alteration of Inorganic N:P Supply in a Shallow Marsh by Ecosystem Retention and Nitrogen Transformations

Introduction

Primary and secondary production in aquatic ecosystems can be limited by the availability of nitrogen (N) and phosphorus (P) and depends on inputs from various sources, such as the landscape, atmosphere, and/or internal recycling. In freshwater systems, P is considered to be a primary element controlling production over long time scales, thereby shaping many ecosystem functions (Schindler 1977; Vitousek 2002). The biological fixation of atmospheric nitrogen (N_2) can provide an inexhaustible N source to bring N into balance with other ecosystem elemental requirements (Vitousek et al. 2002). Therefore, imbalanced N:P supply to an ecosystem should favor a biological community capable of fixing atmospheric N_2 and ameliorating N deficits (e.g. Levine and Schindler 2002).

A variety of other N transformation processes exist, in addition to N_2 fixation, which may supplement or counteract biologically available N supply to ecosystems. For example, denitrification may decrease available N by converting nitrate (NO_3^-) to N_2 , while nitrification (conversion of ammonium [NH_4^+] to NO_3^- by aerobic bacteria) and dissimilatory NO_3^- reduction to NH_4^+ (DNRA, anaerobic conversion of NH_4^+ to NO_3^- ; An and Gardner 2002) shift the chemical form of N between two biologically available compounds. Although denitrification may provide a substantial N sink (Seitzinger 1988), the process can be limited by NO_3^- availability and coupled with nitrification in many

ecosystems (Risgaard-Petersen and Jensen 1997; Risgaard-Petersen 2003). Nitrate can be lost from the system through denitrification and NH_4^+ can be lost via coupled nitrification-denitrification (Jenkins and Kemp 1984). Assimilative uptake and N regeneration (via planktonic and benthic pathways), as well as DNRA (Gardner et al. 2006), retain biologically available N in the ecosystem as NH_4^+ . Additional N losses can occur by burial, although the proportion of this loss compared with N transformation rates is generally minimal (Seitzinger 1988). The sum of these transformation rates and allochthonous N input determine the total N supply to an ecosystem.

Phosphorus cycling is less complicated. Aquatic P sources are generally limited to watershed inputs and internal recycling by organisms. Furthermore, P is lost only through physical transport or burial. Phosphorus forms buried in aquatic systems may include organically bound P, P adsorbed to sediments, and/or P chemically bound with iron or calcium (see review by Reddy et al. 1999). Phosphorus may be released from sediments during resuspension or under low redox (freeing Fe bound P) and low pH conditions (freeing Ca bound P; Reddy et al. 1999). Allochthonous P supply, along with any internal loading, determines the total P supply rate to an ecosystem.

Shallow freshwater ecosystems, such as marshes and shallow lakes, are productive “hot spots” for nutrient biogeochemical cycling. These systems have a high affinity for N retention (Bowden 1987) but store less P, particularly when inputs exceed $1 \text{ g P m}^{-2} \text{ y}^{-1}$ (Richardson and Qian 1999). The combination of efficient N transformation and storage and inefficient P retention may affect the functioning of shallow ecosystems by altering available N and P ratios. In hydrologically open ecosystems, such as marshes, external N and P supplies may be modified by internal processes with implications for

“downstream” ecological communities. However, the role of internal N and P processing in ecosystem nutrient supply often is considered only at coarse scales using mass balance approaches (Seitzinger 1988). Although these studies indicate ecosystem retention rates, mass balance approaches are not sufficient to evaluate internal cycling (i.e. sediment nutrient flux and biogeochemical transformation rates, such as denitrification, nitrogen fixation, etc.). In more recent studies, sediment nutrient fluxes and several N transformation processes have been quantified (e.g. Gardner et al. 2006). The relative magnitude of internal and external nutrient loading has seldom been quantified simultaneously (except see Levine and Schindler 1992).

In this study, we quantify external and internal nutrient loading and the rates of specific biogeochemical transformations to characterize the impact of these ecosystem processes on inorganic nutrient availability in a freshwater marsh. Specifically, we consider the following questions: 1. Are sediments a net source or sink of dissolved N and P to the marsh ecosystem? 2. What are the rates of sediment N transformations, such as N_2 fixation, denitrification, and DNRA? 3. To what extent are sediment nutrient fluxes, and associated biogeochemical transformations, correlated with ecosystem nutrient fluxes? 4. Do sediment nutrient dynamics impact inorganic N and P supply? Overall goals were to examine how a freshwater wetland affects nutrient dynamics and availability ratios as water passes through the system and estimate the importance of wetlands in modifying N loads before deliverance to rivers or other waterways.

Materials and Methods

Sediment Nutrient Flux and N Transformations

Continuous-flow experiments with intact cores were used to quantify sediment nutrient and dissolved gas fluxes following the methods outlined by Gardner et al. (2006) and references therein. Three intact sediment cores (7.6 cm inner diameter; 10 to 20 cm depth) were collected from sampling areas 1A, 1B, 2A, and 2B (Figure 1.1) in January, April, and July 2005. Cores were collected in sampling areas 1A, 1B, and 2B in August 2004. Cores were collected with a coring device equipped with a one-way rubber valve to maintain structural integrity of the core and overlying water. In addition to cores, approximately 20 L of site water was collected from each sampling area for nutrient analysis and sediment core incubations. Sediment cores were transferred the same day to the laboratory in Port Aransas, Texas, and fitted with an adjustable flow-through plunger with O-ring seal and Teflon inlet and outlet tubes to create a continuous flow chamber. Water column depth over the sediment surface was maintained at ~5 cm to give an overlying water volume of ~230 ml. Continuous flow chambers were incubated in a water bath at in situ temperature, and water from each sampling area was passed over the core surface at $\sim 1.2 \text{ ml min}^{-1}$. Flow through water was aerated, and incubations were conducted under ambient indoor lighting to represent the shaded conditions of a shallow marsh. Cores were incubated overnight to allow establishment of “steady state” conditions. After initial stabilization, triplicate inflow and outflow samples were collected once daily from each chamber for dissolved gas analysis by membrane inlet mass spectrometry (MIMS). Dissolved N_2 , O_2 , and Ar were measured with MIMS using the method described by Kana et al. (1994) and modified by An et al. (2001). The N_2 -

scavenging effect observed by Eyre et al. (2002) was evaluated on the MIMS used in this study and was not significant.

Additional samples were collected with sediment cores to determine dissolved nutrients. On these samples, NO_2^- , NO_3^- , and PO_4^{3-} were measured colorimetrically using a Lachat QuikChem 8000 flow injection autoanalyzer. Ammonium concentration and isotopic content were measured by HPLC (Gardner et al. 1995). Sediment flux for each compound was calculated as the concentration difference between inflow and outflow water divided by the flow rate and cross-sectional area (Lavrentyev et al. 2000) so that final units were expressed as $\mu\text{mol N (or P) m}^{-2} \text{ h}^{-1}$. After the second sampling day, inflow water was enriched with $^{15}\text{NO}_3^-$ (40 to 100 $\mu\text{mol L}^{-1}$ final concentration). Production of mass-specific N_2 ($^{28}\text{N}_2$ from $^{14}\text{NO}_3^-$, $^{30}\text{N}_2$ from $^{15}\text{NO}_3^-$, and $^{29}\text{N}_2$ from $^{14}\text{NO}_3^-$ and $^{15}\text{NO}_3^-$) was used to estimate gross denitrification and calculate N_2 fixation, potential DNRA rates (as $^{15}\text{NH}_4^+$ production), and the percentage of denitrification coupled to nitrification (Nielson 1992; An et al. 2001; An and Gardner 2002).

Hydraulic and Nutrient Loading Estimates

Wetland inflow volume was estimated daily throughout the course of the study, and water chemistry was monitored weekly during each sampling month to estimate dissolved nutrient loading rates. Daily flow into the wetland (area 1A; Figure 1.1) was determined from the number of hours that two inflow pumps (rated at 865 $\text{m}^3 \text{ hour}^{-1}$ each) were run each day. Flow through areas 1B and 2B was estimated as the difference between inflow volume and the loss of water from wetland cell one and wetland cells one and two, respectively. Water loss was assumed to occur by two major mechanisms: evapotranspiration (ET) and infiltration of water into shallow groundwater. Monthly ET

rates (mm month^{-1}) were estimated using the Thornthwaite model (Mitsch and Gosselink 2000) and multiplied by the area of each wetland cell to determine a monthly volumetric water loss from ET ($\text{m}^3 \text{ month}^{-1}$). Infiltration losses were estimated by subtracting the outflow rate below cell 2 from the inflow rate when ET was at an annual low (December to February). Infiltration loss was normalized to total area of wetland cells 1 and 2. The measured loss during this period was $0.05 \text{ m}^3 \text{ m}^{-2} \text{ day}^{-1}$. Estimated infiltration loss was calculated for each wetland cell and summed with estimates of ET loss from each wetland cell to derive a total daily water loss and, ultimately, a flow estimate ($\text{m}^3 \text{ day}^{-1}$) at the outflow of wetland cells 1 and 2 (sampling areas 1B and 2B, respectively). Infiltration losses were assumed to be constant across all seasons. Flow was calculated as the difference between inflow and water loss rates from cell 1 (station 1B flow) and cells 1 and 2 combined (station 2B flow). Flow estimates were not derived for station 2A because surface flow in this area was not restricted to a confined sampling area (Figure 1).

Water chemistry was monitored weekly at stations 1A, 1B, and 2B during each sampling month. Water chemistry samples were collected in acid-washed 1 liter polyethylene bottles and returned to the laboratory for analysis of NO_2^- , NO_3^- , NH_4^+ , and PO_4^{3-} . $\text{NO}_2^- + \text{NO}_3^-$ was determined by colorimetry on a Beckman DU 650 spectrophotometer following cadmium reduction (Clesceri et al. 1998). Ammonium and PO_4^{3-} were determined colorimetrically on the same instrument using phenate and molybdenum blue methods, respectively (Clesceri et al. 1998). DIN was calculated as the sum of $\text{NO}_2^- + \text{NO}_3^-$ and NH_4^+ in each sample. Water temperature was measured during sample collection using a YSI 6600 multiparameter datasonde. Surface water nutrient

loading rates were estimated for sampling areas 1A, 1B, and 2B by multiplying the average monthly nutrient concentration (DIN or PO_4^{3-}) by the estimated monthly flow rate at each station. Loading rates were expressed in hourly units for direct comparison with sediment nutrient flux data ($\mu\text{mol N or P m}^{-2} \text{ h}^{-1}$).

Contribution of Sediments to Ecosystem Nutrient Dynamics

The role of sediment nutrient flux and N transformations in ecosystem nutrient dynamics was explored using two approaches: 1. the relationship between sediment and ecosystem areal nutrient flux (*e.g.* $\mu\text{mol N m}^{-2} \text{ h}^{-1}$), and 2. the total supply of inorganic nutrients to a specific sampling area (via surface water loading and sediment loading; *e.g.* mol N h^{-1}). In the first approach, ecosystem areal nutrient flux was estimated as the difference between surface water nutrient loading rates at the inflow and outflow of a wetland cell divided by the cell area. For example, the difference between surface water loading rates between stations 1A and 1B was divided by the area of wetland cell 1 to estimate the ecosystem nutrient flux from this wetland cell. A negative value indicated the rate of nutrient retention, and a positive value indicated the rate of nutrient release. Furthermore, average sediment nutrient fluxes ($\text{NO}_2^- + \text{NO}_3^-$, NH_4^+ , and PO_4^{3-}) for each wetland cell were derived by averaging sediment nutrient fluxes from each sampling area within the respective wetland cells (*i.e.* stations 1A and 1B in cell 1, and stations 2A and 2B in cell 2). Because station 2A was not sampled in August 2004, sediment nutrient fluxes from station 2B were used as estimates for cell 2 during this event. Sediment NO_2^- and NO_3^- fluxes were summed and expressed as $\text{NO}_2^- + \text{NO}_3^-$ to match the simultaneous measured parameter in the routine water chemistry monitoring.

In the second approach, sediment NO_2^- , NO_3^- , and NH_4^+ fluxes were summed to estimate sediment DIN flux. Sediment DIN and PO_4^{3-} fluxes were multiplied by the representative wetland areas to calculate sediment nutrient loading rates (i.e. sediment fluxes in area 1A were multiplied by one-half the area of cell 1, 1B by one-half the area of cell 1, and 2B by one-half the area of cell 2). Sediment nutrient loading rates were summed with surface water loading rates (DIN and PO_4^{3-}) from the respective areas to estimate the total nutrient supply rates (mol h^{-1}) to that area. The DIN supply rate was then divided by the PO_4^{3-} supply rate to characterize the DIN: PO_4^{3-} ratio of supply in each wetland area.¹

Results

Physical and Chemical Data at Sediment Coring Stations

Table 2.1 provides physical and chemical data at sediment coring stations through the course of the study. Stations 1A and 2A were shallower (0.1 – 0.6 m) than stations 1B and 2B (0.3 – 1.0 m). Water temperature ranged from 7.4 °C in January 2005 to 30.8 °C in July 2005. Water column PO_4^{3-} concentration was higher in summer and lower in spring but did not demonstrate a clear spatial pattern within the wetland. Although NH_4^+ and NO_2^- concentrations varied, neither seasonal nor spatial patterns were evident. However, NO_3^- concentration demonstrated a distinct spatial pattern within the wetland. Nitrate concentration was always highest at station 1A and decreased sequentially at each downstream station.

Table 2.1. Physical and chemical characteristics of water for each sampling station in all events.

Date	Station	Depth (m)	Temp. (°C)	PO ₄ ³⁻ (μmol P L ⁻¹)	NH ₄ ⁺ (μmol N L ⁻¹)	NO ₂ ⁻ (μmol N L ⁻¹)	NO ₃ ⁻ (μmol N L ⁻¹)
Aug 2004	1A	0.6	28.6	0.41	5.73	1.09	30.0
	1B	0.5	27.3	0.80	1.89	0.40	15.7
	2A						
	2B	0.4	28.9	1.51	1.45	0.28	0.04
Jan 2005	1A	0.1	10.1	0.17	0.75	0.29	25.4
	1B	0.4	8.0	0.18	0.44	0.12	20.7
	2A	0.3	7.4	0.11	0.89	0.20	7.45
	2B	0.7	8.1	0.14	1.14	0.44	9.86
Apr 2005	1A	0.1	21.4	0.05	1.87	0.44	36.8
	1B	0.3	19.6	0.28	1.38	0.26	8.86
	2A	0.3	20.9	0.04	0.31	0.05	0.22
	2B	0.5	20.0	0.04	2.18	0.10	0.73
Jul 2005	1A	0.1	30.8	0.13	2.71	0.68	18.6
	1B	1.0	27.1	0.37	0.53	0.13	4.38
	2A	0.5	28.1	0.08	BDL*	BDL*	0.09
	2B	0.8	29.2	0.24	0.95	0.13	0.81

*BDL = below detection limit

Sediment Nutrient Flux and N Transformations

Nutrient and dissolved gas fluxes, as well as N transformation rates for all sampling events, are provided in Table 2.2. For nutrient and dissolved gas fluxes, positive values indicate compound flux out of the sediment (increasing concentration in overlying water), and negative values indicate compound flux into the sediment (decreasing concentration in overlying water). Phosphate flux was positive but low (0.1 – 10.7 μmol P m⁻² h⁻¹) except in July 2005, where PO₄³⁻ fluxed into the sediments at stations 1B and 2A. In most cores, NH₄⁺ was released from the sediments, with the exception of station 2A in July 2005. The addition of ¹⁵NO₃⁻ increased NH₄⁺ flux out of sediments 2 – 4 fold in wetland cell 2 but had little impact on NH₄⁺ flux in cell 1. Nitrite flux was low and varied between positive (August 2004 and January 2005) and negative values (April and

Table 2.2. Nutrient flux and nitrogen transformation rates; NF, nitrogen fixation; DNF, potential denitrification; DNRA, dissimilatory NO_3^- reduction to NH_4^+ ; % Coupled, percent of denitrification coupled with nitrification. Positive values indicate flux out of sediments and negative values indicate flux into sediments. All rates expressed as $\mu\text{mol N m}^{-2} \text{h}^{-1}$ except PO_4^{3-} flux ($\mu\text{mol P m}^{-2} \text{h}^{-1}$) and % coupled.

Date	Station	PO_4^{3-}	NH_4^{+*}	$\text{NH}_4^{+†}$	NO_2^{-*}	$\text{NO}_2^{-†}$	NO_3^{-*}	$\text{NO}_3^{-†}$	Net N_2 Flux*	NF†	DNF†	DNRA†	% Coupled
Aug 2004	1A	10.7	626	566	24.2	182	-87.7	-629	184	35.6	278	28.3	8.3
	1B	5.9	328	262	4.0	57.3	-144	-453	32.1	40.4	268	17.4	4.2
	2A												
	2B	3.1	86.8	169	1.5	68.3	-1.68	-410	-48.7	207	217	22.1	2.7
Jan 2005	1A	0.4	28.4	46.6	3.1	6.6	-61.8	-205	-57.6	30.0	131	0.0	31.3
	1B	0.7	79.5	103	4.4	3.3	-30.6	-122	13.8	30.9	99.4	0.0	33.3
	2A	0.1	18.2	16.5	0.7	0.2	-30.1	-94.4	-55.0	0.0	53.9	0.0	20.0
	2B	0.8	179	270	1.0	21.5	-28.2	-119	37.9	0.0	225	0.0	32.3
Apr 2005	1A	0.6	434	227	5.9	5.7	-213	-206	69.4	66.6	149	0.0	38.5
	1B	2.5	135	188	-1.0	4.0	-68.0	-295	48.5	10.6	161	0.0	8.6
	2A	0.1	3.2	23.7	-1.4	5.8	2.3	-169	27.0	7.7	73.3	0.0	2.0
	2B	2.4	75.5	149	-0.3	6.9	-5.57	-160	-8.6	0.0	88.9	0.0	2.9
Jul 2005	1A	4.2	245	265	-0.5	52.0	-113	-645	93.8	74.8	268	2.5	4.9
	1B	-0.5	27.1	18.0	1.3	12.3	-45.2	-251	-126	119	131	1.3	3.9
	2A	-0.2	-2.8	108	-0.1	37.9	-0.7	-283	25.7	14.4	58.0	33.0	0.9
	2B	0.7	26.8	77.4	2.1	20.4	3.2	-336	-270	426	139	10.0	3.9

*Values measured before enrichment of inflow waters with $^{15}\text{NO}_3^-$.

†Values measured after $^{15}\text{NO}_3^-$ addition (40 - 100 $\mu\text{mol L}^{-1}$).

July 2005). However, $^{15}\text{NO}_3^-$ addition induced and/or increased positive NO_2^- flux, particular in summer months. Nitrate was removed from the water at relatively high rates, except in April 2005 at station 2A and July 2005 at station 2B, where NO_3^- fluxes were small but positive. Addition of $^{15}\text{NO}_3^-$ consistently increased NO_3^- flux into the sediments with the exception of station 1A in April 2005. Net N_2 flux ranged from -270 (net N_2 fixation) to 180 (net denitrification). A distinct spatial pattern in N_2 flux was apparent in August 2004 and April 2005, when net denitrification was greatest near the inflow (station 1A) and decreased in the downstream direction before shifting to net N_2 fixation at the outflow of cell 2 (station 2B). Although station 1A was characterized by net denitrification and station 2B by net N_2 fixation in July 2005, the spatial trend was not apparent at intermediate stations (1B and 2A) on this date or at any stations in January 2005. Nitrogen (N_2) fixation rates, calculated after $^{15}\text{NO}_3^-$ additions, were highest in summer months and exhibited no significant spatial pattern except in August 2004 when rates increased sequentially at each downstream station. Sediment N_2 flux was negatively correlated with sediment NO_3^- flux when considered across all sites and dates (Figure 2.1). Potential denitrification rates were high year round and exhibited little spatial pattern except that rates were highest near the wetland inflow (station 1A). Potential DNRA was observed in summer sampling in both 2004 and 2005 but was not observed in January or April 2005. Finally, the percent of denitrification coupled with nitrification at all stations in January 2005 and at station 1A in April 2005 was 3 to 4 times higher (20.0 – 38.5 %) than any other observation throughout the study (0.9 – 8.6 %).

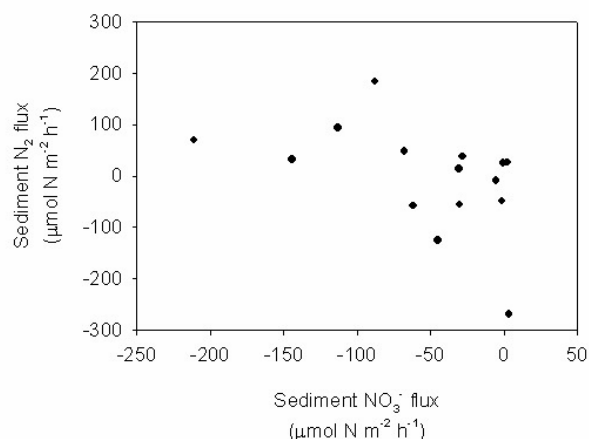


Figure 2.1. Relationship between sediment NO₃⁻ flux and sediment N₂ flux for all sampling events.

Hydraulic and Nutrient Loading Estimates

Hydraulic loading to the Lake Waco Wetland averaged 25,103 m³ day⁻¹ (± 12,833; SD). Inflow was consistent (approximately 20,000 m³ day⁻¹) from January 2004 to May 2005 when only one pump was being used, but increased to about 40,000 m³ day⁻¹ from June 2005 through August 2005 when both pumps were in use simultaneously (Figure 2.2A). The main inflow pumps failed in November 2004 and were out of service until early January 2005. During this time, a temporary pump rated at 19,000 m³ day⁻¹ was used, and inflow rates were assumed to be constant at the pump rating. Water loss from evapotranspiration and infiltration resulted in a 20 % water loss in cell 1 and > 40 % water loss in cells 1 and 2 combined (Figure 2.2B). Of this water loss, only 1 to 10 % was from evapotranspiration, and 90 to 99 % of the loss was from infiltration (Figure 2.2C).

Estimated hourly flow and average DIN and PO₄³⁻ concentrations at stations 1A, 1B, and 2B for each sediment core sampling month are provided in Table 2.3. The product of average nutrient concentration and estimated flow is the average surface water nutrient loading condition for stations 1A, 1B, and 2B (Table 2.3). Average DIN surface

water loading (DIN SWL, Table 2.3) exhibited a clear spatial pattern in all months. DIN loading was greatest at the wetland inflow (station 1A) and decreased 2 – 6 fold by the outflow of cell one (station 1B) and another 2 – 6 fold by the outflow of cell two (station 2B).

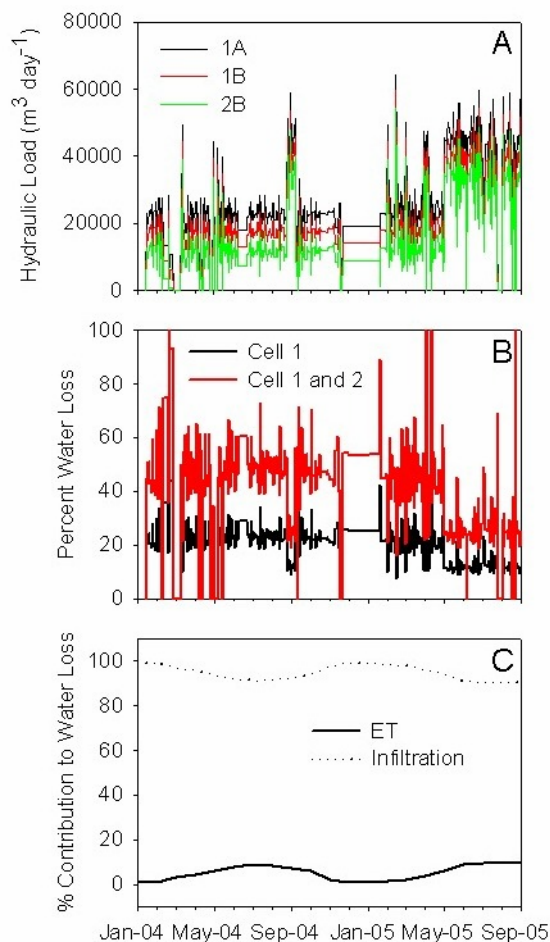


Figure 2.2. Hydraulic loading, water loss, and relative contribution of evapotranspiration (ET) and infiltration to water loss.

Contribution of Sediments to Ecosystem Nutrient Dynamics

On average, 94 % of inflowing DIN was retained in the first two wetland cells.

Nitrite + NO_3^- was the DIN form most efficiently retained. Negative ecosystem NO_2^- +

Table 2.3. Average monthly water column nutrient concentrations, estimated flow rates, nutrient supply rates from water column and sediments, and total nutrient supply rates at each station in the confined flow path. SWL, surface water load; SDL, sediment load. All values \pm SD.

Date	Site	DIN* ($\mu\text{mol L}^{-1}$)	N	PO ₄ ^{3-*} ($\mu\text{mol L}^{-1}$)	P	Est. Flow [†] ($\text{m}^3 \text{h}^{-1}$)	DIN SWL (mol h^{-1})	PO ₄ ³⁻ SWL (mol h^{-1})	DIN SDL [‡] (mol h^{-1})	PO ₄ ³⁻ SDL [‡] (mol h^{-1})	Total supply (mol h^{-1})	DIN Total supply (mol h^{-1})	PO ₄ ³⁻ Total supply (mol h^{-1})	DIN:PO ₄ ³⁻
Aug 2004	1A	23.7 \pm 7.1		0.23 \pm 0.1		1150	27.2 \pm 8.17	0.26 \pm 0.10	26.2 \pm 6.84	0.50 \pm 0.13	53.4 \pm 15.0	0.76 \pm 0.23		70.2 \pm 0.58
	1B	6.56 \pm 3.9		0.39 \pm 0.2		929	6.09 \pm 3.64	0.36 \pm 0.16	8.72 \pm 4.63	0.28 \pm 0.20	14.8 \pm 8.27	0.64 \pm 0.36		23.1 \pm 1.21
	2B	1.08 \pm 0.3		0.42 \pm 0.4		689	0.74 \pm 0.23	0.29 \pm 0.25	4.96 \pm 1.44	0.16 \pm 0.05	5.70 \pm 1.67	0.45 \pm 0.35		12.7 \pm 1.07
Jan 2005	1A	39.5 \pm 7.0		0.10 \pm 0.0		834	32.9 \pm 5.84	0.08 \pm 0.03	-1.42 \pm 1.24	0.02 \pm 0.01	31.5 \pm 7.08	0.10 \pm 0.04		315 \pm 0.62
	1B	28.7 \pm 5.9		0.27 \pm 0.1		634	18.2 \pm 3.71	0.17 \pm 0.10	2.49 \pm 2.16	0.03 \pm 0.01	20.7 \pm 5.87	0.20 \pm 0.11		103 \pm 0.83
	2B	6.92 \pm 2.7		0.12 \pm 0.1		412	2.85 \pm 1.10	0.05 \pm 0.02	7.89 \pm 2.91	0.04 \pm 0.01	10.7 \pm 4.01	0.09 \pm 0.03		119 \pm 0.71
Apr 2005	1A	37.3 \pm 1.5		0.06 \pm 0.0		1080	40.2 \pm 1.61	0.06 \pm 0.00	10.7 \pm 11.6	0.03 \pm 0.01	50.9 \pm 13.21	0.09 \pm 0.01		566 \pm 0.37
	1B	7.62 \pm 2.8		0.21 \pm 0.1		877	6.69 \pm 2.41	0.17 \pm 0.05	3.06 \pm 2.69	0.12 \pm 0.08	9.75 \pm 5.10	0.29 \pm 0.13		33.6 \pm 0.97
	2B	3.87 \pm 2.1		0.10 \pm 0.0		664	2.57 \pm 1.42	0.07 \pm 0.03	3.61 \pm 3.13	0.13 \pm 0.07	6.18 \pm 4.55	0.20 \pm 0.10		30.9 \pm 1.04
Jul 2005	1A	24.1 \pm 2.6		0.11 \pm 0.0		1340	32.2 \pm 3.45	0.15 \pm 0.02	6.11 \pm 1.58	0.19 \pm 0.06	38.3 \pm 5.03	0.34 \pm 0.08		113 \pm 0.37
	1B	5.31 \pm 0.7		0.35 \pm 0.0		1160	6.16 \pm 0.86	0.41 \pm 0.03	-0.78 \pm 1.25	-0.02 \pm 0.03	5.38 \pm 2.11	0.39 \pm 0.06		13.8 \pm 0.54
	2B	2.08 \pm 0.4		0.18 \pm 0.0		963	2.00 \pm 0.39	0.17 \pm 0.03	1.66 \pm 1.09	0.04 \pm 0.02	3.66 \pm 1.48	0.21 \pm 0.05		17.4 \pm 0.64

*n = 3 – 4

[†]Estimated from pumping hours and modeled loss from evapotranspiration and infiltration

[‡]n = 3

NO_3^- flux was correlated with sediment $\text{NO}_2^- + \text{NO}_3^-$ influx, and the rate of sediment $\text{NO}_2^- + \text{NO}_3^-$ influx accounted for one half of the rate of total ecosystem $\text{NO}_2^- + \text{NO}_3^-$ retention (slope of best fit line = 2.03; Figure 2.3A). Interestingly, sediment NH_4^+ flux was inversely correlated with ecosystem NH_4^+ flux (Figure 2.3B). In other words, highest rates of sediment NH_4^+ efflux corresponded with highest rates of ecosystem NH_4^+ influx.

Conversely, PO_4^{3-} was not well retained in the ecosystem. A clear spatial pattern in PO_4^{3-} loading was not evident in August 2004 but became increasingly apparent in subsequent sampling. In January, April, and July 2005, PO_4^{3-} loading was always greatest at the outflow of cell one (station 1B) while lower, and similar, PO_4^{3-} loading was observed at the wetland inflow (station 1A) and outflow of cell 2 (station 2B; Table 2.3). Therefore, wetland cell 1 was a net source of PO_4^{3-} , and cell 2 was a net sink leaving the PO_4^{3-} inputs and outputs (at least for the first two wetland cells) relatively balanced. Although higher sediment PO_4^{3-} efflux resulted in less ecosystem influx in cell 2, ecosystem PO_4^{3-} efflux from cell 1 varied independently of sediment PO_4^{3-} efflux (Figure 2.3C).

Total DIN and PO_4^{3-} supply rates, and the corresponding ratio of DIN: PO_4^{3-} , are provided in Table 2.3. Supply rates were derived by summing surface water nutrient loads (SWL) and sediment nutrient loads (SDL) for sampling stations 1A, 1B, and 2B. Surface water and sediment loading appeared to contribute equally to total DIN supply in August 2004. However, surface water loading was the dominant contributor to total DIN supply in all other months, except at station 2B where sediment loading rates from DIN efflux approached or exceeded surface water loading rates. Surface water loading and

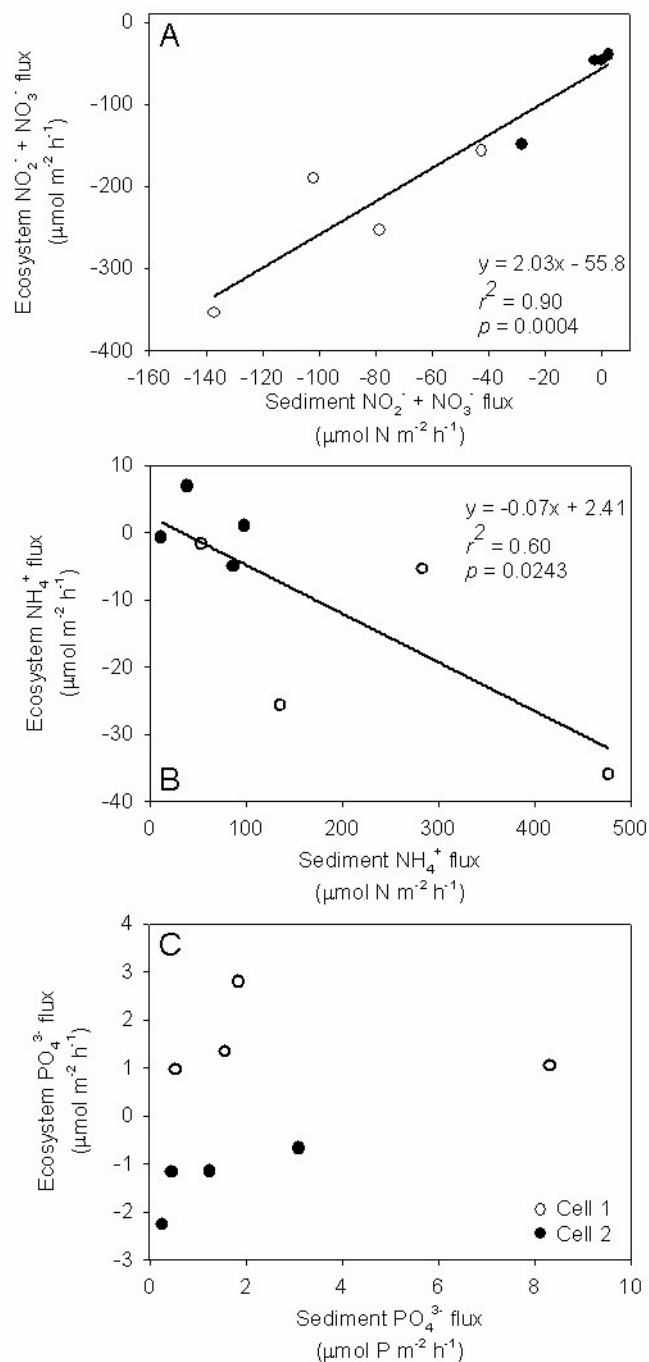


Figure 2.3. Relationship between sediment nutrient flux and ecosystem nutrient flux.

sediment loading appeared to contribute equally to total PO_4^{3-} supply (Table 2.3). The consistent decrease in DIN supply to areas at increasing distances from the wetland inflow, and the relatively variable pattern of PO_4^{3-} supply, caused DIN: PO_4^{3-} to decrease

substantially in the downstream direction. Although this relative pattern was consistent during all sampling months, DIN:PO₄³⁻ approached or fell below 16:1 (Redfield ratio) only in summer months. Interestingly, periods when the DIN:PO₄³⁻ of the total nutrient supply rate fell below 20 were associated with periods of sediment N₂ influx (net N₂ fixation), while sediment N₂ efflux (net denitrification) corresponded to DIN:PO₄³⁻ ratios greater than 20. Furthermore, four of the five sediment N₂ influx observations occurred when DIN supply was $\leq 6 \text{ mol N h}^{-1}$ (Figure 2.4).

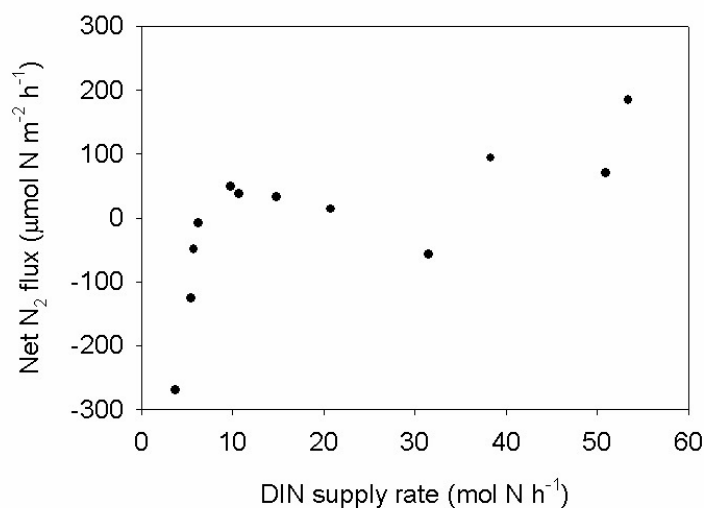


Figure 2.4. Relationship between DIN supply rate and sediment net N₂ flux.

Discussion

Are Sediments a Net Source or Sink of Dissolved N and P?

Intact core experiments in this study revealed that sediment NH₄⁺ production (net source) and sediment NO₃⁻ influx (net sink) were the most important processes regulating the magnitude of sediment nutrient flux (Table 2.2). The rate of NH₄⁺ production often exceeded the influx of combined NO₂⁻ + NO₃⁻, resulting in net DIN efflux. Only in

January 2005 at site 1A and July 2005 at site 2B were the sediments a net sink for DIN. The sediments were usually a net source of PO_4^{3-} , although the magnitude of PO_4^{3-} flux was much less than NH_4^+ and $\text{NO}_2^- + \text{NO}_3^-$ flux.

Rates of sediment NH_4^+ production observed in this study are higher than rates for lentic freshwater systems reviewed by Seitzinger (1988), but are similar to more recently derived estimates for a freshwater wetland (Tomaszek et al. 1997), freshwater lake (Nowlin et al. 2005), and Texas estuaries (Gardner et al. 2006). Sediment NO_3^- retention/removal observed in this study is in agreement with NO_3^- removal observed in similar freshwater wetland systems in Michigan (Whitmire and Hamilton 2005) and North Carolina (Poe et al. 2003), but exceeds NO_3^- retention/removal observed in Texas estuarine systems (Gardner et al. 2006). However, NO_3^- concentration in overlying water measured in this study was 2 – 5 times higher than estuarine NO_3^- concentration measured by Gardner et al. (2006), suggesting a fundamental difference in potential NO_3^- gains or losses between systems.

What are the Rates of Sediment N Transformations such as N_2 fixation, Denitrification, and DNRA?

Sediment N_2 fixation and denitrification proceeded simultaneously in all sampling events except in January 2005 at sites 2A and 2B and in April 2005 at site 2B, where N_2 fixation was zero (Table 2.2). Sediment N_2 fixation rates measured in this study fluctuated between 0 – 426 $\mu\text{mol N m}^{-2} \text{ h}^{-1}$. When seasonal rates were averaged and extrapolated to yearly estimates, the average annual contribution of N_2 fixation was approximately 8.7 $\text{g N m}^{-2} \text{ y}^{-1}$, which aligns with relatively high rates reported for similar ecosystems (0.01 – 6.0 $\text{g N m}^{-2} \text{ y}^{-1}$; see review by Howarth et al. 1988). Sediment

denitrification rates measured in this study ranged from 54 – 278 $\mu\text{mol N m}^{-2} \text{ h}^{-1}$, which was similar to rates from other freshwater wetland sediments in Ohio (40 – 428 $\mu\text{mol N m}^{-2} \text{ h}^{-1}$; Tomaszek et al. 1997) and North Carolina (71 – 285 $\mu\text{mol N m}^{-2} \text{ h}^{-1}$; Poe et al. 2003). Denitrification was not strongly coupled to nitrification during most sampling events (0.9 – 8.6 %) except in January 2005 and at site 1A in April 2005, where 20 – 40 % of denitrification was coupled to nitrification (Table 2.2). It is possible that the high-level $^{15}\text{NO}_3^-$ additions used in this study had a “decoupling” effect, but generally high ambient NO_3^- concentrations and observed NO_3^- influx into sediments before isotope addition suggests that nitrification does not satiate denitrifiers in these sediments.

Potential DNRA rates observed in the summer sampling events in this study (1.3 – 33 $\mu\text{mol N m}^{-2} \text{ h}^{-1}$) are among the highest reported for freshwater systems, although DNRA was zero in the winter and spring. DNRA was positively correlated with salinity in Texas estuaries and always less than 5 $\mu\text{mol N m}^{-2} \text{ h}^{-1}$ when salinity was less than 10 ppt (Gardner et al. 2006). Interestingly, the highest DNRA rate observed in the present study occurred at station 2B in July 2005 and was associated with net NH_4^+ influx into sediments before isotope addition (Table 2.2). However, $^{15}\text{NO}_3^-$ addition to these samples resulted in a change to high NH_4^+ efflux, suggesting that DNRA was limited by NO_3^- availability. The percentage of NO_3^- influx, following $^{15}\text{NO}_3^-$ addition, transformed by DNRA was relatively low (4.6 % in August 2004, 0.0 % in January and April 2005, and 3.9 % in July 2005) when compared with the percentage of NO_3^- influx transformed by denitrification (52 % in August 2004, 68 % in January 2005 [not including site 2B where denitrification exceeded NO_3^- flux following isotope addition], 56 % in April 2005, and 39 % in July 2005). This suggests that even though observed DNRA rates were relatively

high in this system, NO_3^- influx had a much greater probability of being denitrified rather than reduced to NH_4^+ by DNRA.

Because the absolute rates of sediment N_2 fixation and denitrification were determined using the isotope pairing approach (An et al. 2001), they may not portray actual rates if fluxes were changed by $^{15}\text{NO}_3^-$ addition. However, net N_2 flux prior to $^{15}\text{NO}_3^-$ addition can be used as an indicator of the relative importance of these processes. In August 2004 and April 2005, net N_2 flux was positive (net denitrification) and relatively high at site 1A, but was decreased at downstream sites (1B and 2A) and negative (net N_2 fixation) at site 2B (Table 2.2). This spatial pattern was also apparent at sites 1A (net denitrification) and 2B (net N_2 fixation) in July 2005, but was less apparent at the middle wetland sites (1B and 2A; Table 2.2). Because sediment N_2 flux was negatively correlated with sediment NO_3^- flux (Figure 2.1), the spatial pattern of diminishing N_2 efflux to increasing N_2 influx may relate to the decreasing availability of NO_3^- along the flow path of water (Table 2.1). Similar patterns have been reported in a created wetland ecosystem with a well defined flow path (Poe et al. 2003) and in the Florida Everglades, where denitrifying enzyme activity was limited by NO_3^- availability (White and Reddy 1999).

To What Extent are Sediment Nutrient Fluxes, and Associated Biogeochemical Transformations, Correlated with Ecosystem Nutrient Fluxes?

Nitrite + NO_3^- influx into sediments accounted for one-half the rate of ecosystem $\text{NO}_2^- + \text{NO}_3^-$ influx (Figure 2.3A). Combining NO_2^- and NO_3^- sediment fluxes was necessary for comparisons with ecosystem fluxes because NO_2^- and NO_3^- concentrations in routine sampling were not differentiated (*i.e.* determined simultaneously as $\text{NO}_2^- +$

NO_3^-). The combined $\text{NO}_2^- + \text{NO}_3^-$ flux (sediment or ecosystem) was primarily a function of NO_3^- flux. Nitrite concentrations measured during sediment core sampling events were less than 10 % of the combined $\text{NO}_2^- + \text{NO}_3^-$ concentration, except in cell 2 where NO_3^- concentration was low ($< 1 \mu\text{mol L}^{-1}$; Table 2.1). Sediment NH_4^+ production appeared to result from assimilative uptake and regeneration, which was likely supported by the relatively high sediment N_2 fixation rates. However, potential DNRA accounted for 1 to 5 % of NH_4^+ production in cell 1 (stations 1A and 1B) and 23 to 37 % of NH_4^+ production at station 2B in the summer months of both years. The negative correlation between sediment NH_4^+ production and ecosystem NH_4^+ retention was unexpected (Figure 2.3B). However, this relationship appears to have varied with season. Sediment NH_4^+ production was highest in summer (Table 2.2) during peak production by the benthic microbial community. Therefore, the high ecosystem NH_4^+ retention observed during high sediment NH_4^+ production may have been caused by efficient NH_4^+ uptake and retention by epiphytic and epipelagic microbes. Sediment PO_4^{3-} flux was always positive but relatively low and not strongly correlated with ecosystem PO_4^{3-} flux (Figure 2.3C). Interestingly, ecosystem PO_4^{3-} flux was always positive in cell 1 and negative in cell 2. This difference may have been due to higher sediment PO_4^{3-} flux in cell 1. Average sediment PO_4^{3-} flux in cell 1 was ~ 2.5 times higher than sediment PO_4^{3-} flux in cell 2 in August 2004 and ~ 4 times higher in July 2005, but displayed little or no difference in January and April 2005 (Figure 2.3C).

Do Sediment Nutrient Dynamics Impact Inorganic N and P Supply?

Average DIN surface water loading was highest at the wetland inflow (site 1A = $33.1 \text{ mol N h}^{-1}$) and was diminished by 50 – 80 % at site 1B and by 91 – 97 % at site 2B

(Table 2.3). The reduction of DIN was probably due in large part to assimilation microbial epiphytes and microphytobenthos. However, sediment $\text{NO}_2^- + \text{NO}_3^-$ influx accounted for one half of $\text{NO}_2^- + \text{NO}_3^-$ ecosystem retention/removal (Figure 2.3A). As previously mentioned, 40 – 70 % of sediment $\text{NO}_2^- + \text{NO}_3^-$ influx was transformed by denitrification or DNRA, which was supported by evidence from increased NO_3^- influx and NH_4^+ and NO_2^- efflux following $^{15}\text{NO}_3^-$ addition in the intact core experiments. The rate of sediment NH_4^+ production often counterbalanced $\text{NO}_2^- + \text{NO}_3^-$ loss to sediments, but sediment NH_4^+ was probably quickly assimilated or transformed by the microbial community and did not result in ecosystem NH_4^+ efflux (Figure 2.3B). Average sediment DIN loading comprised 0 – 49 % of the total DIN supply at site 1A, 0 – 58 % of the total DIN supply at site 1B, and 45 – 87 % of the DIN supply at site 2B. The increased importance of sediment N loading to total N supply at downstream sites, site 2B in particular, was supported by sediment NH_4^+ production. Furthermore, sediment NH_4^+ production remained high at site 2B perhaps due to sediment N_2 fixation. Ammonium production was usually a function of biological regeneration as a result of assimilative processes, but DNRA accounted for as much as 37 % of sediment NH_4^+ production during summer. Overall, the sediments were an important sink for N when the water column N supply was high (near inflow), but the sediments were an important source of N when water column N supply was low.

Average PO_4^{3-} surface water loading was variable but highest at site 1B, consistent with higher PO_4^{3-} efflux from cell 1. Sediment PO_4^{3-} loading accounted for 20 – 66 % of total PO_4^{3-} supply at site 1A, 15 – 56 % of total PO_4^{3-} supply at site 1B, and 19 – 65 % of total PO_4^{3-} supply at site 2B. Wetlands receiving more than $1 \text{ g P m}^{-2} \text{ y}^{-1}$ often

have higher P outputs than inputs (Richardson and Qian 1999). Average surface water P loading approached the upper limit of the “one gram rule” for cell 1 ($0.76 \text{ g P m}^{-2} \text{ y}^{-1}$) and cell 2 ($0.94 \text{ g P m}^{-2} \text{ y}^{-1}$), but only cell 1 was consistently a source of P (i.e. P loading at sites 1A was greater than P loading at site 1B; Table 2.3). Although cell 2 reduced P concentrations to the original inflow value, this cell may have retained a higher percentage of the original P load to the wetland if the incoming load had not been increased by P efflux from cell 1.

The ratio of DIN to PO_4^{3-} supply was greatest at the wetland inflow and decreased in the downstream direction, except in January and July 2005 when DIN: PO_4^{3-} at site 2B was greater than that at site 1B. Interestingly, DIN: PO_4^{3-} usually indicated P-limitation (i.e. > 20) except at site 2B in both summers and at site 1B in July 2005 when this ratio approached the threshold for N-limitation (Table 2.3). Low DIN: PO_4^{3-} supply, and low DIN supply alone, was often associated with sediment N_2 influx (Figure 2.4). It should be noted that DIN: PO_4^{3-} may not be the best proxy for identifying limiting nutrients (Dodds 2003), but total N and P data were not available for this study.

Conclusions

The results of this study support the importance of sediment nutrient flux and N transformations in shaping inorganic N and P supplies in wetland ecosystems. Denitrification appeared to be an important sink for N when NO_3^- supply was sufficient. Conversely, N_2 fixation and DNRA were important sources of biologically available N when inorganic N was low, particularly in summer months. Overall, the system was a net sink for inorganic N but a net source of inorganic P. This trend caused a shift in the relative importance of atmospheric N_2 inputs and outputs in order to balance ecosystem

N:P supply and may have been responsible for inducing periods of N-limitation within the ecosystem. Temporal shifts between N and P limitation is likely to have implications for the structure and function of wetland microbial communities dependent on inorganic nutrient supplies.

Results of this study also demonstrate the potential of created wetlands as N sinks. The efficacy by which N may be removed or retained in wetland ecosystems may decrease the N load to downstream systems, particularly coastal systems, impacted by accelerated eutrophication. Increasing wetland acreage in areas such as the Mississippi drainage basin could reduce the amount of N loading to receiving waters and aid in preventing such problems as Gulf of Mexico hypoxia.

CHAPTER THREE

Periphyton Nutrient Limitation and Nitrogen Fixation Potential Along the Wetland Nutrient-Depletion Gradient¹

Introduction

The role of algal assemblages in wetlands remains a relatively understudied component in wetland ecology. Although some extensive reviews have stated the importance of periphyton and phytoplankton in wetlands (Vymazal 1995, Goldsborough and Robinson 1996), the major factors controlling algal dynamics in wetland systems continue to be poorly understood. Nutrient control of periphyton has been confirmed in both temperate and subtropical wetlands (McDougal et al. 1997, McCormick et al. 2001). Wu and Mitsch (1998) observed that periphyton biomass was generally greatest near the inflow of a newly constructed wetland where available nutrient concentrations were greatest, and then decreased along with available nutrients as the distance from inflow increased. A similar trend was observed between decreasing algal growth potential and nutrient concentrations in the Florida Everglades (McCormick et al. 1996). Although periphyton nutrient limitation status has been widely reported for streams (e.g. Matlock et al. 1999, Tank and Dodds 2003) and lake littoral zones (e.g. Fairchild et al. 1985, Havens et al. 1999, Rodusky et al. 2001), few studies have directly assessed nutrient limitation status of periphyton in wetlands (Toetz 1995).

Nutrient availability gradients develop in freshwater wetlands as water column nutrients are depleted along the flow path of water. This trend has been widely

¹Previously published in *Wetlands* 25 (2): 439-448. 2006. Scott JT, Doyle RD, Filstrup CT. Reproduced with permission.

documented in created wetlands (Kadlec and Knight 1996) and for areas of the Florida Everglades (Vaithianathan and Richardson 1997). Studies of biological responses to such gradients have focused mostly on aquatic macrophytes (Vaithianathan and Richardson 1999, Olde Venterink et al. 2001). However, significant effort has been given to understand periphyton response to nutrient gradients in the Everglades, where periphyton P limitation intensifies in a downstream direction by a concurrent increase in N:P ratio and depletion of N and P (Vymazal and Richardson 1995, McCormick et al. 1996, 1998). Other studies, as reviewed by Goldsborough and Robinson (1996), have demonstrated short periods of N and P limitation of wetland periphyton, however, to our knowledge no studies have demonstrated a shift in periphyton nutrient limitation status in response to a spatial gradient of nutrient concentration and N:P ratio.

Nitrogen limitation along wetland nutrient depletion gradients may occur as a result of unequal removal efficiencies of N and P. Evidence for a maximum P assimilative capacity in wetlands has been suggested (Richardson and Qian 1999). Due to the potential for permanent N removal from wetlands via denitrification, a falling N:P ratio may be relatively common under various nutrient loading scenarios.

A shift to N limitation within a wetland ecosystem would likely favor organisms capable of molecular nitrogen (N_2) fixation, a well known trend observed in phytoplankton assemblages of lakes (Levine and Schindler 1999). Bowden (1987) suggested that N_2 fixation by periphytic cyanobacteria may be an important component of nitrogen dynamics in some freshwater wetlands, with contributions as high as $11.9 \text{ g N m}^{-2} \text{ y}^{-1}$. Because periphyton form a major portion of the base of the aquatic food web in wetlands (Goldsborough and Robinson 1996), it is imperative to develop an

understanding of how environmental factors such as nutrient status may influence periphyton productivity, biomass accumulation, growth limitation, and species composition in these assemblages. The objectives of this study were to: 1) evaluate nutrient limitation status of periphyton along a known nutrient depletion gradient in a freshwater marsh, 2) characterize changes in available nutrient concentrations and N:P ratio along this gradient, and 3) measure changes in N₂ fixation potential by periphyton along the observed gradient.

Materials and Methods

Nutrient Limitation Status

In situ nutrient diffusing substrata (NDS) were utilized for the determination of nutrient limitation status at the station 1A and station 1B in April, July, and September 2003 (See Figure 1.1 for locations). This technique has been described in detail by Matlock et al. (1998) and is briefly discussed here. NDS were constructed by cutting a 5.07 cm² circular hole in the lid of 1 liter polyethylene bottles. The modification allowed bottles to be capped by resting a Whatman 0.45 µm pore size nylon filter (NF), overlaid with a Whatman 1.2 µm pore size glass fiber filter (GFF), over the mouth of the bottle and attaching the modified lid. The filter series allowed passive diffusion of concentrated nutrients from within the bottle to the surrounding water column, thereby providing a nutrient rich substrate for periphyton growth. The 0.45 µm NF minimized contamination of nutrient concentrate by microorganisms while the 1.2 µm GFF provided substrate for attachment of periphyton. Modified lids on each NDS were covered with 1 mm mesh screen to reduce grazing pressure by large organisms (Rodusky et al. 2001).

Four nutrient treatments were used in this experiment, a control (C = deionized water), nitrogen treatment (N = 21.85 mg l⁻¹ nitrate), phosphorus treatment (P = 12.17 mg l⁻¹ phosphate), and a combined nitrogen plus phosphorus treatment (N+P = 21.85 mg l⁻¹ nitrate + 12.17 mg l⁻¹ phosphate). Diffusion rates of nutrients across NF and GFF at 26 °C were reported as $27 \pm 17 \mu\text{g cm}^{-2} \text{ h}^{-1}$ for nitrate and $17 \pm 16 \mu\text{g cm}^{-2} \text{ h}^{-1}$ for phosphate (Matlock et al. 1998). Although these estimated diffusion rates include the influence of boundary layer conditions caused by periphyton accumulating on GFF's, it is important to recognize that variability in periphyton accumulation may change the degree to which boundary layer conditions influence diffusion rates (Borchardt 1996). In this study, we assumed differences in diffusion rates due to variability in periphyton accumulation were negligible.

Each treatment was replicated four times during the April bioassay and six times in all bioassays thereafter. Replicated treatments were attached to a floating rack using a randomized block design to account for across-row sunlight effects. For each bioassay, NDS were placed at stations 1A and 1B of the wetland for a period of 14-16 days. Following retrieval, GFF's were harvested and periphyton accumulation was measured as pheophytin-corrected chlorophyll- α using a Beckman DU® 650 multiple wavelength spectrophotometer (Clesceri et al. 2000). Although pigment content of an individual algal cell can vary with growth conditions and viability (Wetzel 2001), chlorophyll- α is widely used as a surrogate for algal biomass (Wetzel and Likens 2000).

Periphyton accumulation data from bioassays were log transformed for statistical analysis to correct non-normal distribution and unequal variances among treatments. Data were analyzed using the REGWQ multiple comparison procedure in SAS 8e (SAS

Institute Inc. 1999) to determine differences among treatments. Familywise error rate was controlled at $p < 0.05$ for all pairwise comparisons between treatments and control. A significant difference between periphyton accumulation on controls and individual nutrient treatments (N or P) was considered a response to limitation by that nutrient. A significant difference between periphyton accumulation on controls and the combined nutrient treatments (N+P) was considered a response to N+P co-limitation. However, a response in the combined treatment (N+P) was not considered co-limitation if one of the individual nutrient treatments (N or P) caused a significant response in periphyton accumulation within the same bioassay. In that circumstance, the individual nutrient stimulating growth was considered the limiting nutrient. For instance, if the combined N+P treatment resulted in the greatest difference between treatments and controls, but the P treatment also resulted in significantly greater periphyton accumulation, P would be considered the limiting nutrient.

Periphyton accumulation on controls and N+P treatments were used to calculate an ecosystem trophic status index (ETSI). Assuming periphyton accumulation on N+P treatments represented the maximum growth potential under saturating nutrient conditions, the ETSI is calculated by the following equation:

$$\text{ETSI} = \text{PP} / \text{MPP}$$

where PP represents natural primary productivity (periphyton accumulation on controls) and MPP represents maximum primary productivity (periphyton accumulation on N+P enriched treatments). Theoretically, the ETSI ranges between 0.0 and 1.0. An ETSI value of 1.0 indicates that periphyton productivity is at 100% relative to nitrogen and phosphorus needs (i.e. no nutrient limitation), while an ETSI value near 0.0 indicates

strong nutrient limitation (Matlock et al. 1999). Analysis of variance in SAS 8e (SAS 1999) was used to determine differences in ETSI among locations and dates.

Water Quality and Nitrogen Fixation

During each bioassay period, water samples were collected every 2-3 days at stations 1A, B, C, D, E, and 1B (Figure 1.1) and returned to the laboratory for chemical analysis. Turbidity samples collected in April and July were analyzed in the laboratory using a HACH® 2100N Turbidimeter while turbidity in September was monitored *in situ* using a YSI 6600 multiparameter datasonde. Once in the laboratory, water quality samples were filtered through a Whatman 0.45 µm membrane filter and analyzed for soluble reactive phosphorus (SRP), ammonia-nitrogen (NH₃-N), and nitrate-nitrogen (NO₃-N). Soluble reactive phosphorus concentrations were determined using the ascorbic acid colorimetric method on a Beckman DU® 650 spectrophotometer with 4 cm sample cell (Clesceri et al. 2000). Ammonia-nitrogen and NO₃-N were determined spectrophotometrically on the same instrument using the phenate method (Clesceri et al. 2000) and a modified cadmium reduction method with HACH® preconditioned chemicals, respectively.

Periphyton from stations 1A and 1B (Figure 1.1) were sampled during the July and September bioassays to assess N₂ fixation potential utilizing the acetylene reduction assay (Flett et al. 1976). Plastic slides were placed on a floating rack at the wetland inflow and outflow to allow periphyton colonization over the 14-16 day bioassay period. Intact periphyton samples on artificial substrate were transferred into Popper® Micromate 50 ml syringes filled with water from the sampling location. Separate syringes were filled with water samples alone to assess any background level of

planktonic N₂ fixation. Additional water collected from each site was filtered through a Whatman 0.45 µm membrane filter to create an N₂ fixation assay method blank.

In the laboratory, water volume in syringes was adjusted to 30-32 ml and inoculated with 5 ml acetylene. The syringes were gently mixed to allow rapid dissolution of acetylene gas. Syringes were then incubated overnight (14-20 hours) in the laboratory at constant temperature (adjusted to mean temperature measured at periphyton harvest) and artificial light conditions (330 – 435 µmol s⁻¹ m⁻²). Following incubation, 15 ml of air was drawn into each syringe, which was then vigorously agitated to establish equilibrium conditions of ethylene between dissolved and vapor phases. Aqueous and vapor volumes were recorded following equilibration to account for partitioning of ethylene between aqueous and vapor phases (Flett et al. 1976, Doyle and Fisher 1994). A 100 µl air sub-sample was drawn from each syringe and injected into a Carle® AGC Series gas chromatograph equipped with a flame ionization detector and a 1.8 m stainless steel column packed with 80% Porapack N and 20% Porapack Q (80/100 mesh). The column temperature was 70 °C, helium was used as the carrier gas, and 10 ppm ethylene standards were used to calibrate the instrument daily. Ethylene production rates were converted to N₂ fixation potential using a conversion of 3 µM ethylene per 1 µM N₂ (Doyle and Fisher 1994). Nitrogen fixation rates were normalized to biomass by measuring dry weight (DW) of assayed periphyton. Dry weights were assessed by scraping periphyton from artificial substrate and collecting material on a washed, dried, and pre-weighed glass fiber filter. Samples on filters were dried overnight at 60 °C and dry weight assessed as the difference between total dry weight of sample and filter minus the original filter dry weight. Nitrogen fixation potential was calculated as µg N g DW⁻¹

h^{-1} . Differences in N_2 fixation potential between locations in July and September were determined using individual one-tailed t-tests with Bonferroni corrected error rates. For these analyses, we hypothesized that N_2 fixation would be greater at the outflow. Differences in N_2 fixation between months were determined for each location using individual two-tailed t-tests with Bonferroni corrected error rates.

Periphyton Assemblage Composition

To identify the occurrence of autotrophs capable of molecular N_2 fixation, a qualitative assessment of periphyton taxonomic composition was conducted on samples collected from artificial substrata in September 2003. Periphytic autotrophs were identified using bright-field illumination of a Nikon Eclipse E600 light microscope at 1500x total magnification. To verify diatom identifications based on light microscopy, diatom frustules were cleaned via 30% H_2O_2 oxidation of organic matter. Frustules were dried onto coverslips coated with gold and viewed using a JEOL JSM 5410 scanning electron microscope at 10 kV. All periphyton taxonomic designations were based on Krammer and Lange-Bertalot (1999, 2000) and Wehr and Sheath (2003).

Results

Nutrient Limitation Status

Log transformed (LT) periphyton accumulation at station 1A was never stimulated by the addition of N or P alone (Table 3.1). At station 1B, LT periphyton accumulation was always stimulated by N addition alone. Addition of both N+P resulted in significantly greater accumulation in all bioassays where stimulation was observed. In April, only LT periphyton accumulation on the N+P treatment was significantly greater

than the control at station 1A. At station 1B, LT periphyton accumulation on the N and N+P treatments were significantly greater than the control. At station 1A in July, only LT periphyton accumulation on N+P treatment was significantly greater than other treatments. Log transformed periphyton accumulation on all enrichments were significantly greater than the control at station 1B during this period. No statistical differences were noted in LT periphyton accumulation at station 1A in September. At station 1B, however, LT periphyton accumulation on N and N+P treatments were significantly greater than accumulation on P treatments and controls.

ETSI values for inflow and outflow locations during each bioassay period are given in Figure 3.1. ETSI values decreased significantly from station 1A to 1B in the July and September bioassay periods. Mean ETSI values at 1B were consistently low among all bioassays (0.05-0.17), indicating strong nutrient control on biomass accumulation at this site. The ETSI varied considerably at station 1A, but showed a consistent increase from April (0.15) to September (0.88), indicating declining nutrient limitation through the summer.

Water Quality and Nitrogen Fixation

Mean dissolved inorganic nitrogen ($\text{DIN} = \text{NH}_3\text{-N} + \text{NO}_3\text{-N}$) concentrations, SRP concentrations, and turbidity levels over the study period at each location are displayed in Figure 3.2. Although turbidity and DIN levels declined substantially as water flowed through the first wetland cell, SRP did not follow a similar trend. Over the study period, average DIN concentrations decreased by 89.0% from station 1A to station 1B while SRP concentrations decreased by 34.1%.

Table 3.1. Mean responses of periphyton to nutrient enrichment and results of REGWQ multiple comparison procedure conducted on log transformed values using REGWQ in SAS 8e. Means with same grouping letter are not significantly different at $\alpha_{FW}=0.05$. Differences among means at this significance level were interpreted as response to nutrient limitation.

Treatment	N	Mean Periphyton Accumulation (μg Chlorophyll- α cm^{-2}) \pm SE	Mean Log Periphyton Accumulation (μg Chlorophyll- α cm^{-2}) \pm SE	Mean Groupings	Limitation Status
April, 1A: $F_{3,12} = 22.79$, $p = 0.0002$					
Control	4	0.361 \pm 0.033	-1.06 \pm 0.126	A	N+P co-limited
N	4	0.652 \pm 0.200	-0.562 \pm 0.263	A	
P	4	0.694 \pm 0.072	-0.387 \pm 0.104	A	
N+P	4	2.61 \pm 0.391	0.924 \pm 0.147	B	
April, 1B: $F_{3,12} = 42.15$, $p < 0.0001$					
Control	4	0.552 \pm 0.039	-0.618 \pm 0.070	X	N Limited
N	4	2.02 \pm 0.662	0.517 \pm 0.309	Y	
P	4	0.881 \pm 0.149	-0.175 \pm 0.149	XY	
N+P	4	10.9 \pm 2.03	2.33 \pm 0.186	Z	
July, 1A: $F_{3,20} = 11.23$, $p = 0.0004$					
Control	6	1.55 \pm 0.156	0.410 \pm 0.105	A	N+P co-limited
N	6	1.49 \pm 0.178	0.364 \pm 0.111	A	
P	6	1.70 \pm 0.303	0.437 \pm 0.205	A	
N+P	6	3.67 \pm 0.525	1.23 \pm 0.175	B	
July, 1B: $F_{3,20} = 36.45$, $p < 0.0001$					
Control	6	0.649 \pm 0.059	-0.452 \pm 0.086	X	N+P co-limited
N	6	1.45 \pm 0.251	0.305 \pm 0.161	Y	
P	6	1.44 \pm 0.116	0.350 \pm 0.074	Y	
N+P	6	4.39 \pm 0.698	1.43 \pm 0.143	Z	
September, 1A: $F_{3,20} = 3.27$, $p = 0.051$					
Control	6	0.784 \pm 0.072	-0.266 \pm 0.096	A	No nutrient limitation
N	6	0.886 \pm 0.118	-0.157 \pm 0.113	A	
P	6	0.663 \pm 0.030	-0.416 \pm 0.042	A	
N+P	6	0.883 \pm 0.063	-0.138 \pm 0.076	A	
September, 1B: $F_{3,20} = 199.30$, $p < 0.0001$					
Control	6	0.612 \pm 0.070	-0.526 \pm 0.119	X	N Limited
N	6	5.23 \pm 0.631	1.62 \pm 0.117	Y	
P	6	0.686 \pm 0.071	-0.404 \pm 0.105	X	
N+P	6	8.26 \pm 0.447	2.10 \pm 0.059	Z	

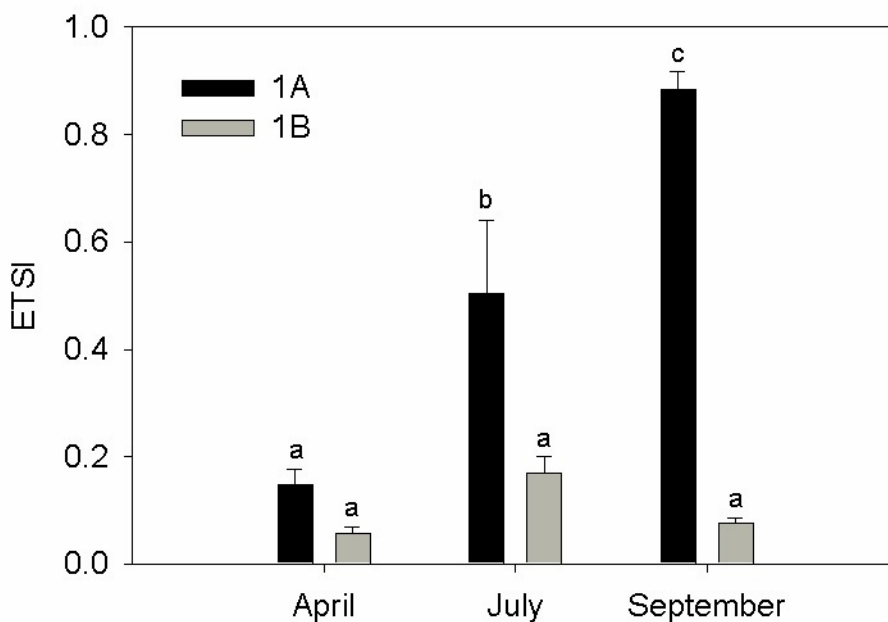


Figure 3.1. Ecosystem trophic status index at areas 1A and 1B for all nutrient enrichment bioassays ($F_{5,26} = 27.92$, $p < 0.0001$).

Mean nutrient concentrations, turbidity levels, and N_2 fixation potentials associated with individual bioassays are summarized in Table 3.2. Turbidity levels and nutrient concentrations, with the exception of SRP during the July bioassay, decreased from station 1A to station 1B during all bioassays (Table 3.2). Both NO_3 -N and SRP values at station 1A and 1B were greatest in September, while lowest SRP and lowest NO_3 -N occurred at station 1B in April and July, respectively. Station 1A NH_3 -N was greatest in April and subsequently decreased in July and September. Station 1B NH_3 -N consistently increased through the spring and summer from a minimum of $6.4 \mu g\ l^{-1}$ in April to a maximum of $18.1 \mu g\ l^{-1}$ in September.

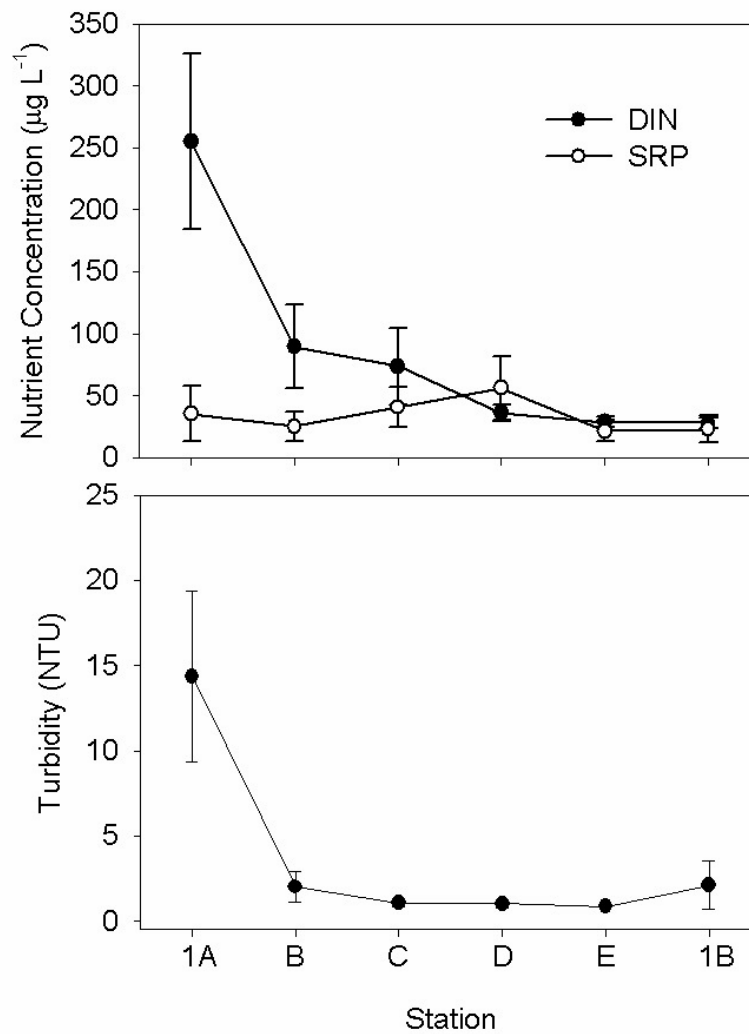


Figure 3.2 Mean dissolved inorganic nitrogen (DIN), soluble reactive phosphorus (SRP), and turbidity for summer 2003 at each station in cell 1 (error bars represent SE).

Nitrogen fixation potential at the wetland outflow was significantly greater than at the wetland inflow for both assayed periods (July, $t_{0.025, 10} = -6.61$, $p < 0.0001$; September, $t_{0.025, 10} = -7.97$, $p < 0.0001$). Analysis of temporal data revealed a significant increase in N_2 fixation potential from July to September at the wetland inflow ($t_{0.0125, 10} = -3.98$, $p = 0.0026$) and outflow ($t_{0.0125, 10} = -7.20$, $p < 0.0001$).

Table 3.2. Water column nutrient content and periphyton N₂ fixation potential for each bioassay period (mean \pm SE [n]).

Bioassay Period	SRP ($\mu\text{g l}^{-1}$)	NO ₃ -N ($\mu\text{g l}^{-1}$)	NH ₃ -N ($\mu\text{g l}^{-1}$)	DIN:SRP	Turbidity (NTU)	Periphyton N fixation Potential ($\mu\text{g N g DW}^{-1} \text{h}^{-1}$)
1A						
April	7.6 \pm 2.4 [3]	228.6 \pm 24.0 [3]	85.0 \pm 37.1 [2]	44.91 \pm 13.96 [3]	19.27 \pm 2.95 [3]	NA
July	5.7 \pm 1.2 [5]	14.7 \pm 2.5 [5]	48.4 \pm 7.4 [5]	13.58 \pm 3.28 [5]	11.44 \pm 0.676 [5]	0.038 \pm 0.009 [6]
September	81.2 \pm 55.2 [5]	374.8 \pm 132.4 [5]	45.4 \pm 17.7 [5]	12.20 \pm 3.16 [5]	18.7 \pm 0.562*	0.374 \pm 0.084 [6]
1B						
April	3.9 \pm 3.0 [3]	12.2 \pm 3.3 [3]	6.4 \pm 2.1 [2]	10.41 \pm 9.19 [2]	3.63 \pm 0.695 [3]	NA
July	8.6 \pm 2.5 [5]	6.4 \pm 2.3 [5]	11.4 \pm 2.7 [5]	3.40 \pm 1.33 [5]	1.21 \pm 0.174 [5]	3.29 \pm 0.491 [6]
September	49.4 \pm 26.1 [5]	22.7 \pm 2.0 [5]	18.1 \pm 4.0 [5]	1.61 \pm 0.48 [5]	2.0 \pm 0.235*	32.4 \pm 4.02 [6]

* September turbidity data logged *in situ* using a multiparameter datasonde logging at 15 minute intervals

Periphyton Assemblage Composition

The qualitative assessment of periphyton assemblage composition from station 1B revealed that the pennate diatoms *Epithemia adnata* (Kützinger) Brébisson and *Rhopalodia gibba* (Ehrenberg) O. Müller var. *gibba* were common in the downstream location. All species of *Epithemia* are reported to contain N₂ fixing cyanobacterial endosymbionts, while some species of *Rhopalodia* contain endosymbiotic cyanobacteria (Round et al. 1990). Both heterocystous and non-heterocystous N₂ fixing cyanobacteria appeared to be uncommon or absent. Although a quantitative assessment was not conducted, the abundance of *E. adnata* appeared high relative to other taxa capable of molecular N₂ fixation. Because N₂ fixation potential at station 1A was low, a qualitative assessment of periphyton assemblages composition was not completed for this site.

Discussion

A pronounced nutrient depletion gradient is evident in the Lake Waco Wetland (Figure 3.2), suggesting the potential for increased nutrient limitation of periphyton at downstream locations. This increased likelihood of nutrient limitation was supported by nutrient enrichment bioassay data. The low ETSI values (< 0.20) observed for both stations 1A and 1B in April indicate strong nutrient limitation of periphyton accumulation in the wetland during this period (Figure 3.1). Although nutrient limitation of periphyton at station 1A was diminishing in July (ETSI = 0.50) and was practically absent in September (ETSI = 0.88), nutrient limitation of periphyton at station 1B remained strong throughout the summer (ETSI of 0.06, 0.17, and 0.08 for April, July, and September, respectively). The increased severity of periphyton nutrient limitation along the Lake

Waco Wetland nutrient gradient is similar to that demonstrated in other wetland systems (McCormick et al. 1996).

However, during the study period the Lake Waco Wetland consistently removed N more efficiently than P from the water column (also see Chapter 1). This trend differs from that previously described in wetlands, such as the Florida Everglades, where P concentrations are depleted from the water column more efficiently than N, thereby resulting in increased N:P (Vaithiyathan and Richardson 1997). The nutrient depletion trend in the Lake Waco Wetland resulted in a continuous decrease of DIN:SRP mass ratio from 20.2 ± 5.0 at station 1A to 3.8 ± 1.6 at station 1B. Consequently, differences in nutrient limitation status of periphyton existed between stations 1A and 1B. Nitrogen additions alone never stimulated periphyton accumulation at station 1A. However, sole N additions always stimulated periphyton accumulations at station 1B. To our knowledge, a shift in nutrient limitation from one nutrient to another within wetland ecosystems has only been previously suggested for macrophytes (Richardson et al. 1999).

During the April and September bioassays, nutrient limitation status of periphyton shifted from N+P co-limitation or no nutrient limitation respectively at station 1A, to N limitation at station 1B (Table 3.1). Water column nutrient content, DIN:SRP ratios, and N₂ fixation potential during these time periods provide further evidence for a shift to N deficiency (Table 3.2).

Only in July did periphyton at station 1A and 1B exhibit similar characteristics in nutrient limitation status (i.e. both N+P co-limited), but even then, the type and severity of co-limitation differed. Periphyton accumulation at station 1A in July was significantly higher on N+P treatments only, while the N, P, and N+P treatments all had a stimulatory

effect at station 1B. These results suggest that the periphyton assemblage at station 1A required simultaneous enrichment of N and P to stimulate growth and were therefore truly N+P co-limited. On the other hand, periphyton accumulation at station 1B was stimulated individually by N and P, and to a larger degree by the combined N+P. This suggests that a portion of the downstream assemblage was limited individually by N and another portion was limited simultaneously by P. The large response to combined N+P is likely a consequence of satisfying the secondary nutrient requirement (Borchardt 1996). For instance, the N limited portion of the assemblage may have been stimulated by N enrichment to a point where P became limiting, and the P limited portion of the assemblage may have been stimulated by P to a point where N became limiting. Therefore, the combined nutrient treatment (N+P) provided the primary and secondary limiting nutrients to both portions of the assemblage at station 1B, resulting in greater periphyton accumulation.

The significant increase in N_2 fixation potential between stations 1A and 1B in July also indicates a definitive response to N deficiency. This is supported by the occurrence of comparable N_2 fixation trends at stations 1A and 1B in September, when N deficiency at 1B was known. Doyle and Fisher (1994) report a similar periphyton N_2 fixation response along a NO_3 -N gradient as nutrient rich river waters flooded onto the Amazon floodplain.

Nitrogen fixation potential at the outflow of the Lake Waco Wetland ($3.29 - 32.4 \mu\text{g N g DW}^{-1} \text{ h}^{-1}$) exceeds recently reported (Inglett et al. 2004) per gram rates of periphyton N_2 fixation in the Florida Everglades under ambient light ($0.61 - 1.09 \mu\text{g N g DW}^{-1} \text{ h}^{-1}$). An estimated contribution of $9.7 \text{ g N m}^{-2} \text{ y}^{-1}$ by periphyton N fixation in the

Everglades, derived from the aforementioned per gram rates, are described by Inglett et al. (2004) to be among the highest reported for aquatic and wetland ecosystems. This is in agreement with a range of reported annual estimates ($0.5 - 31.3 \text{ g N m}^{-2} \text{ y}^{-1}$) from a variety of other freshwater ecosystems (Doyle and Fisher 1994). However, the relatively high annual estimate for the Everglades is influenced by the large standing crop of periphyton biomass known to occur in this ecosystem (Turner et al. 1999). The absence of information on periphyton standing crop in the Lake Waco Wetland prevents us from estimating areal rates of N_2 fixation for this system.

The observed spatial shift in nutrient deficiency and relatively high, per gram N_2 fixation potential at station 1B may be influenced to a certain degree by wetland age. Tyler et al. (2003) found that N_2 fixation rates in younger salt marshes were 2 or 3 times greater than N_2 fixation rates in intermediate and older marshes, respectively. However, evidence for similar trends in freshwater wetlands appears absent. If in fact, a maximum P assimilative capacity for a wetland exists (Richardson 1997), and nitrogen transformations along a nutrient gradient (see Chapter 1 and Poe et al. 2003) can provide a permanent sink for nitrogen, the potential for falling N:P ratio and subsequent N limitation of periphyton may exist in many freshwater wetlands (e.g. Doyle and Fisher 1994). However, this assumes that periphyton rely primarily on water column nutrient content and not upon alternate nutrient sources. Goldsborough and Robinson (1996) point out that epiphyton and epipelon in most systems likely derive a significant portion of their nutritional requirements from the substrate to which they are attached (macrophytes and sediment, respectively). The extent to which water column nutrient content may control these assemblages, or how wetland nutrient depletion gradients may

influence nutrient signatures in their attachment substrate is poorly understood. More research on periphyton successional characteristics in developing freshwater wetlands is needed to further understand how functions of periphyton assemblages change during wetland development.

Given the observed shifts in N:P ratio and nutrient limitation status in the Lake Waco Wetland, and the known competitive advantage *Epithemia adnata* (Kützing) Brébisson and *Rhopalodia gibba* (Ehrenberg) O. Müller var. *gibba* have in N poor habitats (Lowe et al. 1984), the appearance of these organisms is not surprising. However, the ecological significance of *E. adnata*'s contribution to total periphyton N₂ fixation in this and other systems may be of interest. The absence of other heterocystous and non-heterocystous cyanobacteria in periphyton of N poor areas suggest that *E. adnata* may be responsible for the majority of N₂ fixation in these assemblages. Although the competitive advantage of *Epithemia* sp. and *Rhopalodia* sp. with other diatoms in N poor habitats has been explored (Mayer and Galatowitsch 2001), more research is needed to investigate the competitive ability and contribution to periphyton N₂ fixation rates of these organisms relative to heterocystous and non-heterocystous cyanobacterial N₂ fixers.

Conclusions

Nutrient depletion gradients may commonly develop along the flow path of water in many freshwater wetlands. Results of this study suggest that unequal nutrient retention in wetlands can lead to a spatial heterogeneity in both the severity of nutrient limitation and the specific nutrient limiting growth. Further, our results suggest that a shift towards N limitation in wetland periphyton assemblages may result in ecologically significant rates of periphyton N₂ fixation.

The relative abundance of *Epithemia* sp. and *Rhopalodia* sp. over other potential N₂ fixing autotrophs found in this study is interesting. Currently, little is known about the rate of supply or transfer of fixed nitrogen from the endosymbionts to diatoms, much less the ecological significance of fixed nitrogen supplied from periphyton dominated by these diatom genera. More research is needed to identify the cell specific rates of N₂ fixation associated with *Epithemia* sp. and *Rhopalodia* sp. dominated assemblages.

CHAPTER FOUR

Elemental, Isotopic, and Enzymatic Evidence for Seasonally-Evolving Phosphorus Limitation in a Nitrogen-Fixing Metaphyton Community

Introduction

Primary production in freshwater aquatic ecosystems will proceed until limited by resource availability. In general, photoautotrophs become limited by either the availability of light energy or elemental resources (*e.g.* nitrogen (N) or phosphorus (P)). When elemental resources are sufficient, photoautotrophs will grow until their own biomass decreases the amount of available light energy or until nutrients have been exhausted. Schindler (1977) suggested that N resources of lakes could only be exhausted temporarily and therefore P would limit primary production in these systems over extended time scales. This hypothesis was based on the ability of planktonic heterocystous cyanobacteria to fix atmospheric N (N_2) at a rate sufficient to supplement the N supply to an ecosystem. Cyanobacterial N_2 fixation rates, and conditions controlling the establishment of cyanobacteria and initiation of N_2 fixation, have since been widely described for a variety of aquatic habitats (see reviews by Howarth et al. 1988a and 1988b) with the greatest attention given to planktonic systems (Vitousek 2002). Although Schindler's hypothesis (1977) did not hold true for estuarine and marine systems (due to trace element limitation of the nitrogenase enzyme; see Howarth et al. 1988b for details), "evolving" P-limitation in phytoplankton has often since been assumed for freshwater systems. However, the rate at which N_2 fixation can supplement ecosystem N supply has not been rigorously tested, even for planktonic systems.

Howarth et al. (1999) derived a mechanistically-based simulation model to test the interacting effects of molybdenum-limitation and zooplankton grazing on cyanobacterial exclusion from estuarine phytoplankton. Although the model could accurately predict the timing and magnitude of N_2 fixing cyanobacterial blooms in lakes, the model did not include a mass balance term that would suppress N_2 fixation in response to N accumulation. In that and subsequent papers, the authors suggested the need to refine the model to include the inherent feedback of N accumulation in the N_2 -fixing community (Howarth 1999, Vitousek et al. 2002). Although many studies have identified dissolved inorganic N (DIN) concentrations at which cyanobacterial N_2 fixation diminishes (see Horne et al. 1979, Doyle and Fisher 1994), few studies, if any, have characterized how feedback conditions such as N accumulation might suppress N_2 fixation or even stimulate P-limitation of primary production.

In wetland and shallow lake environments (lentic ecosystems), periphyton communities can dominate microbial primary production. In particular, floating periphyton mats or “metaphyton” (Stevenson 1996), which form by fragmentation of epipelagic, epilithic, or epiphytic communities, can be highly productive and radically alter ecosystem nutrient cycling (Wetzel 1996). These communities often efficiently retain and recycle sequestered nutrient stocks. However, nutrient-limitation of periphyton primary production has been widely demonstrated in enrichment experiments utilizing both whole-system (McDougal et al. 1997, Havens et al. 1999, McCormick et al. 2001) and diffusion substrate approaches (Chapter Three of this dissertation, Fairchild et al. 1985). Many of these studies demonstrated periods of N and/or P-limitation, and/or periods of N+P co-limitation. Co-limitation describes a scenario whereby only combined

enrichments of N and P (and possibly other micronutrients as well) resulted in growth stimulation. When N or both N and P are in low supply and cyanobacteria are present, N₂ fixation should commence when the energetic costs of N-limitation (*i.e.* unrealized primary production) exceed the energetic cost of N₂ fixation. When N stocks have been replenished, N₂ fixation will cease as its energetic cost begins to exceed the potential production achievable solely with DIN (Tyrell 1999).

To our knowledge, no studies have assessed the impact of N accumulation derived from N₂ fixation in lentic periphyton communities. In fact, few studies on periphyton nutrient limitation have included N₂ fixation measurements at all. Results from Chapter Three of this dissertation indicated that periphyton were increasingly N-limited and exhibited increasing N₂ fixation potential along the longitudinal axis of a created wetland. However, that study did not attempt to quantify N accumulation within the periphyton community. In a Florida Everglades metaphyton community, Inglett et al. (2004) found that N accumulated with increasing N₂ fixation throughout the summers of 1998 and 1999 and that metaphyton N content was always greatest in September when N₂ fixation rates began to decline. Although these results suggest that N₂ fixation may have been sufficient to balance metaphyton N content within one summer season, this study did not assess the limitations to metaphyton primary production over any time scale.

Interestingly, N₂-fixing metaphyton communities are conspicuous in tropical and sub-tropical marshes, such as the Florida Everglades, which are generally considered strongly P-limited. For instance, Rejmánková et al. (2000) found that P enrichment increased metaphyton primary production but that N enrichment did not change metaphyton primary production in three marshes of northern Belize. In two of the three

marshes where P enrichment increased primary production, a simultaneous increase in N_2 fixation rates and decrease alkaline phosphatase activity (APA) were observed. This suggests that P availability may have limited primary production but that P enrichment may have resulted in an N deficiency. Additionally, metaphyton N content was generally higher in the third marsh where N_2 fixation and APA did not change when enriched with P, than it was in the two marshes where N_2 fixation and APA responded to P enrichment. This further suggests that N rich metaphyton did not waste energy on N_2 fixation to bring N supply into balance, which is in general agreement with trends observed in phytoplankton (Tyrell 1999). Considered collectively, the results of Rejmánková et al. (2000) suggest that cyanobacterial N_2 fixation could have been sufficient to maintain N balance during the 10 day experimental period but the process was only initiated under relatively low metaphyton N content.

If we are to understand the role of nutrient limitations to primary production in any ecosystem, it is imperative that we have a complete understanding of the role of biological N_2 fixation in ecosystem production (Vitousek 2002). Aquatic ecosystems, and periphytic communities in particular, provide a unique opportunity to study the role of N_2 fixation in alleviating N-limitations to community production. In this study, we attempted to quantify the seasonal role of periphytic N_2 fixation in balancing community N stocks and inducing P-limitation to primary production. Specifically, the objectives of the study were to: 1) quantify metaphyton primary production along a nutrient availability gradient, 2) quantify rates of biological N_2 fixation relative to metaphyton primary production and nitrogen content, 3) quantify metaphyton phosphatase activity relative to primary

production, and 4) describe both short-term (instantaneous) and long-term (seasonal) limitations to metaphyton primary production.

Materials and Methods

Metaphyton samples were randomly collected from areas 1A, 1B, and 2B of the LWW (Figure 1.1) in May, July, and September 2004. These sampling areas were positioned along the gradient of nutrient availability which corresponds to the flow path of water (Figure 1.1; see Chapters 1 and 2). Approximately 400 cm² of metaphyton were harvested, placed into a plastic container with site water, and transported to the laboratory. Eight replicate samples were collected from each area on all dates. In the laboratory, metaphyton samples were subsampled for measurements of primary production, N₂ fixation via acetylene reduction, phosphatase activity, C, N, and P content, and $\delta^{15}\text{N}$ composition. In addition to metaphyton samples, four liters of water were collected on each sampling date to use as incubation water in laboratory bioassays for primary production and N₂ fixation. Water samples were also collected in each sampling area on a biweekly basis during the course of the study for water chemistry analysis.

Primary Production

Metaphyton primary production was determined by measuring the rate of O₂ production in high-light, low-light, and dark incubations (Wetzel and Likens 2000). Three small subsamples ($\leq 1 \text{ cm}^2$) were cut away from each metaphyton sample. Two portions were transferred into transparent BOD bottles with 300 ml site water and the third portion was transferred into an opaque BOD bottle with 300 ml site water. The concentration of dissolved O₂ was determined to a precision of 0.1 ppm before incubation

with a YSI 5000 dissolved O₂ meter. Prior to addition to BOD bottles, dissolved O₂ concentration of incubation water was reduced to ~ 3.0 ppm by bubbling with N₂ gas amended with 350 ppm CO₂. All BOD bottles were placed in a water bath incubation set to *in-situ* temperature conditions. One transparent bottle was incubated under high-light intensity (~ 390 - 460 $\mu\text{mol m}^{-2} \text{s}^{-1}$) and the other under low light intensity (~ 45 - 55 $\mu\text{mol m}^{-2} \text{s}^{-1}$). Samples were incubated until dissolved O₂ concentrations increased by ~ 1 to 1.5 ppm in low light incubations (~ 1-4 hours). Final dissolved O₂ concentration, incubation time, and photon flux density were recorded at the end of incubation. The photon flux density encountered by each incubation bottle was determined by measuring irradiance at the location of each bottle in the water bath with a LI-COR LI-250 light meter equipped with a spherical sensor. In addition to metaphyton samples, samples containing only site water from each sampling location were incubated in duplicate at each light level to account to photosynthesis and respiration by plankton.

Following incubation, the samples were filtered onto a pre-washed, -dried, and – weighed glass fiber filter then oven-dried at 60 °C overnight. The dry weight of sample was calculated as the final weight of the sample and filter minus the original filter weight. Gross photosynthesis for samples at each light level was calculated as:

$$GP = \frac{[(O_{2e} - O_{2r}) \times 0.375 \times 0.3]}{(PQ) \times (t) \times (DW)}$$

where *GP* is the rate of gross photosynthesis ($\text{mg C g DW}^{-1} \text{h}^{-1}$), O_{2e} is the change in dissolved O₂ concentration ($\text{mg O}_2 \text{L}^{-1}$) in the transparent bottle over time *t*, O_{2r} is the change in dissolved O₂ concentration ($\text{mg O}_2 \text{L}^{-1}$) in the opaque bottle over time *t*, *PQ* is the photosynthetic quotient (dimensionless constant = 1.2; see Wetzel and Likens 2000),

and DW is the dry weight of the sample in grams. The constant 0.375 represents the ratio of carbon fixed to oxygen generated during photosynthesis, and the constant 0.3 was the incubation volume in liters. Low-light photosynthetic rates were standardized to the average low-light condition by dividing the photosynthetic rate by the measured incubation light intensity and multiplying by the average low-light incubation condition ($40 \mu\text{mol m}^{-2} \text{s}^{-1}$). Standardized low-light gross photosynthesis was multiplied by 8 hours, light-saturated (determined from high-light incubations) gross photosynthesis was multiplied by 4 hours, and these rates were summed to derive an estimate of daily metaphyton primary production expressed as $\text{mg C g DW}^{-1} \text{day}^{-1}$.

N₂ fixation

Acetylene reduction was used to estimate the rate of N_2 fixation in metaphyton samples. In this assay, acetylene is reduced to ethylene by the nitrogenase enzyme at a rate proportional to the reduction of N_2 to NH_4^+ (Flett et al. 1976). The measurement is indicative of N_2 fixation in a sample at a given point in time (*i.e.* instantaneous N_2 fixation). In the laboratory, three small subsamples ($\leq 1 \text{ cm}^2$) were cut away from each metaphyton sample and placed into Popper Micromate syringes with 30 ml site water. One syringe was wrapped in foil for dark incubation while the other two were used for high-light and low-light incubations. Five milliliters of acetylene gas were injected into each syringe which was then gently mixed to allow rapid dissolution of acetylene. Syringes were incubated as described above for primary production. At the end of incubation, 15 ml of air were drawn into each syringe which was then vigorously agitated to establish equilibrium conditions of gases between aqueous and vapor phases. Water and vapor volumes were recorded to account for partitioning between phases and

ethylene concentration of the vapor was determined using a Carle AGC Series gas chromatograph (GC). The GC was equipped with a flame-ionization detector and a 1.8 m column packed with 80% Porapak N and 20% Porapak Q (80/100 mesh). The column temperature was 70 °C, helium was used as the carrier gas, and 10 ppm ethylene standards were used to calibrate the instrument daily. For each light level (dark, low-light, high-light), the hourly ethylene production rate was converted to an hourly N₂ fixation rate assuming that the production of 3 µmol ethylene was equivalent to the fixation of 1 µmol N₂ (Flett et al. 1976). Low-light N₂ fixation rates were standardized to average low-light conditions and used with light-saturated N₂ fixation rates to derive estimates of daily metaphyton N₂ fixation (µg N g DW⁻¹ day⁻¹) following the same method described above for primary production.

Phosphatase Activity

Phosphatase activity may be used as an indicator of P-limitation in metaphyton. Organisms will increase phosphatase production in an attempt to increase P availability. In this study, phosphatase activity in metaphyton was measured fluorometrically using methylumbelliferone phosphate (MUP) as a substrate. In the presence of phosphatase enzymes the phosphate group on MUP is hydrolyzed yielding methylumbelliferone (MU). MU fluoresces when irradiated at 365 nm wavelength. In samples saturated with MUP, the rate of increasing fluorescence is proportional to the rate of MU production, and subsequently, phosphatase activity (Pettersen 1980). Metaphyton subsamples were transferred into 15 ml culture tubes with 9 ml 1.2 % TRIS buffer (pH 8.3). One milliliter of 10⁻⁴ mol L⁻¹ MUP was added to each tube and samples were mixed gently. Samples were incubated at room temperature under ambient indoor lighting. Fluorescence was

measured after 5, 15, and 45 minutes on a Turner 10 AU fluorometer calibrated with 50, 100, 250, 500, and 1000 ppb MU standards. Dry weight of all samples was determined as previously described and phosphatase activity expressed as $\text{nmol P}_{\text{ase}} \text{ g DW}^{-1} \text{ min}^{-1}$.

Metaphyton Elemental and Isotopic Composition

A subsample of each metaphyton sample was oven-dried overnight at 60 °C and ground to a fine powder for determination of C, N, and P content and N isotopic composition. C and N content were determined simultaneously using a Thermo Finnigan FlashEA 1112 elemental analyzer. Phosphorus content was determined colorimetrically on a Lachat Quickchem 8500 following a 3 hour digestion in concentrated H_2SO_4 at 370 °C (Clesceri et al. 1998). Nitrogen isotopic composition was measured using a continuous flow isotope ratio mass spectrometer connected to a Carlo Erba NA1500 elemental analyzer. Measured $^{15}\text{N}/^{14}\text{N}$ ratios are expressed in delta notation (δ):

$$\delta^{15}\text{N}_{\text{sample}} = \left[\left(\frac{R_{\text{sample}}}{R_{\text{air}}} \right) - 1 \right] \times 1000$$

where $\delta^{15}\text{N}_{\text{sample}}$ is the isotopic composition of the sample expressed in units of per mil (‰), R_{sample} is $^{15}\text{N}/^{14}\text{N}$ ratio measured in the sample, and R_{air} is the $^{15}\text{N}/^{14}\text{N}$ ratio of air.

Contribution of N_2 fixation to Total N Uptake

We estimated the contribution of N_2 fixation to total N uptake by metaphyton using two separate methods: 1) acetylene reduction measurements with gross N assimilation estimates, and 2) $\delta^{15}\text{N}$ composition of metaphyton. Estimates from acetylene reduction assays were derived by dividing the rate of N_2 fixation measured by acetylene reduction by the rate of gross N assimilation. Gross N assimilation was estimated by

multiplying the rate of primary production of a sample by its measured ratio of N:C. The quotient of N_2 fixation, expressed as $\text{mg N g DW}^{-1} \text{ h}^{-1}$, and gross N assimilation, also expressed as $\text{mg N g DW}^{-1} \text{ h}^{-1}$, is the percent contribution of N_2 fixation to total N uptake.

The use of $\delta^{15}\text{N}$ as an indicator of the contribution of N_2 fixation to total N uptake is based on the general isotopic difference between atmospheric N_2 and DIN. Atmospheric N_2 has a constant N isotopic composition. When air is used as the reference standard in mass spectrometry (as is usually done for N), $\delta^{15}\text{N}$ of atmospheric N_2 is 0 ‰. The isotopic composition of DIN in freshwaters however, is usually relatively heavy ($\delta^{15}\text{N} \approx 5 - 15$ ‰; Heaton 1986). Because N isotopic composition of autotrophs will usually reflect the isotopic composition of their inorganic N source (Lajtha and Marshall 1994), it is often possible to estimate the relative contribution of DIN and atmospheric N_2 to autotrophic communities that can utilize either N source by measuring the N isotopic composition of the community itself (Gu and Alexander 1993; France et al. 1998).

For our purposes, a two-end member mixing model was developed to predict the relative contribution of N_2 fixation to total N uptake by metaphyton. The model was constructed as follows:

$$\delta^{15}N_{\text{periphyton}} = \left[(C_{N_2}) \times (\delta^{15}N_{N_2} + f_{N_2}) \right] + \left[(C_{\text{DIN}}) \times (\delta^{15}N_{\text{DIN}} + f_{\text{DIN}}) \right]$$

where $\delta^{15}N_{\text{metaphyton}}$ is the N isotopic composition of metaphyton, C_{N_2} is the percent contribution of atmospheric N_2 to total nitrogen uptake by metaphyton, $\delta^{15}N_{N_2}$ is the isotopic composition of N_2 (0 ‰), and f_{N_2} is the fractionation value associated with N_2 fixation (assumed to be -2.0 ‰ based on the value of fractionation reported for cyanobacterial cultures using N_2 as their sole source of N (Gu and Alexander 1993)),

respectively. C_{DIN} is the percent contribution of DIN to total N uptake which was set equal to $1 - C_{N_2}$ in this mixing model. $\delta^{15}N_{DIN}$ is the isotopic composition of DIN in waters flowing into the LWW (assumed to be 9.7 ‰; from Dworkin 2003), and f_{DIN} is the fractionation value associated with DIN uptake. In general, fractionation with DIN uptake will occur only when DIN is in relatively abundant supply and should approach zero when DIN availability is at limiting or near-limiting levels (see Fogel and Cifuentes 1993). Because DIN has been shown to limit metaphyton production in the LWW (Chapter Three), f_{DIN} was assumed to be 0 ‰ in this study.

Metaphyton $\delta^{15}N$, along with the previously stated assumptions, were used to solve the mixing model for the percent contribution of N_2 fixation to total N uptake (C_{N_2}). An important assumption inherent within the model was that N was not efficiently retained and recycled within the metaphyton community. If this assumption was correct, the percent contribution of N_2 fixation to total N uptake derived from the isotopic model (C_{N_2}) should be equal to the instantaneous estimate derived from acetylene reduction measurements and gross N assimilation estimates. Predicted values of C_{N_2} calculated by the isotope mixing model were compared to instantaneous estimates using linear regression analysis in Sigma Plot 9.0 (Sigma Plot 2005).

Water Chemistry

Biweekly water chemistry samples were collected in acid-washed 1 liter polyethylene bottles and returned to the laboratory for analysis of nitrite-nitrogen plus nitrate-nitrogen (NO_2-N+NO_3-N), ammonia-nitrogen (NH_4-N), and soluble reactive phosphorus (SRP). NO_2-N+NO_3-N was determined colorimetrically on a Beckman DU 650 spectrophotometer following cadmium reduction (Clesceri et al. 1998). NH_4-N and

SRP were also determined colorimetrically using the phenate and molybdenum blue methods, respectively (Clesceri et al. 1998). Water temperature, specific conductance, and pH were measured during sample collection with a YSI 6600 multiparameter datasonde.

Results

Water Chemistry

Average water chemistry conditions observed during the study are provided in Table 4.1. Conductivity was generally greatest at site 1A (wetland inflow), diminished at site 1B, and lowest at 2B, except in September when this pattern was reversed. Both $\text{NO}_2\text{-N} + \text{NO}_3\text{-N}$ and $\text{NH}_4\text{-N}$ followed a similar pattern of decreasing concentration along the flow path of water. However, this pattern was not observed in SRP. In May and July, SRP concentrations were generally similar amongst all sites. In September, average SRP concentration was highest at site 1B, followed by sites 1A then 2B. However, all

Table 4.1. Water chemistry values for sites on each sampling date (mean \pm SD; n=2 for all events).

Site	Water Temp($^{\circ}\text{C}$)	Spec Cond ($\mu\text{S cm}^{-1}$)	pH	$\text{NO}_2\text{-N} + \text{NO}_3\text{-N}$ (ppb)	$\text{NH}_4\text{-N}$ (ppb)	DIN (ppb)	SRP (ppb)	DIN:SRP
May								
1A	25 \pm 2	736 \pm 59	7.8 \pm 0.0	194 \pm 6	22 \pm 1	217 \pm 5	4 \pm 3	84 \pm 69
1B	25 \pm 3	715 \pm 51	7.9 \pm 0.2	44 \pm 29	19 \pm 6	63 \pm 23	6 \pm 4	14 \pm 12
2B	26 \pm 3	642 \pm 65	7.8 \pm 0.2	6 \pm 2	14 \pm 11	20 \pm 10	5 \pm 4	5 \pm 2
July								
1A	30 \pm 1	708 \pm 344	8.0 \pm 0.3	227 \pm 136	69 \pm 4	296 \pm 132	8 \pm 4	38 \pm 4
1B	27 \pm 0	665 \pm 344	8.0 \pm 0.3	42 \pm 8	44 \pm 27	87 \pm 19	11 \pm 8	12 \pm 10
2B	29 \pm 0	592 \pm 399	8.0 \pm 0.7	5 \pm 3	15 \pm 3	21 \pm 1	4 \pm 3	7 \pm 5
September								
1A	26 \pm 0	490 \pm 12	8.1 \pm 0.3	210 \pm 89	74 \pm 20	284 \pm 69	3 \pm 0	30 \pm 115
1B	23 \pm 1	501 \pm 83	7.8 \pm 0.6	100 \pm 112	14 \pm 13	115 \pm 125	8 \pm 5	12 \pm 10
2B	24 \pm 1	507 \pm 83	7.8 \pm 1.1	6 \pm 3	8 \pm 7	15 \pm 4	1 \pm 0	11 \pm 4

differences observed in SRP concentrations between sites were minor when compared to differences observed in dissolved inorganic nitrogen ($\text{DIN} = \text{NO}_2\text{-N} + \text{NO}_3\text{-N} + \text{NH}_4\text{-N}$). The ratio of DIN:SRP consistently decreased along the flow path of water during all months.

Metaphyton Primary Production and Enzyme Activity

Metaphyton primary production did not follow a consistent pattern among sites and dates (Table 4.2). In May, average primary production was at site 1A, lower at site 1B, and lowest at site 2B. However, this trend disappeared in July when highest rates were observed at site 1B, followed by 1A then 2B. Site 1B remained the most productive site in September, but site 2B displayed higher primary production than site 1A during this month. N_2 fixation measured using acetylene reduction (AR) was not detected at site 1A on any sampling event, but was always measurable at sites 1B and 2B (Table 4.2). N_2 fixation measured by AR was always light-dependent (Figure 4.1). Furthermore, the N_2 fixation rate was negatively correlated with average DIN concentration in the water column (Figure 4.2A) which resulted in a consistent spatial pattern of decreasing DIN and increasing metaphyton N_2 fixation along the flow path of water. Phosphatase activity was always greatest at site 2B followed by site 1A then site 1B, except in September when phosphatase activity at site 1A exceeded that observed at site 2B (Table 4.2). In general, phosphatase activity was negatively correlated with SRP concentration in the water column (Figure 4.2B).

Table 4.2. Primary production, enzyme activities, elemental composition, and isotopic composition of metaphyton community for sites on each sampling date. All values are mean \pm SD. For all values, n=8 except where indicated parenthetically.

Month Site	Primary Production (mg C g DW ⁻¹ day ⁻¹)	Acetylene Reduction ¹ (μ g N g DW ⁻¹ day ⁻¹)	Phosphatase Activity (nmol P _{ase} g DW ⁻¹ min ⁻¹)	Carbon (wt. %)	Nitrogen (wt. %)	Phosphorus (wt. %)	$\delta^{15}\text{N}$ (‰; Air)
May							
1A	39.0 \pm 12.0 (7)	BDL ²	60.5 \pm 16.6	20.9 \pm 3.3	1.21 \pm 0.31	IS ³	10.5 \pm 1.2
1B	22.0 \pm 11.7	42.6 \pm 33.6	41.6 \pm 21.2 (7)	22.0 \pm 3.2	1.08 \pm 0.20	IS ³	7.3 \pm 1.0
2B	10.6 \pm 3.2	221.7 \pm 38.1	104.4 \pm 24.3 (4)	21.0 \pm 1.7	1.41 \pm 0.12	IS ³	3.1 \pm 0.5
July							
1A	65.0 \pm 23.8	BDL ²	23.9 \pm 12.6 (7)	23.3 \pm 3.9	1.86 \pm 0.45	0.26 \pm 0.10	12.2 \pm 1.2
1B	82.3 \pm 36.2 (7)	67.8 \pm 106.3 (7)	14.2 \pm 5.1 (7)	26.4 \pm 2.6 (7)	1.93 \pm 0.51 (7)	0.27 \pm 0.08 (7)	9.2 \pm 0.6 (7)
2B	41.4 \pm 16.3	384.9 \pm 284.8	76.4 \pm 33.8	24.3 \pm 1.3	1.80 \pm 0.15	0.18 \pm 0.05	3.4 \pm 0.5 (7)
September							
1A	27.1 \pm 10.5 (7)	BDL ²	95.7 \pm 50.8	19.9 \pm 2.1	1.49 \pm 0.20	0.10 \pm 0.02	9.6 \pm 0.9
1B	107.3 \pm 46.5	6.1 \pm 6.3	31.9 \pm 15.1	27.6 \pm 4.1	2.28 \pm 0.53	0.21 \pm 0.05	8.5 \pm 0.4
2B	42.2 \pm 6.7	60.7 \pm 32.6	77.2 \pm 25.0	32.1 \pm 1.8	2.02 \pm 0.27	0.16 \pm 0.01	1.2 \pm 0.6

¹N₂ fixation determined from acetylene reduction assays with intact metaphyton.

²BDL – below detection level (1 ppm ethylene).

³IS – Insufficient sample for phosphorus analysis.

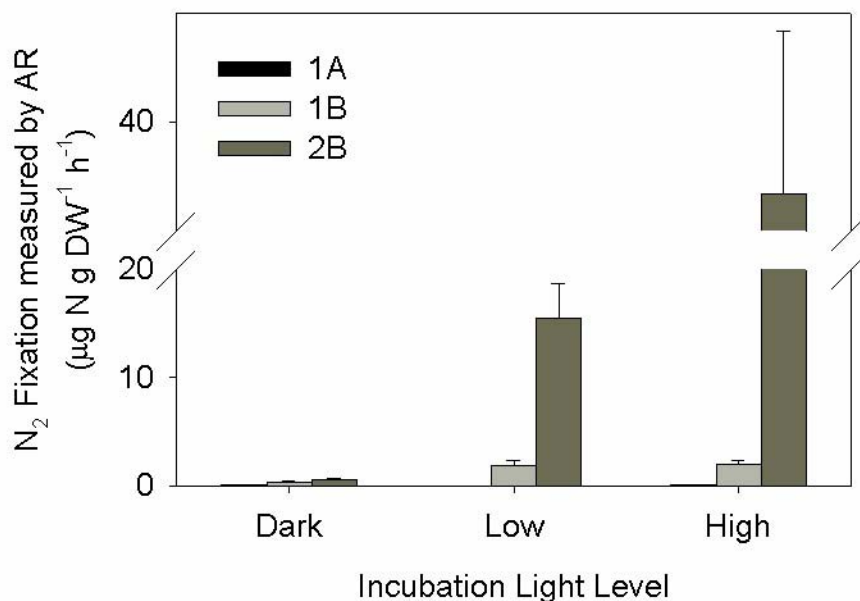


Figure 4.1. N₂ fixation measured by acetylene reduction (expressed in hourly units) at each incubation light level for the entire study. Bars indicate mean rate determined at each site for the entire summer (\pm SE).

Metaphyton Elemental and Isotopic Composition

The elemental composition of metaphyton exhibited both spatial and temporal heterogeneity (Table 4.2). Carbon content at all sites was relatively low in May but generally increased through July and September. The only exception was at site 1A where C content appeared to slightly decrease from July to September. Nitrogen content followed a temporal pattern almost identical to C. Nitrogen content increased throughout the summer at all sites except 1A where N content was greatest in July but slightly decreased by September. Insufficient sample was collected for the determination of P content in the May samples. Data from the remainder of the summer show that metaphyton P content was greater in July than in September for all sample sites. Elemental composition of metaphyton did not appear to follow a spatial pattern similar to

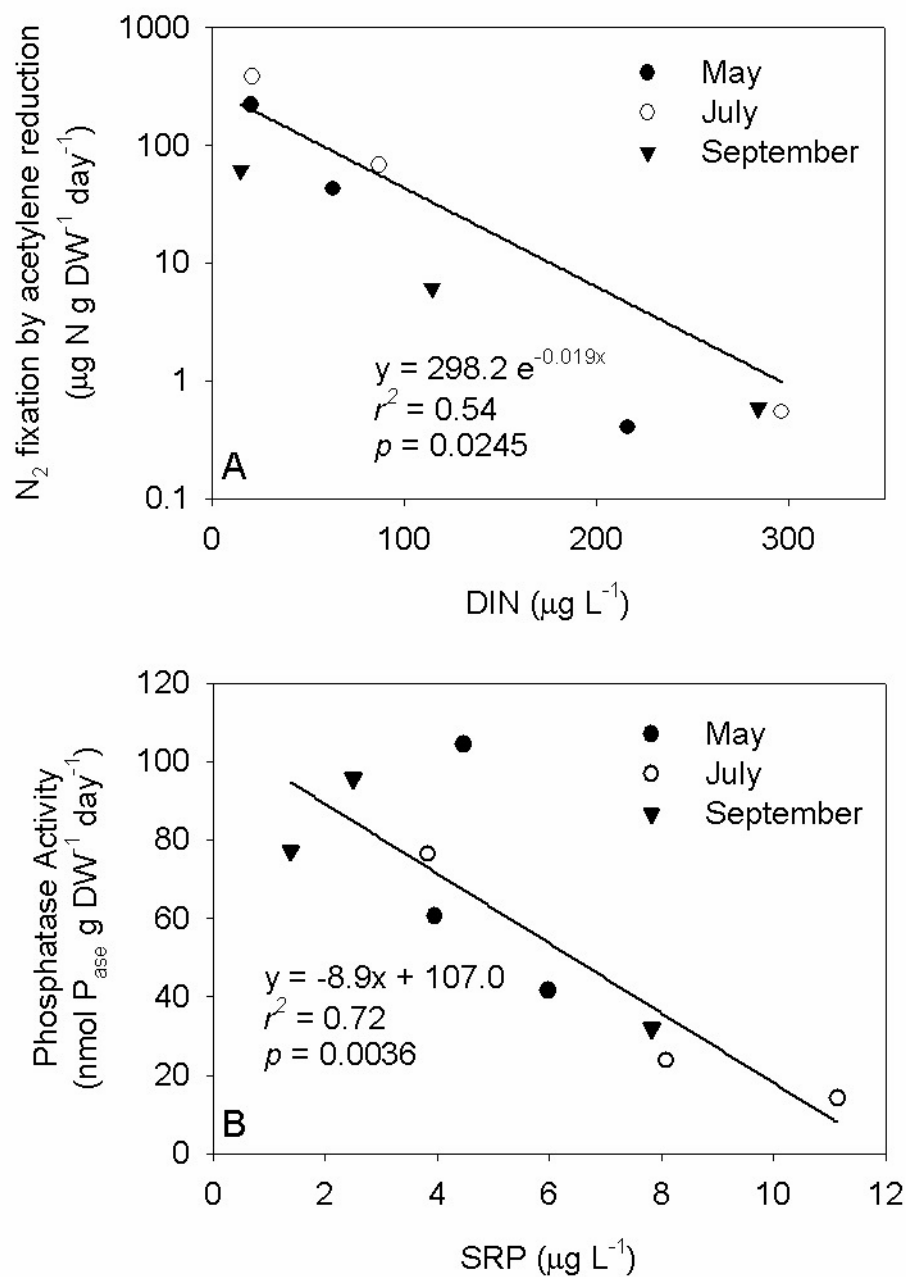


Figure 4.2. Enzymatic activity versus nutrient concentrations for each sampling event. A) Daily N_2 fixation, measured by acetylene reduction, versus mean DIN concentration in the water column. B) Phosphatase activity versus mean SRP concentration in the water column.

the distribution of dissolved inorganic nutrients except in September when metaphyton C content was negatively correlated with mean DIN and metaphyton P content was positively correlated with mean SRP (Tables 4.1 and 4.2). The carbon to nitrogen ratio

(C:N) of metaphyton was consistently between 12 and 15 except at sites 1A and 1B in May where values ranged between 18 and 21 (Figure 4.3). The ratio of carbon to phosphorus (C:P) and nitrogen to phosphorus (N:P) tended to exhibit more heterogeneity. In July, C:P and N:P were similar at sites 1A and 1B but higher at site 2B (Figure 4.3). This difference was due to diminished metaphyton P content at site 2B in July (Table 4.2). In September, C:P and N:P were greatest at site 1A, followed by site 2B then site 1B (Figure 4.4). Again, these differences were primarily the result of the relatively large difference in metaphyton P content observed between sites (Table 4.2). The N:P ratio in metaphyton was not strongly related to the ratio of DIN:SRP in July but appeared to be more positively correlated in September (Figure 4.3 and Table 4.1).

Contribution of N_2 fixation to Total N Uptake

Estimates of the contribution of N_2 fixation to total N uptake determined by AR assays and $\delta^{15}N$ composition of metaphyton are shown in Figure 4.4. In general, $\delta^{15}N$ derived values tended to overestimate the percent contribution of N_2 fixation as measured via AR. Although a strong correlation between estimates existed in May ($r^2 = 0.88$; Figure 4.4), $\delta^{15}N$ derived values were 1.4 times greater than estimates derived from AR. Furthermore, the correlation between these estimates was greatly reduced in July and September. The poor correlation was the result of greatly reduced estimates of the percent contribution of N_2 fixation determined via AR (0 – 30%) but relatively high estimates from the $\delta^{15}N$ derivation, particularly from site 2B (Figure 4.4).

Interestingly, both AR and $\delta^{15}N$ derived estimates demonstrated unique relationships with metaphyton N content (Figure 4.5). Metaphyton N content and AR derived estimates appeared to correlate on a temporal scale. In particular, AR derived

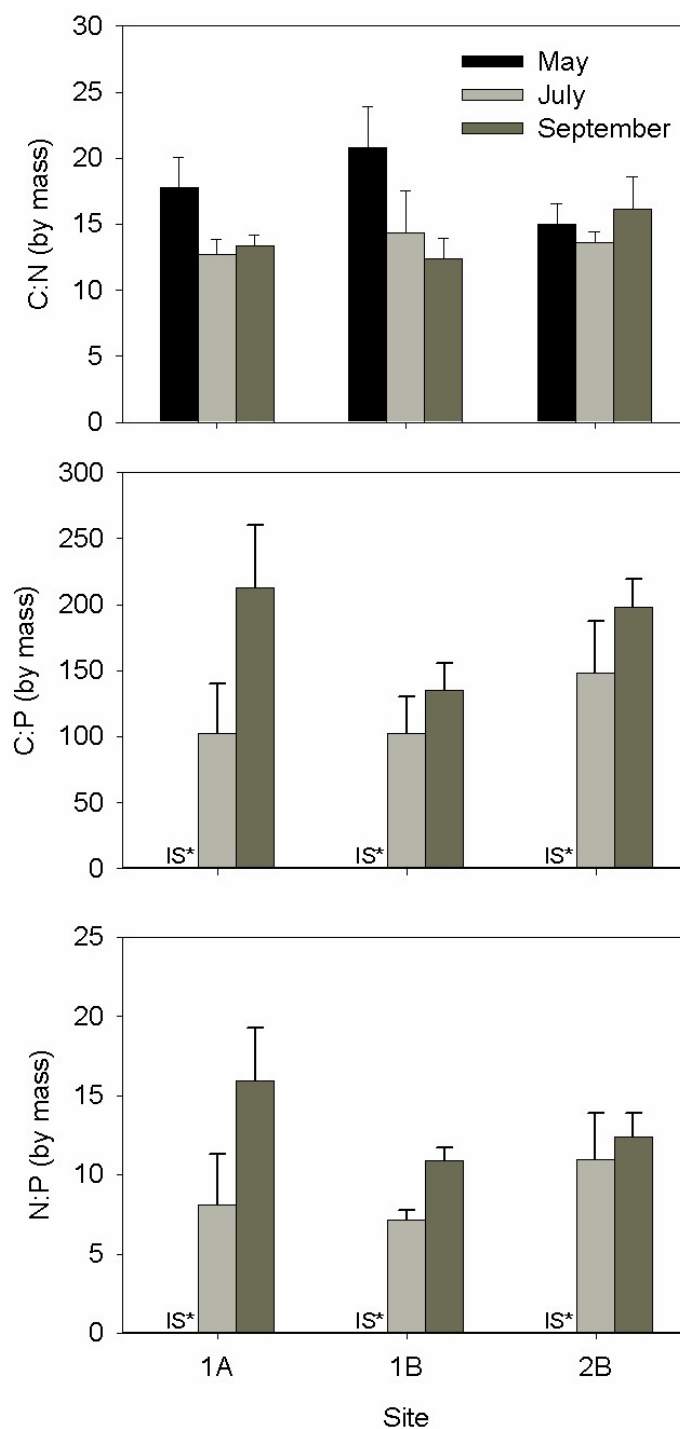


Figure 4.3. Elemental ratios of metaphyton for each sampling event (mean \pm SD; $n = 7-8$, see Table 2 for details on number of samples). Black bars represent samples collected in May 2004, light gray bars represent samples collected in July 2004, and medium gray represent samples collected in September 2004. Insufficient sample was collected during May 2004 for phosphorus determination (IS*), therefore, C:P and N:P values are not available for that sampling event.

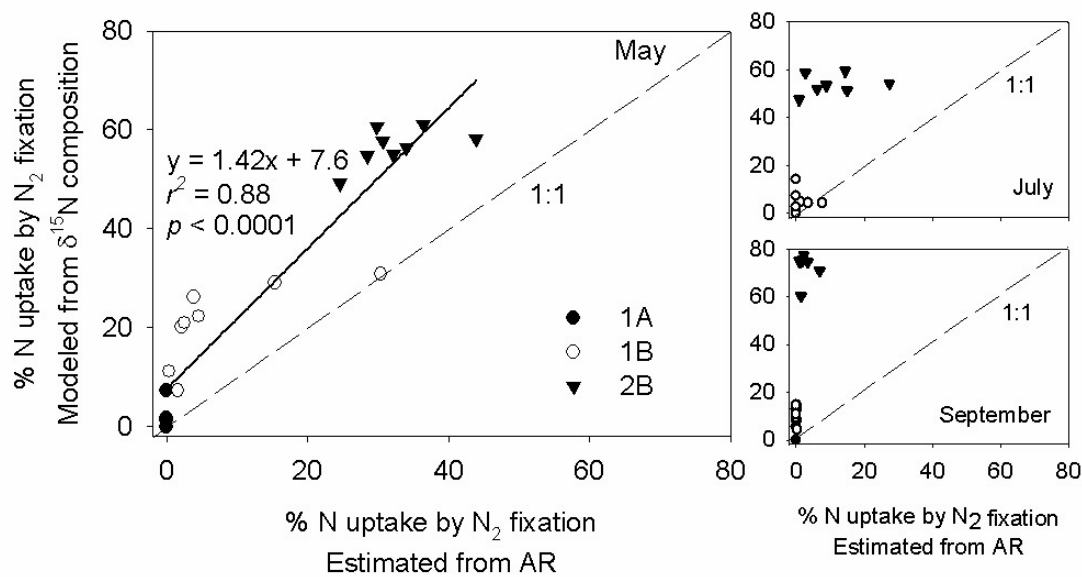


Figure 4.4. Measured versus modeled percentage of N uptake derived from N_2 fixation. Measured values determined by dividing acetylene reduction estimates of N_2 fixation by estimates of gross N uptake. Modeled values determined from isotope mixing model. Black circles represent samples from area 1A, white circles represent samples from area 1B, and black triangles represent samples from 2B. The mixing model estimates generally agreed with empirical estimates from acetylene reduction in May only. In July and September, modeling with $\delta^{15}N$ tended to overestimate the instantaneous contribution of N_2 fixation to total N uptake.

estimates and metaphyton N content were positively correlated in May, but negatively correlated in July and September (Figure 4.5A). Percent contribution of N_2 fixation derived from $\delta^{15}N$ appeared to correlate with metaphyton N content on a temporal and spatial scale. At site 1B in May, the relationship between metaphyton N content and percent contribution of N_2 fixation derived from $\delta^{15}N$ was positive and could be modeled on the same regression line with observations from all months at site 2B (Figure 4.5B). The correlation between these variables was less pronounced at site 1B in July and September and at site 1A during all sampling events (Figure 4.5B).

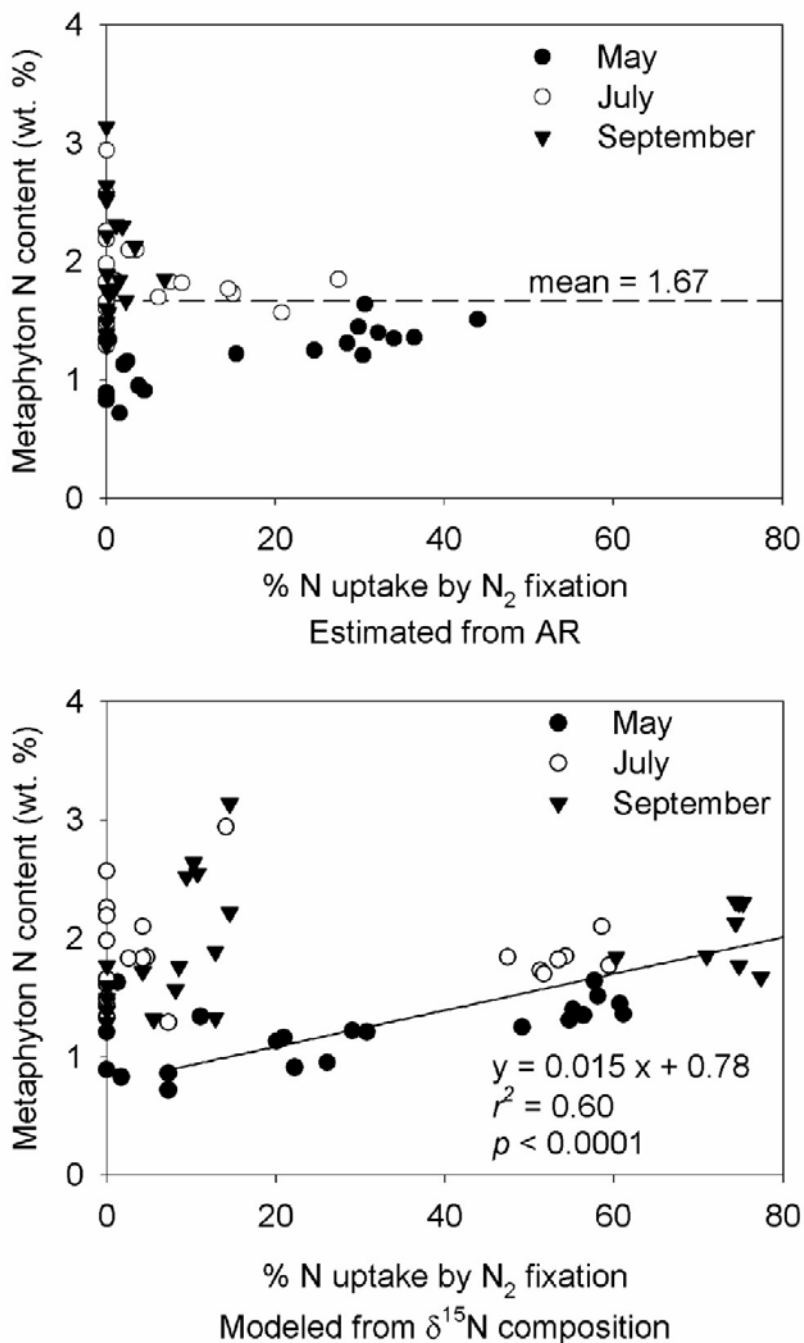


Figure 4.5. Relationship between percent contribution of N_2 fixation to total N uptake, and metaphyton N content. In both plots, black circles represent samples collected in May 2004, white circles represent samples from July 2004, and black triangles represent samples from September 2004. A) Percent contribution of N_2 fixation derived from acetylene reduction and gross N assimilation estimates. B) Percent contribution of N_2 fixation derived from isotope ($\delta^{15}N$) mixing model. Regression line derived for data collected in area 2B and area 1B in May 2004. See discussion for details of these groupings.

Correlates of Metaphyton Primary Production

In May, metaphyton primary production appeared to correlate with water column DIN concentrations (Tables 4.1 and 4.2). However, this relationship did not exist in July or September. In these months, metaphyton primary production was more generally correlated (inversely) with phosphatase activity, and also metaphyton P content in September (Table 4.2). When normalized to metaphyton N content and considered over the entire summer, metaphyton primary production was strongly inversely correlated with phosphatase activity (Figure 4.6).

Discussion

Results of this study demonstrate the seasonal evolution of P-limitation in a lentic metaphyton community. Metaphyton primary production appeared to be N-limited during spring but became P-limited, and remained so, throughout the summer. This was indicated by several relationships between primary production and indicators of nutrient stress. For instance, average primary production was inversely correlated with average DIN in May but became more generally correlated with phosphatase activity in July and September (Tables 4.1 and 4.2). This switch between DIN correlation and phosphatase correlation with primary production corresponded to a 1.5 to 1.6 fold increase in average metaphyton N content from May to July and September, respectively (Table 4.2). Furthermore, the percent contribution of N₂ fixation to total N uptake, estimated via AR, was generally highest in May and decreased iteratively in July and September. This suggests that periphytic cyanobacteria may have down regulated N₂ fixation in response to accumulating N. In fact, this trend is supported by the N isotopic signature of the metaphyton. Metaphyton $\delta^{15}\text{N}$ composition retained the atmospheric signature at site 2B

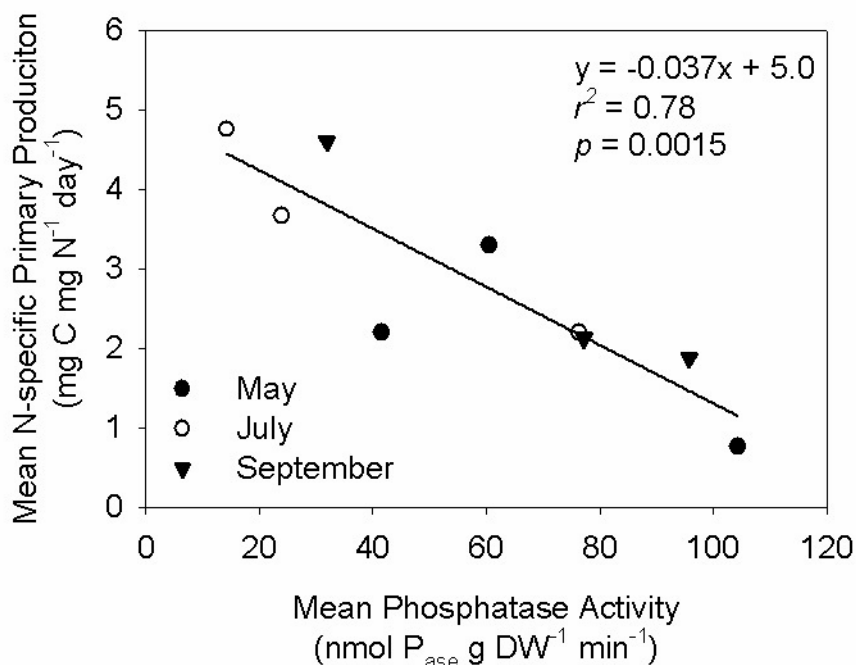


Figure 4.6. Relationship between mean phosphatase activity and mean nitrogen-specific primary production from all sampling events.

even when N₂ fixation measured by AR had diminished (Table 4.2). However, lighter isotopic values, and subsequently larger isotopic estimates of the percent contribution of N₂ fixation to total N uptake (> 20 %), were generally correlated with higher metaphyton N content (Figure 4.5B). We submit that the accumulation and retention of N in the metaphyton mats eventually resulted in P-limited primary production. Interestingly, when primary production was normalized to N content, a strong inverse correlation with phosphatase activity was apparent across all sampling events (Figure 4.6). Therefore, short-term correlates of nutrient limitation (instantaneous from each month) indicate a springtime period of N-limitation followed by an extended period of P-limitation. However, over a seasonal time scale (all months), N-specific primary production appeared limited by P availability (Figure 4.6).

Elemental balance within the metaphyton mats may also indicate nutrient limitation status. Metaphyton C:N was only elevated at sites 1A and 1B in May, and appeared relatively balanced during the remainder of the growing season (Figure 4.3). Because stoichiometric theory tells us that nutrient limitation of photoautotrophs is generally coupled with an increase in the C:nutrient ratio (Sterner and Elser 2002), metaphyton C:N indicate that N may only have been limiting in May. Furthermore, C:P appears to have increased at all sites from July to September. Unfortunately, it remains unknown whether C:P would have been lowest in May because insufficient sample was available for the determination of P content.

The accumulation and retention of N appears to be a critical factor in controlling primary production and inducing P-limitation. Nitrogen availability was primarily driven by DIN supply and secondarily driven by N₂ fixation. For instance, N₂ fixation was never observed nearest inflowing waters (site 1A) where DIN was relatively high. However, N₂ fixation appeared increasingly important at downstream sites where DIN concentrations were greatly reduced (Tables 4.1 and 4.2; Figure 4.2A). Furthermore, N₂ fixation appeared to balance metaphyton N content on the scale of weeks in the downstream, most N poor, areas.

Estimates of the percent contribution of N₂ fixation to total N uptake can be derived using both AR (coupled with estimated of gross N assimilation) and metaphyton $\delta^{15}\text{N}$ composition. Recent studies have attempted to characterize the importance of lentic metaphyton N₂ fixation using the N isotopic method with somewhat mixed results. Inglett et al. (2004) found that average AR rates correlated well with average $\delta^{15}\text{N}$ composition in an Everglades metaphyton community. However, measurements in that study were

limited to one location over a two-year period and potential differences between individual measurements (AR versus $\delta^{15}\text{N}$) were not considered. Rejmánková et al. (2004) did use individual measurements in an attempt to predict N_2 fixation rates (derived using AR) from $\delta^{15}\text{N}$ signatures in a number of tropical wetland metaphyton communities. Although their correlation showed some promise, the dataset had poor resolution when N_2 fixation rates were low. The authors ultimately found that a simple threshold in metaphyton $\delta^{15}\text{N}$ was the most robust indicator of either high or low N_2 fixation.

In this study, we used a mechanistic N isotope approach (*i.e.* a two-end member mixing model) to develop estimates of the percent contribution of N_2 fixation to total N uptake. We hypothesized that the percent contribution of N_2 fixation to total N uptake modeled from isotopic measurements would equal instantaneous estimates derived from AR and gross N assimilation if internal N recycling in the metaphyton community was negligible. When compared with empirical estimates of the percent contribution of N_2 fixation (from AR), $\delta^{15}\text{N}$ estimates tended to overestimate the importance of N_2 fixation. Although a good correlation between estimates was observed in May samples, the isotope model overestimated the percent contribution of N_2 fixation to total N uptake by almost 1.5 fold (Figure 4.4). Furthermore, isotope model values for site 2B were grossly overestimated in July and September (Figure 4.4). We propose that this overestimation was caused by the accumulation of atmospherically derived N in the metaphyton through time. This accumulation violated the model assumption of negligible N recycling and therefore caused overestimates of the percent contribution of N_2 fixation. Although not explicitly measured in this study, metaphyton communities are known to retain and

recycle nutrients with great efficiency (Borchardt 1996). Because instantaneous N_2 fixation (AR) appeared to contribute a large amount of N to metaphyton at site 2B in spring and early summer (Figure 4.5A), accumulation and recycling of this fixed N may have caused metaphyton $\delta^{15}N$ to continually reflect a high contribution of N_2 fixation throughout the summer even though instantaneous N_2 fixation rates (AR) had diminished (Figure 4.4). Therefore, metaphyton $\delta^{15}N$ comprises a time-integrated estimate of the relative contributions of DIN and N_2 fixation to the N content of the community. Although this inherent characteristic was suggested in early comparisons between N_2 fixation measured by AR and estimates from $\delta^{15}N$ composition (Gu and Alexander 1993; France et al. 1998), recent studies have not considered this potential inconsistency and subsequently have generated mixed results on the usefulness of the technique (Rejmánková et al. 2004; Inglett et al. 2004).

Interestingly, relatively low $\delta^{15}N$ (*i.e.* relatively high percent contribution of N_2 fixation total N uptake) was always correlated with metaphyton N content when instantaneous N_2 fixation (measured by AR) was contributing to N content. For example, metaphyton N at site 2B during all months and at site 1B in May increased by 0.015 % for every 1 % increase in the contribution of N_2 fixation to total N uptake (see regression in Figure 4.5B). This trend was not apparent at site 1B in July and September and never apparent at site 1A. This evidence in particular, along with reduced N_2 fixation (AR) observed with increasing metaphyton N content, suggest the importance of accumulating atmospherically derived N to alleviate N deficiency in this metaphyton community. Although an N rich lifestyle could be expected when N_2 fixers are present (Gu and

Alexander 1993), our results indicate that fixed N may be efficiently retained by a metaphyton community long after instantaneous N₂ fixation ceases.

Conclusions

Results of this study suggest that metaphyton communities can rapidly fix and accumulate significant amounts of atmospheric N₂, thereby driving the community toward P-limitation. It appears that the buildup and retention of N to a critical threshold can occur within a matter of weeks during the early growing season, at least within the warm-temperate zone similar to this study. When N content exceeds a critical threshold, instantaneous N₂ fixation rates fall rapidly but isotopic composition continues to reflect an atmospheric N source. We hypothesize that sustained $\delta^{15}\text{N}$ in the range of atmospheric N₂ was caused by the efficient retention and recycling of fixed N₂. Efficient retention brought metaphyton N content into stoichiometric balance causing N-specific primary production to be limited by P availability. This study confirms the importance of fixed N₂ as an N source to metaphyton community production and provides an example of seasonally-evolving P-limitation in a shallow aquatic ecosystem.

CHAPTER FIVE

Coupled Photosynthesis and Heterotrophic Bacterial Biomass Production in a Nutrient-Limited Wetland Metaphyton¹

Introduction

Floating periphyton mats, also termed microbial mats (Paerl and Pinckney 1996), metaphyton (Stevenson 1996), or cyanobacterial mats (Rejmánková et al. 2004), are often conspicuous features of wetland and shallow lake environments. These consortia can provide key ecosystem services such as fixing large quantities of atmospheric N₂ (Rejmánková and Komárková 2000; Inglett et al. 2004), seasonal nutrient storage and retention (Scinto and Reddy 2003), and contributing to basal resources in the food web (Lamberti 1996). However, many aspects on the functioning of metaphyton, and periphyton in general, have received little attention relative to the functioning of their pelagic counterparts (Vadeboncoeur et al. 2002).

Most studies on photosynthetic-bacterial interactions in aquatic systems have focused attention on bacterioplankton use of extracellular organic carbon (EOC) generated by phytoplankton during photosynthesis (i.e. Cole et al. 1982; Coveney and Wetzel 1989; Medina-Sánchez 2004). Few studies have explored similar relationships in periphyton. Murray et al. (1986) were among the first to demonstrate increased rates of bacterial DNA synthesis in response to photosynthetically derived EOC in periphyton. In another study, Neely and Wetzel (1995) demonstrated a positive correlation between photosynthesis (PS) and bacterial biomass production (BBP) in periphyton using short-

¹Previously published in *Aquatic Microbial Ecology* 45(1): 69-77. 2006. Scott JT, Doyle RD. Reproduced with permission.

term incubations (2 hours) across a range of photosynthetically active irradiance (20-400 $\mu\text{mol m}^{-2} \text{s}^{-1}$). Espeland et al. (2001) found that even low rates of PS under low light intensities ($< 100 \mu\text{mol m}^{-2} \text{s}^{-1}$) could substantially increase the rate of BBP in periphyton after long-term exposure (8 hours or more). Other studies have focused attention on the influence of periphytic PS on bacterial enzyme activity (Espeland et al. 2001; Francouer and Wetzel 2003), providing further evidence for the coupling of these processes. The majority of these studies however, were carried out in the laboratory in nutrient-rich media and therefore did not consider any community interactions (commensal, mutual, or competitive) relative to nutrient stress.

Some studies on photosynthetic-bacterial interactions in periphyton have focused on periods when nutrient resources for periphyton were high as a result of decaying macrophyte biomass (Neely 1994; Neely and Wetzel 1997), or have focused on attachment substrate without regard to nutrients supplied by the substrate (Stanley et al. 2003). Furthermore, studies that have tested the effect of nutrient supply to periphyton communities have assumed that interactions between photoautotrophs and bacteria occur, but did not explicitly examine any relationships between PS and BBP (Haglund and Hillebrand 2005). Although it has been established that phytoplankton and bacterioplankton may compete for important nutrient resources in oligotrophic lakes (i.e. Chrzanowski et al. 1996), further research is needed to assess the type and degree of interaction (if any) displayed by photoautotrophs and bacteria in nutrient-limited metaphyton communities.

With respect to nutrient supply, any competitive, commensalistic, or mutualistic interaction between periphytic photoautotrophs and bacteria are poorly understood.

Recently, Sharma et al. (2005) used microscopic evidence on the spatial segregation of chlorophyll and phosphatase in Everglades metaphyton to propose a cooperative interaction between photoautotrophs and bacteria in that system. They suggested that bacterial phosphatase activity might increase the availability of inorganic phosphorus to photoautotrophs, thereby increasing the rate of P-limited PS and subsequently the supply of “photosynthetically fixed carbon” to bacteria. However, this hypothesis contrasts the findings and interpretations of other researchers. Specifically, Espeland and Wetzel (2001) suggested that periphytic bacteria regulated their phosphatase activity in response to photosynthetic production of EOC in order to maximize their competitive ability for phosphates.

In this study, we attempted to identify the degree of coupling between photosynthesis and heterotrophic bacterial biomass production in a nutrient-limited metaphyton. To that end, we measured PS and BBP simultaneously in a series of light and nutrient enrichment experiments. The objectives of the study were to 1) identify the degree of correlation between PS and BBP across a range of photosynthetically active irradiance in a nutrient-limited metaphyton community and, 2) determine the simultaneous response of PS and BBP to increased supply of N and P.

Materials and Methods

In this study, metaphyton samples from the N-limited region of the LWW (Station 2B; Figure 1.1) were collected by cutting approximately 100 cm² of material from the center of an intact mat and returned to the laboratory for experiments and radioassays. Samples were collected on 27 June 2005, 9 July 2005, and 13 July 2005 for use in a methodological experiment (¹⁴C retention by photoautotrophs), a light saturation, and a

nutrient enrichment experiment, respectively. Details of each of these experiments are provided below, following a brief description of the dual-labeled radioassay.

Dual-Labeled Radioassay

We used a dual-labeled radioassay similar to that of Neely and Wetzel (1995) to simultaneously measure PS and BBP in metaphyton. PS was measured by ^{14}C -bicarbonate uptake and BBP was measured by ^3H -L-leucine incorporation into protein. Assays were conducted under in-situ temperature conditions in the laboratory. Metaphyton samples were subdivided into replicate samples by cutting small portions (~10 mg dry weight) from the surface of a mat and transferring the material into borosilicate scintillation vials with Teflon open-top caps. Each vial was filled to capacity (~23.5 ml) with filtered site water. Replicate samples were acclimated to incubation conditions for 1 hour prior to the addition of any isotope to establish experimental conditions (details of incubation conditions provided in experiment descriptions below). At the end of this acclimation period, 50 μl of ^{14}C -bicarbonate (final activity 0.0125 $\mu\text{Ci ml}^{-1}$) were injected into each vial and incubations were continued for a period of 1.5 hours. After that time, 20 μl of 500 nmol L^{-1} ^3H -L-leucine (3.4 nmol L^{-1} labeled, 496.6 nmol L^{-1} unlabeled; specific activity = 0.85 $\mu\text{Ci nmol leucine}^{-1}$) were injected into each vial and incubations were continued for 30 minutes. Previous experiments on metaphyton from this wetland indicated 500 nmol L^{-1} was sufficient to saturate leucine incorporation into protein (Scott, unpubl.). Both formalin killed controls and dark incubations were used in all experiments to account for background retention of both isotopes. At the end of the incubation period, assays were stopped in all samples by the addition of formalin to a final concentration of 2%. The precipitation of proteins for bacterial production

measurements followed the method of Buesing and Gessner (2003). Trichloroacetic acid (TCA) was added to each vial to a final concentration of 5% by volume and samples were homogenized. Samples were placed on ice for 1 hour to allow protein precipitation by cold TCA. A 10 ml aliquot of each sample was then filtered onto a pre-washed, dried, and weighed glass fiber filter. Filters were then dried at 60 °C for one hour then re-weighed to determine the dry weight (DW) of material used in the radioassay. A second 10 ml aliquot of the TCA precipitated sample was filtered onto a polycarbonate filter (0.2 µm pore size) and washed, twice with 5% TCA, once with 80% ethanol, and once with deionized water. Polycarbonate filters were then placed in scintillation vials with an alkaline solution (0.5 mol L⁻¹ NaOH, 25 mmol L⁻¹ EDTA, and 0.1 % sodium dodecyl sulfate) and shaken for 1 hour at 85 °C. Material attached to polycarbonate filters dissolved in the alkaline solution and a 5 ml aliquot of this solution was subsequently radioassayed for both ¹⁴C and ³H activity on a Beckman LS 6500 liquid scintillation counter. Measured activities of both isotopes were corrected for quench with external standards then converted to carbon and leucine uptake rates based on the specific activity of each isotope in the incubations. The rate of leucine uptake (nmol leucine h⁻¹) was converted to BBP by assuming the fraction of leucine in protein to be 7.3%, the cellular carbon per protein to be 86%, and that isotope dilution was negligible (Kirchman 2001). BBP was normalized to dry weight and expressed as µg C g DW⁻¹ h⁻¹. The ratio of labeled to unlabeled bicarbonate in samples was calculated using the concentration of dissolved inorganic carbon (DIC) in filtered incubation water. DIC concentration of incubation water was estimated from measures of temperature, pH (Orion model 720 pH meter), and alkalinity (gran titration; Wetzel and Likens 2000). The rate of carbon uptake

was normalized to dry weight and expressed as photosynthetic production in $\mu\text{g C g DW}^{-1} \text{ h}^{-1}$.

Effect of TCA Precipitation on Autotrophic ^{14}C Retention

TCA protein precipitation is needed to accurately determine the rate of ^3H -L-leucine incorporation into bacterial protein. However, this step is not generally used in ^{14}C -bicarbonate uptake assays for measuring PS. In a previous study on the use of dual-radioassays, Neely and Wetzel (1995) found that 44-66% of ^{14}C taken up by periphytic photoautotrophs was lost when samples were taken through a hot TCA precipitation step. To account for this potential loss in our assays, we tested the effect of the cold TCA precipitation/alkaline dissolution method (Buesing and Gessner 2003) on ^{14}C retention by photoautotrophs in metaphyton. A ^{14}C -bicarbonate uptake radioassay was carried out on floating metaphyton samples as previously described but excluding ^3H -L-leucine additions. After samples were killed with formalin and homogenized, three 10 ml aliquots were subsampled from each vial. The first aliquot was used to measure the dry weight of radioassayed material and the second was taken through the TCA precipitation/alkaline dissolution method then radioassayed. The third aliquot was filtered onto a nitrocellulose filter (0.45 μm pore size), placed in a scintillation vial and allowed to dry overnight. After drying, 1.0 ml ethyl acetate was added to each vial to dissolve filters, samples were mixed thoroughly and radioassayed as described previously. Radioactivity in disintegrations per minute from paired samples were normalized to dry weights then compared using a paired t -test in SAS 9.1 (SAS 1999).

Light Saturation of PS and Relationship of PS to BBP

We tested the effect of increasing irradiance on PS and BBP using the dual-labeled radioassay method. Freshly collected metaphyton samples were incubated under increasing photosynthetically active radiation (photon flux density levels were 0, 19, 44, 94, 202, and 480 $\mu\text{mol m}^{-2} \text{s}^{-1}$) under in-situ temperature conditions in the laboratory. The relationship between photon flux density (PFD) and PS in metaphyton was modeled with Michaelis-Menten kinetics using nonlinear regression analysis in SigmaPlot 9.0 (SigmaPlot 2004). The effect of each light level and the effect of dark versus pooled light levels on BBP were tested using a Kruskal-Wallis test in SAS 9.1 (SAS 1999). Finally, the correlation of PS and BBP across all light levels was tested using linear regression analysis on the paired samples in SigmaPlot 9.0 (SigmaPlot 2004).

Effect of Nutrient Enrichment on PS and BBP

The effect of nutrient enrichment on PS and BBP was tested using a completely randomized-nested design on laboratory enrichments of nitrogen (N) and phosphorus (P) in metaphyton samples. Equal portions of metaphyton (approximately 2 g dry weight) were divided into fifteen separate glass jars with 300 ml filtered site water (background DIN and $\text{PO}_4\text{-P}$ were approximately 13 $\mu\text{g L}^{-1}$, and 5 $\mu\text{g L}^{-1}$, respectively; see Chapters Two and Three). At random, five jars were enriched with N (664 $\mu\text{g L}^{-1} \text{NO}_3\text{-N}$), five more were enriched with P (20 $\mu\text{g L}^{-1} \text{PO}_4\text{-P}$), and five were left untreated to serve as a control. The enrichment concentrations were based on the average concentration of dissolved N and P in waters flowing into the wetland (Scott unpubl.). Jars were randomly placed under artificial lights in a water bath in the laboratory and incubated at 26 °C for 48 hours under a 13.5 hour/10.5 hour light/dark cycle (photon flux density was 250 μmol

$\text{m}^{-2} \text{s}^{-1}$ during light period). At the end of 48 hours, three replicate samples ($\sim 10 \text{ mg}$ dry weight) were taken from each jar (nesting factor), put into borosilicate scintillation vials, and filled with newly prepared incubation water for each respective treatment (control, N, P). Samples were placed under artificial lights ($\text{PFD} = 250 \mu\text{mol m}^{-2} \text{s}^{-1}$) at 26°C and allowed to adjust to incubation conditions for a period of 1 hour. Additionally, a single sample was randomly taken from three of the five experimental jars, enriched with the appropriate nutrient, and incubated at 26°C in the dark for 1 hour. These samples were used to assess any dark uptake of ^{14}C and the rate of BBP without the influence of PS. At the end of the 1 hour acclimation period, the dual-radioassay method was used to determine PS and BBP rates in all samples as previously described.

The effect of nutrient enrichment on BBP measured in dark bottles was tested using a Kruskal-Wallis test in SAS 9.1 (SAS 1999). For samples incubated under light, the correlation between PS on BBP within each treatment was tested using linear regression analysis in SigmaPlot 9.0 (SigmaPlot 2004). Further, because we were interested in the coupled response of PS and BBP of metaphyton, we chose a multivariate method to test the simultaneous response of PS and BBP to nutrient enrichment. We used the nonparametric multiple analysis of variance (NPMANOVA) method developed by Anderson (2001). NPMANOVA is superior to other multivariate procedures because it is capable of handling complex experimental designs, including nesting. In this method, inter-point distances in bivariate (or multivariate) space are used to derive the sums of squares for a statistical test (F). The use of inter-point distances allows additive partitioning of sums of squares, thereby enabling crossed or nested factors in a design to be partitioned out of the total sums of squares.

Specifically, we used the permutational multivariate analysis of variance (PERMANOVA) software (Anderson 2005a) to test for differences in the bivariate location of PS and BBP data among treatments and the permutational analysis of multivariate dispersion (PERMDISP) software (Anderson 2005b) to test for differences in the bivariate dispersions of PS and BBP data among treatments. Data were standardized to z scores in both analyses to account for the large difference in scale between PS and BBP rates. Euclidean distance was used to calculate inter-point distances, and sample nesting within each level of the nutrient treatment was included as a factor in both analyses. Post-hoc multiple comparisons with Bonferroni error correction were used to identify differences between individual treatments when overall statistical tests were significant at $\alpha = .05$.

Results

Effect of TCA Precipitation on Autotrophic ^{14}C Retention

Cold TCA protein precipitation had no effect on the degree of ^{14}C retention by photosynthetic organisms in metaphyton ($t = 0.01$, $p = 0.9915$, $df = 20$). In all subsequent assays, we assumed no loss of ^{14}C due to cold TCA treatment.

Light Saturation of PS and Relationship of PS to BBP

The mean rate of PS in nutrient-limited metaphyton followed Michaelis-Menten kinetics when incubated under increasing light intensities (Figure 5.1B). Although

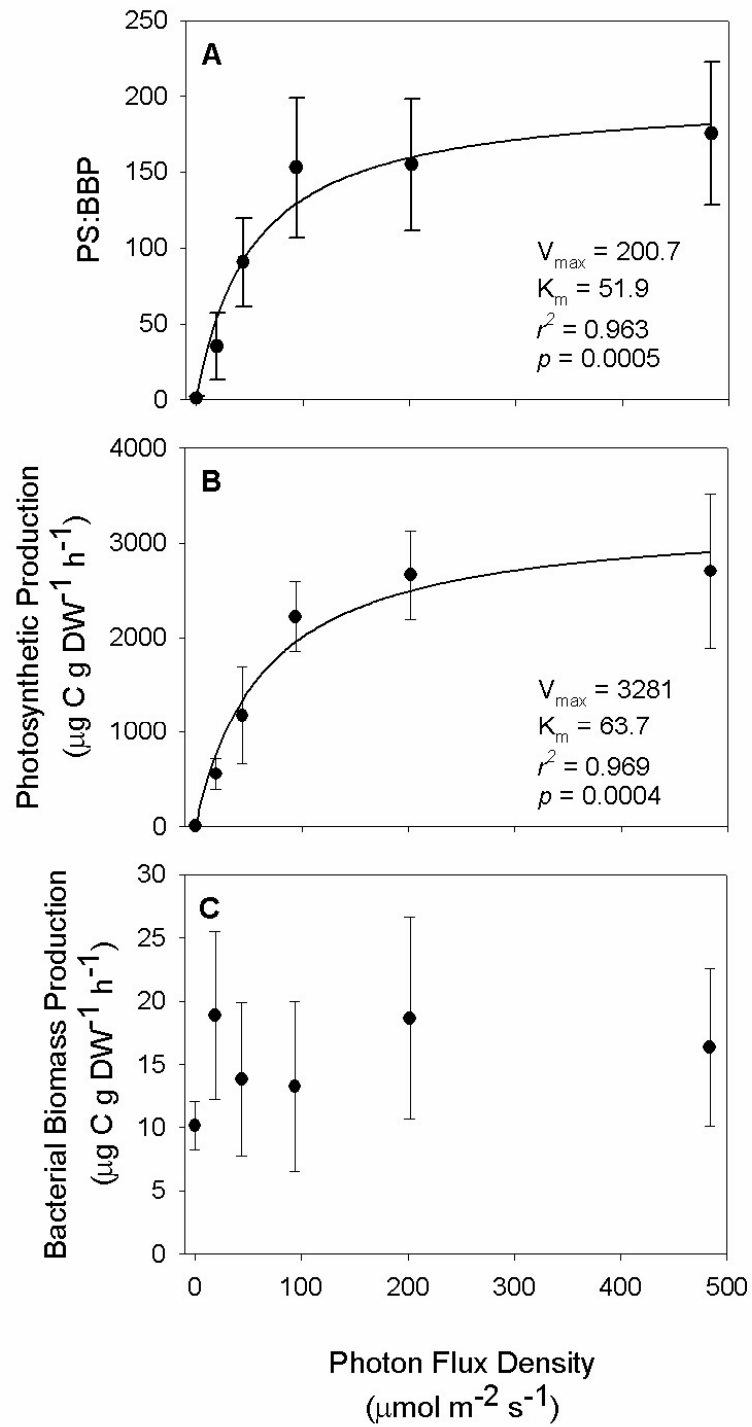


Figure 5.1. Response of photosynthesis (PS) and bacterial biomass production (BBP) to varying light. A) Ratio of PS:BBP observed with increasing irradiance; B) Response of mean PS to increasing irradiance; C) Response of BBP to increasing irradiance. Error bars in all panels indicate standard deviation (SD).

the mean rate of BBP in the dark incubations was statistically lower than the mean BBP in the pooled data from light incubations (Kruskal-Wallis test, $\chi^2 = 5.3$, $df = 1$, $p = 0.0209$), a statistical difference was not observed between discrete light levels (Kruskal-Wallis test, $\chi^2 = 7.32$, $df = 5$, $p = 0.1947$). Further, no pattern was apparent between increasing light intensity and mean BBP (Figure 5.1C). Because mean BBP remained relatively constant across the increasing light levels, the ratio of PS to BBP (PS:BBP) exhibited a pattern similar to PS when examined across light intensities (Figure 5.1A).

Although the mean rates of PS and BBP did not appear coupled in the light saturation experiments, regression analysis of the individual observations indicated a weak positive correlation between PS and BBP across the range of all light intensities (Figure 5.2).

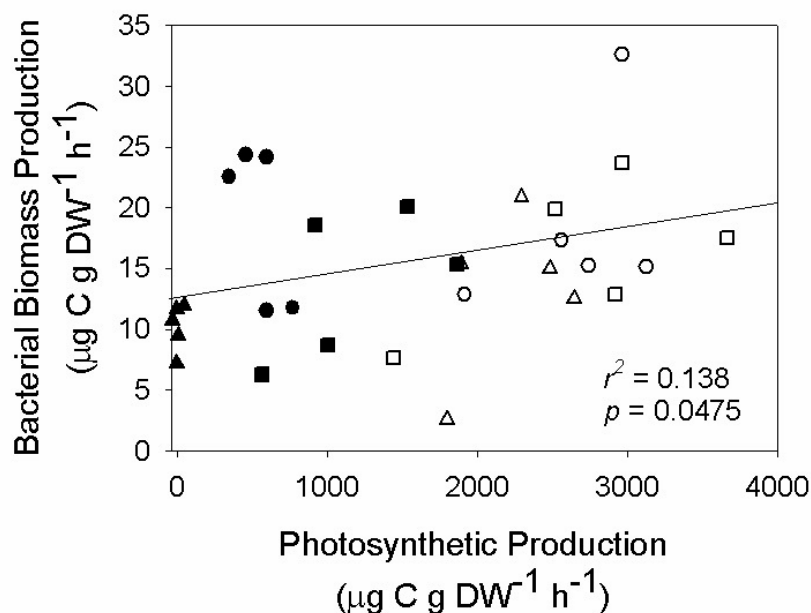


Figure 5.2. Scatterplot of metaphyton photosynthetic production and bacterial biomass production in light saturation experiment; samples incubated across a range of photon flux density. The following symbols represent each respective light level: $\blacktriangle = 0 \mu\text{mol m}^{-2} \text{ s}^{-1}$; $\bullet = 19 \mu\text{mol m}^{-2} \text{ s}^{-1}$; $\blacksquare = 44 \mu\text{mol m}^{-2} \text{ s}^{-1}$; $\triangle = 94 \mu\text{mol m}^{-2} \text{ s}^{-1}$; $\circ = 202 \mu\text{mol m}^{-2} \text{ s}^{-1}$; $\square = 484 \mu\text{mol m}^{-2} \text{ s}^{-1}$.

Effect of Nutrient Enrichment on PS and BBP

Results from the PERMANOVA and PERMDISP tests, along with the results of the corresponding post-hoc tests are provided in Table 5.1. Nutrient enrichment had a statistically significant effect on the location (PERMANOVA) and dispersion (PERMDISP) of PS and BBP data in bivariate space. Although the effect of nesting was statistically significant in the bivariate location test (PERMANOVA), the magnitude of this effect did not appear to dampen the nutrient effect. The nesting factor was not important in the bivariate dispersion test (PERMDISP). In the multiple comparison tests within PERMANOVA, we found that the location of PS and BBP data in bivariate space was only different between the N enrichment and the control. Multiple comparisons from PERMDISP revealed that the dispersion of PS and BBP data was not different between the N enrichment and control. Although mean PS in the P enrichment was 3.6 times greater than mean PS in the control group, the variance of PS data from the P enrichment was 2.5 times greater than the control (Table 5.1). Because of this large variation in PS and BBP data, the bivariate location of data was not statistically different between the P enrichment and control. However, the dispersion of PS and BBP data in the P enrichment was statistically greater than the dispersion in both the control and N enrichment (Table 5.1).

In addition to the differences observed in bivariate location and dispersion of PS and BBP data, the relationship between PS and BBP was different among the three experimental groups. A strong positive correlation between PS and BBP was evident in the control group (Figure 5.3C) but was weaker in each of the nutrient enrichments (Figure 5.3A and 5.3B). In the N enrichment, PS rates were never lower than 20 mg C g

Table 5.1. ANOVA tables for bivariate test of location (PERMANOVA) and the bivariate test of dispersion (PERMDISP), and the results of post-hoc multiple comparisons for both statistical tests. Mean photosynthesis (PS) and bacterial biomass production (BBP) rates and the average ratio of PS:BBP in the nutrient enrichment experiment are reported with the results of the post-hoc comparisons. SE represents standard error of mean.

PERMANOVA					
Source	df	SS	MS	<i>F</i>	<i>p</i>
Nutrient enrichment	2	34.9	17.9	7.93	0.0060
Nesting	12	26.4	2.2	2.46	0.0136
Residual	30	26.8	0.9		
Total	44	88.0			

PERMDISP					
Source	df	SS	MS	<i>F</i>	<i>p</i>
Nutrient enrichment	2	6.2	3.1	17.7	0.0008
Nesting	12	2.1	0.2	1.4	0.2418
Residual	30	3.7	0.1		
Total	44	12.0			

POST-HOC COMPARISONS			
Treatment	Mean PS \pm SE ($\mu\text{g C g DW}^{-1} \text{ h}^{-1}$)	Mean BBP \pm SE ($\mu\text{g C g DW}^{-1} \text{ h}^{-1}$)	Mean PS:BBP \pm SE
Control	8673 \pm 2210	5.79 \pm 1.77	1852 \pm 213
Nitrogen	34909 \pm 1767*	15.67 \pm 0.54*	2236 \pm 96.1
Phosphorus	31235 \pm 5453 [†]	12.25 \pm 1.74 [†]	2586 \pm 212

*Statistically different from the control group ($t=4.05$, $p=0.0082$) in the bivariate location test.

[†]Statistically different from the control group ($t=4.93$, $p=0.0064$) and nitrogen group ($t=5.12$, $p=0.0078$) in the bivariate dispersion test.

$\text{DW}^{-1} \text{ h}^{-1}$ and BBP rates were never lower than $10 \mu\text{g C g DW}^{-1} \text{ h}^{-1}$. However, the range of PS and BBP data observed in the P enrichment spanned the minimum and maximum of all observed values, as indicated by the statistically significant outcome in the bivariate dispersion test. The slope of the best fit line in the control group was four times steeper than the slope of the best fit lines in each of the nutrient enrichments indicating that PS in the nutrient enrichments changed with greater magnitude than did BBP (Figure 5.3). This trend was also illustrated in the mean PS:BBP for each of the treatments. Mean PS:BBP in the N enrichment was 20% greater than the mean PS:BBP of the control and mean PS:BBP in the P enrichment was 40% greater than the mean PS:BBP of the control

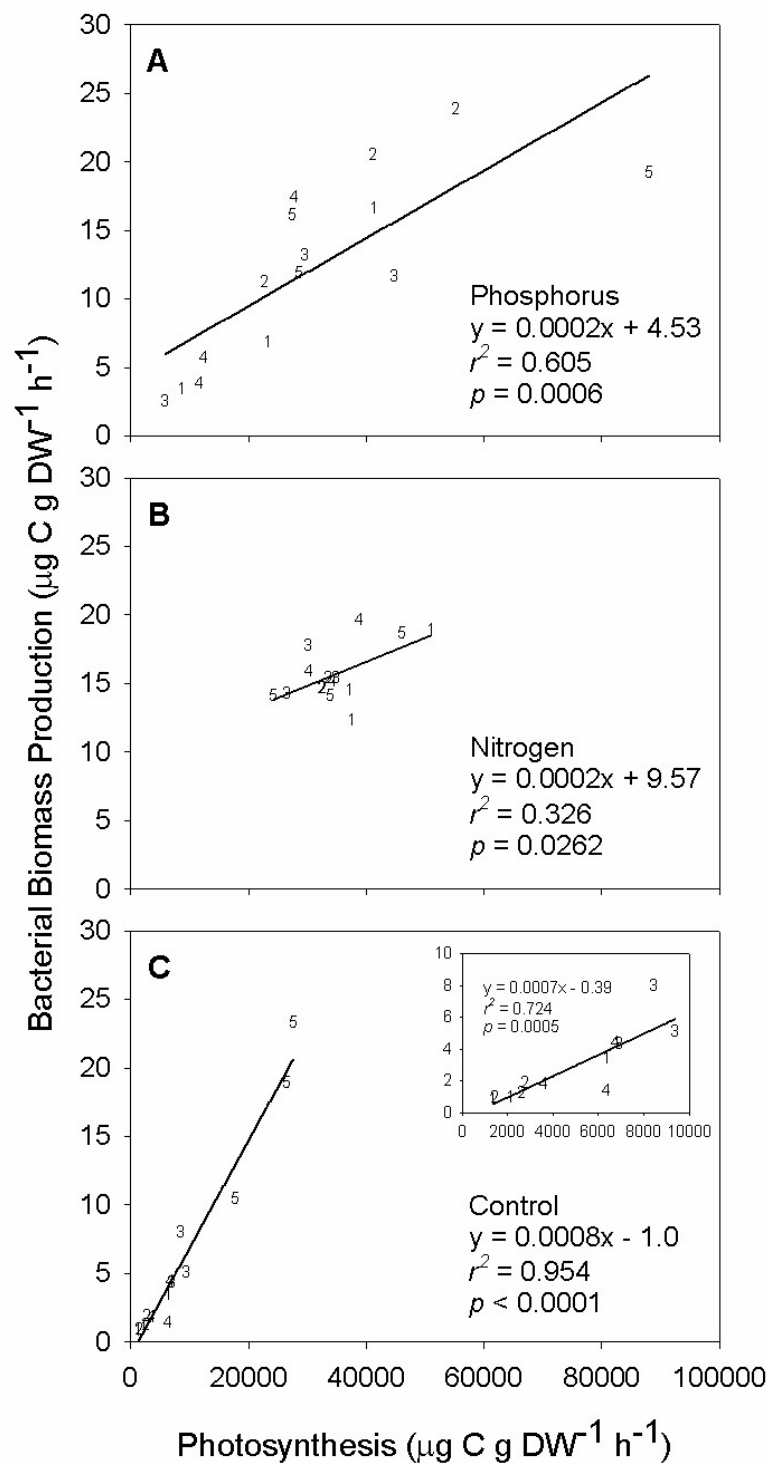


Figure 5.3. Scatterplots of metaphyton photosynthetic production and bacterial biomass production across each nutrient enrichment where all samples were incubated under equal photon flux density ($250 \mu\text{mol m}^{-2} \text{s}^{-1}$): A) phosphorus enrichment, B) nitrogen enrichment, C) control (inset in panel C shows the relationship of data when jar 5 is excluded). Numbers represent jars (nesting factor in PERMANOVA and PERMDISP) from which triplicate measures were made.

(Table 5.1). These data indicate a larger increase in PS relative to BBP by both N and P enrichment.

There were no statistically significant differences in dark BBP (independent from PS) rates among the control and nutrient enrichments (Kruskal-Wallis test, $\chi^2 = 3.2$, $df = 2$, $p = 0.2019$). Although a general pattern of higher dark BBP was observed in the N enrichment (Figure 5.4), the low sample size ($n = 3$) and subsequent reduced statistical power were not sufficient for detecting statistical differences.

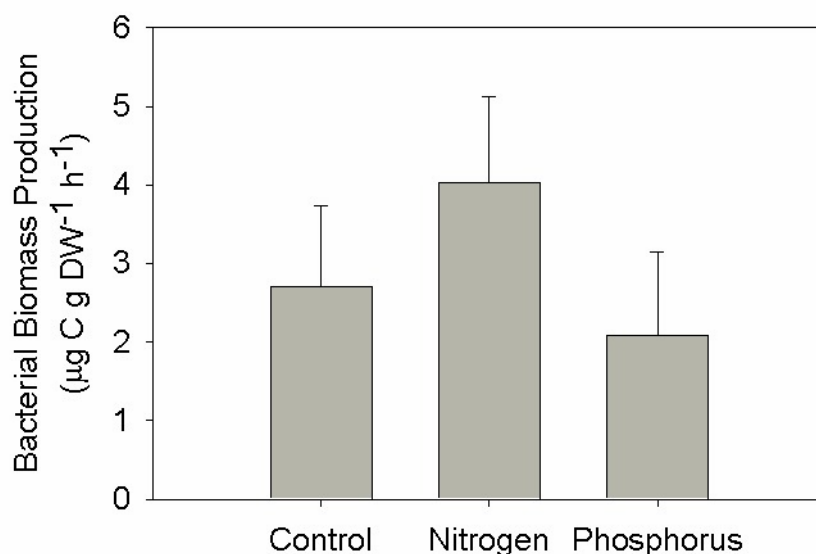


Figure 5.4. Bacterial biomass production rates for samples incubated under dark conditions in the nutrient enrichment experiment (mean \pm SD; $n=3$).

Discussion

Results of this study indicated that photosynthesis (PS) and heterotrophic bacterial biomass production (BBP) were generally coupled in nutrient-limited wetland metophyton under light intensities greater than $\sim 20 \mu\text{mol m}^{-2} \text{s}^{-1}$. In the light saturation experiment, mean PS rates increased in a predictable pattern with increased light intensity (Figure 5.1B). Conversely, mean BBP rates did not follow any pattern across increasing

light intensity (Figure 5.1C). However, when individual PS and BBP measurements were combined in a scatterplot, a positive linear relationship became apparent in the data across all light intensities (Figure 5.2). Furthermore, the relationship between PS and BBP was stronger under saturating light ($\geq 90 \mu\text{mol m}^{-2} \text{s}^{-1}$).

Although the correlation between PS and BBP data across all light intensities was weak ($r^2 = 0.14$) compared to another published value ($r^2 = 0.79$ in Neely and Wetzel 1995), assays in that study were conducted on nutrient-rich media as opposed to the nutrient-limited community used in this study. We believe that the strength of coupling between PS and BBP will be diminished in an environment where both photoautotrophs and bacteria may be experiencing nutrient limitation. Further, samples for the light saturation experiment in this study were generally collected during early morning and only provided 1 hour acclimation and 2 hours of incubation. Espeland et al. (2001) found that BBP tended to be higher in metaphyton receiving 8 hours or more of relatively low irradiance ($< 100 \mu\text{mol m}^{-2} \text{s}^{-1}$). Therefore, the short-term experiments used in this study probably provide a conservative estimate of the degree of coupling between PS and BBP in nutrient-limited metaphyton.

As shown in the multivariate statistical tests, both the location and dispersion of PS and BBP data were affected by nutrient enrichment. In particular, N enrichment (but not P enrichment) resulted in a statistically significant increase in both PS and BBP rates relative to the control. These findings suggest that photoautotrophs in floating metaphyton sampled in this study were N-limited, which supports the findings of previous studies on periphyton in this ecosystem (Chapter Three). The response of BBP however, was more difficult to interpret. Had the increased BBP measured in dark

incubations during N enrichment been statistically greater than BBP in control, we might have concluded with confidence that bacteria were also N-limited. Although the trend in the data suggests that N might have had some influence on dark BBP (Figure 5.4), it is difficult to know whether increased BBP observed under light saturated N enrichment was caused by increased N supply or simply increased EOC supplied at higher rates of PS. However, because light saturated N enrichment decreased the strength of correlation between PS and BBP (Figure 5.3), we suspect bacteria were responding more to inorganic N than they were increased EOC supplied by PS.

The bivariate test of location was not significant when comparing the P enrichment to the control, however, the bivariate dispersion of data was statistically different between these treatments (Table 5.1). The dispersion of data in the P enrichment was also statistically greater than the dispersion observed in the N treatment. We conclude that PS and BBP were responding in some fashion to P enrichment, however, the mechanism at work is difficult to interpret using results of the statistical tests only.

PS in the control group was assumed to be N-limited (see Chapter Three). Therefore, the addition of P alone would only have increased the degree of N-limitation. The N treatment however, likely shifted PS from N to P-limitation. A shift to P-limitation may explain the apparent decoupling of PS and BBP observed in the N treatment. P-limitation may have induced a competitive interaction for P between photoautotrophs and bacteria (Currie and Kalff 1984).

Because PS and BBP remained more strongly coupled during P enrichment (i.e. strengthened N-limitation), a commensalistic or perhaps mutualistic interaction may be occurring during N deficiency. It is possible that a mutualistic relationship exists whereby

bacteria regulate P availability to photoautotrophs, and photoautotrophs supply fixed N to bacteria (rather than simply EOC as suggested by Sharma et al. 2005). A mutualistic relationship of this sort would help explain the ecological necessity of periphytic N₂ fixation in strongly P-limited environments such as tropical and sub-tropical marshes (Rejmánková and Komárková 2000; Inglett et al. 2004). However, more research is needed to identify the nature of photoautotrophic and heterotrophic bacterial interaction across a diverse range of nutrient deficiencies and elemental imbalances.

In this study, we attempted to elucidate the effect of nutrient enrichment on PS and BBP in floating metaphyton using laboratory experiments. It should be noted that the timing of experiments relative to sampling and laboratory conditions of the experiments appeared to change the proportion of measured PS:BBP in floating metaphyton. For instance, in the light saturation experiment where metaphyton samples were collected and radioassayed within a matter of hours, PS:BBP was in the range of typical values found in the literature (Table 5.2). However, PS rates increased slightly and BBP rates decreased substantially when samples were taken through a 48 hour acclimation period. This resulted in an increase in PS:BBP by an order of magnitude (see Table 5.2). Further, when metaphyton were provided a 48 hour acclimation period, the strength of correlation between PS and BBP appeared to increase substantially (see Figure 5.3C versus Figure 5.2). Although the strength of correlation observed in the nutrient enrichment controls was to some degree driven by high PS and BBP rates measured in jar 5, samples from jars 1 - 4 only (Figure 5.3C inset) still exhibited stronger correlation than did PS and BBP in freshly collected samples under saturating light (Figure 2; $r^2 = 0.25$, $p = 0.1463$, for light levels $202 \mu\text{mol m}^{-2} \text{s}^{-1}$ and $494 \mu\text{mol m}^{-2} \text{s}^{-1}$).

Table 5.2. The ratio of photosynthesis to bacterial biomass production (PS:BBP) observed in this study and others.

Study	Community/ Growth Substrate	Incubation Light ($\mu\text{mol m}^{-2} \text{s}^{-1}$)	Incubation Temperature ($^{\circ}\text{C}$)	Nutrient Amendments	PS:BBP	Notes*
Present	Metaphyton	202 – 484	26	None	165	a
Present	Metaphyton	250	26	None	1852	b
Neely and Wetzel (1995)	Periphyton on glass slides	400	20	Agar	29.4	
Neely and Wetzel (1997)	Epiphyton on Typha	500	20	None	14.3 22.5 128.5	c d e

* Notes:

- Measured immediately after sampling.
- Measured following a 48 hour experiment acclimation period where samples were exposed only to artificial photosynthetically active radiation (PAR).
- Following 20 days in direct sunlight.
- Following 40 days in direct sunlight.
- Following 60 days in direct sunlight.

The cause of this change remains unknown, however, we suspect that exposing the photoautotrophs only to the favorable conditions of photosynthetically active radiation may have increased their ability to compete with bacteria for inorganic nutrients. Furthermore, because all treatments in the nutrient enrichment experiment were exposed to the same laboratory conditions, this “bottle effect” does not alter the interpretation of the experimental results.

We used leucine incorporation into protein for heterotrophic bacterial production estimates in order to account for production in cell maintenance as opposed to production via cell division (e.g. using thymidine incorporation into DNA). It should be noted that some studies have shown that leucine can be taken up by photosynthetic cyanobacteria such as *Microcystis aeruginosa* (Kamjunke and Jähnichen 2000) and *Nodularia* spp. (Hietanen et al. 2002). It remains unclear whether N₂-fixing cyanobacteria such as *Anabaena* and *Aphanizomenon*, which are common taxa in metaphyton, exhibit similar capabilities.

Results of this study also support the usefulness of a dual-isotope technique for simultaneous measurements of PS and BBP in microbial communities. The major strength of the dual-isotope technique is in generating a measurement of both PS and BBP on a sample incubated in a single vial. Because metaphyton communities are notoriously heterogeneous (Stevenson 1996), comparing measured rates of biological processes between samples is problematic at best, and using mean rates from a small number of replicates limits the power of detecting statistical differences. Simultaneous measures from a single vial provide increased accuracy and comparability for biological processes in heterogeneous metaphyton communities. One drawback of the dual-isotope

method is the difference in sample preparation between ^{14}C -bicarbonate radioassays for PS and ^3H -L-leucine radioassays for BBP. In a previous study, Neely and Wetzel (1995) reported that as much as 66% of ^{14}C incorporated by periphytic photoautotrophs growing on glass slides was lost during hot TCA precipitation of proteins. However, in our study, the cold TCA protein precipitation/alkaline dissolution method of Buesing and Gessner (2003) had no effect on the degree of ^{14}C retention by photosynthetic organisms in metaphyton. It is difficult to know whether the differences observed between the studies were a function of the different communities assayed, or perhaps a function of using hot versus cold TCA precipitation. What is clear from Neely and Wetzel (1995) and the present study is that the power to detect coupling between PS and BBP increases when measurements originate from the same vial. In our study, the importance of simultaneous measurements was critical for examining PS and BBP coupling in both the light saturation and nutrient enrichment experiments.

Conclusions

The results of the study indicate that although PS and BBP in metaphyton remain coupled under all environmental conditions examined, the magnitude of these rates and the strength of their relationship is influenced by the degree and type of nutrient limitation. N enrichment weakened the relationship between PS and BBP possibly by inducing a competitive interaction between bacteria and photoautotrophs for P. In contrast, coupling of PS and BBP remained high under P enrichment. BBP increased in P enrichments either due to an increased supply of EOC from PS or perhaps due to an increased N supply from light-dependent N_2 fixation. The possibility of linking photoautotrophs and bacteria in metaphyton through multiple elemental interactions

provides an important new line of questioning about the ecological functioning of these communities.

CHAPTER SIX

Summary and Conclusions

Synthesis of Chapter Contents

Research comprising this dissertation demonstrated how biogeochemical processes in wetland ecosystems may influence the supply of inorganic nutrients to organisms relying on water column nutrient supplies. The studies also demonstrated that benthic microbial communities, the metaphyton, are also susceptible to patterns of control and limitation by nutrients supplied in the water column, and use specific mechanisms to overcome nutrient limitation.

The findings from Chapter Two indicated that a differential nutrient availability gradient existed in the Lake Waco Wetlands. Nitrogen (N) in the form of nitrate was efficiently removed from the water column to a large degree by sediment influx and eventual denitrification. Phosphorus (P) however, was not well retained and sediments were often a source of P. The resulting nutrient gradient became diminished in N relative to P along the flow path of water through the wetland.

The results of Chapter Three indicated that periphyton growing in different places along the wetland nutrient gradient responded differently to nutrient enrichment and have different potentials for fixing atmospheric N₂. Near the wetland inflow, both N and P enrichment alone, and in combination, usually resulted in greater periphyton biomass accumulation on artificial substrates. In downstream areas of the wetland only N alone, or in combination with P, stimulated periphyton biomass accumulation. Furthermore, N₂ fixation potential was always zero near the wetland inflow but increased substantially in

downstream locations. These results indicated a substantial shift to N-limitation of periphyton growing in downstream locations.

Functions, such as N_2 fixation and N retention, used by metaphyton to overcome N-limitation were demonstrated in Chapter Four. Nitrogen isotopic composition ($\delta^{15}N$) of the periphyton generally overestimated the contribution of N_2 fixation to total N uptake. This overestimation may have been the result of efficient retention and recycling of fixed N_2 within the metaphyton community. The retention and accumulation of N resulted in a shift toward P-limitation, particularly when production was normalized to metaphyton N content. Although this appears counterintuitive with the findings of the nutrient enrichment experiment in Chapter Three, N enrichment in that study increased periphyton biomass because dissolved N from the water column is much less energetically expensive to acquire than fixed N_2 . Furthermore, dissolved N is immediately available to all organisms in the periphyton community rather than being restricted to certain cyanobacteria which have the capacity to fix N_2 .

Finally, other mechanisms may exist whereby organisms within the metaphyton community, and other periphyton communities, interact in the beneficial exchange of nutrients and energy. Experimental N enrichments, described in Chapter Five, appeared to decouple the relationship between photosynthesis and bacterial biomass production within the metaphyton community. The decoupling could have been in response to a competitive interaction for inorganic P or was perhaps in response to alleviating the reliance of heterotrophic bacteria on fixed N_2 from cyanobacteria.

Future Directions

Although the studies contained in this dissertation shed new light on the interaction between wetland periphyton communities and wetland nutrient biogeochemical cycles, many associated questions remain unanswered. From the ecosystem perspective, future questions may include: What is the spatial distribution of periphyton, and the specific groups such as metaphyton, epipelton, and epiphyton, along wetland nutrient availability gradients, and how important are these communities for carbon and nitrogen supply to the ecosystem? What is the role of metaphyton, epipelton, or epiphyton in benthic and pelagic food webs in wetlands?

Also of interest is the biogeochemical cycling of nutrients within the metaphyton community, and other periphyton groups, and the resulting controls on microbial interactions. Future questions might include: Do bacteria in N-poor periphyton rely on fixed N_2 from cyanobacteria? If bacteria do use fixed N_2 , at what rate is N supplied in this fashion? Also, do bacteria regulate P availability in these situations to stimulate cyanobacterial N_2 fixation? These and other questions should be addressed if we are to truly understand the functional role(s) of periphyton in wetland and shallow aquatic ecosystems.

APPENDIX

APPENDIX

Peer-Reviewed Publications and Manuscripts In-Review for Publication
Derived from this Research*Chapter Two*

Scott JT, McCarthy MJ, Gardner WS, Doyle RD. *In-Review*. Alteration of inorganic N:P supply by ecosystem retention and nitrogen transformations. *Biogeochemistry*.

Chapter Three

Scott JT, Doyle RD, Filstrup CT. 2005. Periphyton nutrient limitation and nitrogen fixation potential along a wetland nutrient-depletion gradient. *Wetlands* 25: 439-448

Reprinted with permission

Chapter Four

Scott JT, Doyle RD, Back JA, Dworkin SI. *Accepted*. Elemental, isotopic, and enzymatic evidence for seasonally-evolving phosphorus limitation in a nitrogen-fixing periphyton community. *Biogeochemistry*.

Chapter Five

Scott JT, Doyle RD. 2006. Coupled photosynthesis and heterotrophic bacterial biomass production in a nutrient limited wetland periphyton mat. *Aquatic Microbial Ecology* 45: 69-77

Reprinted with permission

BIBLIOGRAPHY

- An S, Gardner WS. 2002. Dissimilatory nitrate reduction to ammonium (DNRA) as a nitrogen link, versus denitrification as a sink in a shallow estuary (Laguna Madre/Baffin Bay, Texas). *Marine Ecology Progress Series* 237: 41-50
- An S, Gardner WS, Kana T. 2001. Simultaneous measurement of denitrification and nitrogen fixation using isotope pairing with membrane inlet mass spectrometry. *Applied and Environmental Microbiology* 67: 1171-1178
- Anderson MJ. 2001. A new method for non-parametric multivariate analysis. *Austral Ecology* 26:32-46
- Anderson MJ. 2005a. PERMANOVA: a FORTRAN computer program for permutational multivariate analysis of variance. Department of Statistics, University of Auckland, New Zealand
- Anderson MJ. 2005b. PERMDISP: a FORTRAN computer program for permutational analysis of multivariate dispersions (for any two-factor anova design) using permutation tests. Department of Statistics, University of Auckland, New Zealand
- Bachand PAM, and Horne AJ. 2000. Denitrification in constructed free-water surface wetlands: II Effects of vegetation and temperature. *Ecological Engineering* 14:17-32
- Borchardt MA. 1996. Nutrients p.183-227. In: Stevenson RJ, Bothwell ML, Lowe RL (Eds.). *Algal Ecology: Freshwater Benthic Ecosystems*. Academic Press, New York, NY, USA
- Bowden, WB. 1987. The biogeochemistry of nitrogen in freshwater wetlands. *Biogeochemistry* 4: 313-348
- Buesing N, Gessner MO. 2003. Incorporation of radiolabeled leucine into protein to estimate bacterial production in plant litter, sediment, epiphytic biofilms, and water samples. *Microbial Ecology* 45:291-301
- Casey RE, Taylor MD, Klaine SJ. 2001. Mechanisms of nutrient attenuation in a subsurface flow riparian wetland. *Journal of Environmental Quality* 30:1732-1737
- Chrzanowski TH, Kyle M, Elser JJ, Sterner RW. 1996. Element ratios and growth dynamics of bacteria in an oligotrophic Canadian shield lake. *Aquatic Microbial Ecology* 11:119-125

- Clesceri LS, Greenberg AE, Eaton AD (Eds). 1998. Standard methods for the analysis of water and wastewater, 20th ed. American Public Health Association, Washington DC
- Cole JJ, Likens GE, Stayer DL. 1982. Photosynthetically produced dissolved organic carbon: an important source for planktonic bacteria. *Limnology and Oceanography* 27:1080-1090
- Coveney MF, Wetzel RG. 1989. Bacterial metabolism of algal extracellular carbon. *Hydrobiologia* 79:61-71
- Currie DJ, Kalff J. 1984. Can bacteria outcompete phytoplankton for phosphorus? A chemostat test. *Microbial Ecology* 10:205-216
- Davidsson TE, Leonardson L. 1998. Seasonal dynamics of denitrification activity in two water meadows. *Hydrobiologia* 364:189-198
- Dodds WK. 2003. Misuse of inorganic N and soluble reactive P concentrations to indicate nutrient status of surface waters. *Journal of the North American Benthological Society* 22: 171-181
- Doyle RD, Fisher TR. 1994. Nitrogen fixation by periphyton and plankton on the Amazon floodplain at Lake Calado. *Biogeochemistry* 26:41-66
- Dworkin SI. 2003. The hydrogeochemistry of the Lake Waco drainage basin, Texas. *Environmental Geology* 45: 106-114
- Espeland EM, Wetzel RG. 2001. Effects of photosynthesis on bacterial phosphatase production in biofilms. *Microbial Ecology* 42:328-337
- Espeland EM, Francoeur SN, Wetzel RG. 2001. Influence of algal photosynthesis on biofilm bacterial production and associated glucosidase and xylosidase activities. *Microbial Ecology* 42:524-530
- Eyre BD, Rysgaard S, Dalsgaard T, Christensen PB. 2002. Comparison of isotope pairing and N₂/Ar methods for measuring denitrification rates – assumptions, modifications, and implications. *Estuaries* 25: 1077-1087
- Fairchild GW, Lowe RL, Richardson WB. 1985. Algal periphyton growth on nutrient-diffusing substrates: an in situ bioassay. *Ecology* 66(2):465-472
- Flett RJ, Hamilton RD, Campbell NER. 1976. Aquatic acetylene reduction techniques: solutions to several problems. *Canadian Journal of Microbiology* 22:43-51

- Fogel ML, Cifuentes LA. 1993. Isotope fractionation during primary production. In: Engel MH, Macko SA (Eds) *Organic Geochemistry: Principles and Applications*. Plenum Press, New York, NY
- France R, Holmquist J, Chandler M, Cattaneo A. 1998. $\delta^{15}\text{N}$ evidence for nitrogen fixation associated with macroalgae from a seagrass-mangrove-coral reef system. *Marine Ecology Progress Series* 167: 297-299
- Francoeur SN, Wetzel RG. 2003. Regulation of periphytic leucine-aminopeptidase activity. *Aquatic Microbial Ecology* 31:249-258
- Gardner WS, Bootsma HA, Evans C, St. John PA. 1995. Improved chromatographic analysis of ^{15}N : ^{14}N in ammonium or nitrate for isotope addition experiments. *Marine Chemistry* 48: 271-282
- Gardner WS, McCarthy MJ, An S, Sobolev D, Sell KS, Brock D. 2006. Nitrogen fixation and dissimilatory nitrate reduction to ammonium (DNRA) support nitrogen dynamics in Texas estuaries. *Limnology and Oceanography* 51: 558-568
- Goldsborough LG, Robinson GGC. 1996. Patterns in wetlands p. 77-117. In: Stevenson RJ, Bothwell ML, Lowe RL (Eds.). *Algal Ecology: Freshwater Benthic Ecosystems*. Academic Press, New York, NY, USA
- Gu B, Alexander V. 1993. Estimation of N_2 fixation based on differences in the natural abundance of ^{15}N among freshwater N_2 -fixing and non- N_2 -fixing algae. *Oecologia*. 96: 43-48
- Haglund A, Hillebrand H. 2005. The effect of grazing and nutrient supply on periphyton associated bacteria. *FEMS Microbiology Ecology* 52:31-41
- Havens KE, East TL, Rodusky AJ, Sharfstein B. 1999a. Littoral periphyton responses to nitrogen and phosphorus: an experimental study in a subtropical lake. *Aquatic Botany* 63:267-290
- Havens KE, East TL, Hwang S, Rodusky AJ, Sharfstein B, Steinman AD. 1999. Algal responses to experimental nutrient addition in the littoral community of a subtropical lake. *Freshwater Biology* 42: 329-344
- Heaton THE. 1986. Isotopic studies of nitrogen pollution in the hydrosphere and atmosphere: a review. *Chemical Geology* 59: 87-102
- Heitanen S, Lehtimäki JM, Tuominen L, Sivonen K, Kuparinen J. 2002. *Nodularia* spp. (Cyanobacteria) incorporate leucine but not thymidine: importance for bacterial-production measurements. *Aquatic Microbial Ecology* 28: 99-104

- Horne AJ, Sandusk JC, Carmiggelt CJW. 1979. Nitrogen fixation in Clear Lake, California. 3. Repetitive synoptic sampling of the spring *Aphanizomenon* blooms. *Limnology and Oceanography* 17: 693-703
- Howarth RW, Marino R, Lane J, Cole JJ. 1988a. Nitrogen fixation in freshwater, estuarine, and marine ecosystems. 1. Rates and importance. *Limnology and Oceanography* 33: 669-687
- Howarth RW, Marino R, Cole JJ. 1988b. Nitrogen fixation in freshwater, estuarine, and marine ecosystems. 2. Biogeochemical controls. *Limnology and Oceanography* 33: 688-701
- Howarth RW, Chan F, Marino R. 1999. Do top-down and bottom-up controls interact to exclude nitrogen-fixing cyanobacteria from the plankton of estuaries? An exploration with a simulation model. *Biogeochemistry* 46: 203-231
- Inglett PW, Reddy KR, McCormick PV. 2004. Periphyton chemistry and nitrogenase activity in a northern Everglades ecosystem. *Biogeochemistry* 67:213-233
- Jenkins MC, Kemp M. 1984. The coupling of nitrification and denitrification in two estuarine sediments. *Limnology and Oceanography* 29: 609-619
- Johnston CA, Brigham SD, Schubauer-Berigan JP. 2001. Nutrient dynamics in relation to geomorphology in riverine wetlands. *Soil Science Society of America Journal* 65:557-577
- Kadlec RH, Knight RL. 1996. Treatment Wetlands. Lewis Publishers, CRC Press LLC, Boca Raton, FL, USA
- Kamjunke N, Jähnichen S. 2000. Leucine incorporation by *Microcystis aeruginosa*. *Limnology and Oceanography* 45: 741-743
- Kana TM, Darkangelo C, Hunt MD, Oldham GB, Bennet GE, Cornwell JC. 1994. Membrane inlet mass spectrometer for rapid high-precision determination of N₂, O₂, and Ar in environmental water samples. *Analytical Chemistry* 66: 4166-4170
- Keddy PA. 2000. Wetland Ecology: Principles and Conservation. Cambridge University Press, Cambridge, UK
- Kirchman D. 2001. Measuring bacterial biomass production and growth rates from leucine incorporation in natural aquatic environments. p. 227-336. In: Paul JH (Ed) Methods in Microbiology, Volume 30. Academic Press

- Krammer K, Lange-Bertalot H. 1999. Bacillariophyceae, 2 Teil: Bacillariaceae, Epithemiaceae, Surirellaceae. In: Ettl H., Gerloff J, Heynig H, Mollenhauer D (Eds.). Süßwasserflora von Mitteleuropa, Band 2/2. Spektrum Akademischer Verlag, Heidelberg, Germany
- Krammer K, Lange-Bertalot H. 2000. Bacillariophyceae, Part 5: English and French Translation of the Keys. In: Büdel B, Gärtner G, Krienitz L, Lokhorst GM (Eds.). Süßwasserflora von Mitteleuropa, Band 2/5. Spektrum Akademischer Verlag, Heidelberg, Germany
- Lavrentyev PJ, Gardner WS, Yang L. 2000. Effects of the zebra mussel on nitrogen dynamics and the microbial community at the sediment-water interface. *Aquatic Microbial Ecology* 21: 187-194
- Lajtha K, Marshall JD. 1994. Sources of variation in the stable isotopic composition of plants. p. 1-21. In: Lajtha K, Michener RH (Eds) Stable Isotopes in Ecology and Environmental Science. Blackwell Scientific Publications, Cambridge, MA
- Lamberti GA. 1996. The role of periphyton in benthic food webs. p. 533-564. In: Stevenson RJ, Bothwell ML, Lowe RL (Eds) Algal Ecology – Freshwater Benthic Habitats. Academic Press, New York, NY
- Levine SN, Schindler DW. 1992. Modification of the N:P ratio in lakes by in situ processes. *Limnology and Oceanography* 37: 917-935
- Levine SN, Schindler DW. 1999. Influence of nitrogen to phosphorus supply ratios and physicochemical conditions on cyanobacteria and phytoplankton species composition in the Experimental Lakes Area, Canada. *Canadian Journal of Fisheries and Aquatic Science* 56: 451-466
- Lowe RL, Rosen BH, Fairchild GW. 1984. Endosymbiotic blue-green algae in freshwater diatoms: an advantage in nitrogen poor habitats. *Journal of Phycology* 20:24
- Matlock MD, Matlock ME, Storm DE, Smolen MD, Henley WJ. 1998. Limiting nutrient determination in lotic ecosystems using a quantitative nutrient enrichment periphytometer. *Journal of the American Water Resources Association* 34(5):1141-1147
- Matlock MD, Storm DE, Smolen MD, Matlock ME, McFarland AMS, Hauck LM. 1999. Development and application of a lotic ecosystem trophic status index. *Transactions of the American Society of Agricultural Engineers* 42(3):651-656
- Mayer PM, Galatowitsch SM. 2001. Assessing ecosystem integrity of restored prairie wetlands from species production-diversity relationships. *Hydrobiologia* 443:177-185

- McCormick PV, Rawlik PS, Lurding K, Smith EP, Sklar FH. 1996. Periphyton-water quality relationships along a nutrient gradient in the northern Florida Everglades. *Journal of the North American Benthological Society* 15(4):433-449
- McCormick PV, Shuford III RBE, Backus JG, Kennedy WC. 1998. Spatial and seasonal patterns of periphyton biomass and productivity in the northern Florida Everglades. *Hydrobiologia* 362:185-208
- McCormick PV, O'Dell MB, Shuford III RBE, Backus JG, Kennedy WC. 2001. Periphyton responses to experimental phosphorus enrichment in a subtropical wetland. *Aquatic Botany* 71:119-139
- McCune B, Grace JB. 2002. Analysis of ecological communities. MjM Software Design, Gleneden Beach, OR
- McDougal RL, Goldsborough LG, Hann BJ. 1997. Responses of a prairie wetland to press and pulse additions of inorganic nitrogen and phosphorus: production by planktonic and benthic algae. *Archiv für Hydrobiologie* 140(2):145-167
- McFarland AMS, Hauck LM. 1999. Existing nutrient sources and contributions to the Bosque River Watershed. Texas Institute for Applied Environmental Research, Tarleton State University, Stephenville, TX, USA. PR9911.
- Medina-Sánchez JM, Villar-Argaiz M, Carrillo P. 2004. Neither with nor without you: a complex algal control on bacterioplankton in a high mountain lake. *Limnology and Oceanography* 49:1722-1733
- Mitsch WJ, Gosselink JJ. 2000. Wetlands 3rd Ed. John Wiley and Sons Incorporated, New York, NY, USA
- Murray RE, Cooksey KE, Priscu JC. 1986. Stimulation of bacterial DNA synthesis by algal exudates in attached bacterial consortia. *Applied and Environmental Microbiology* 41:1378-1382
- Nairn RW, Mitsch WJ. 2000. Phosphorus removal in created wetland ponds receiving river overflow. *Ecological Engineering* 14:107-126.
- Neely RK. 1994. Evidence for positive interactions between epiphytic algae and heterotrophic decomposers during decomposition of *Typha latifolia*. *Archiv für Hydrobiologie* 129:443-457
- Neely RK, Wetzel RG. 1995. Simultaneous use of ¹⁴C and ³H to determine autotrophic production and bacterial protein production in periphyton. *Microbial Ecology* 30:227-237

- Neely RK, Wetzel RG. 1997. Autumnal production by bacteria and autotrophs attached to *Typha latifolia* L. detritus. *Journal of Freshwater Ecology* 12:253-267
- Nielson LP. 1992. Denitrification in sediment determined from nitrogen isotope pairing. *FEMS Microbiology Ecology* 86: 357-362
- Nowlin WH, Evarts JL, Vanni MJ. 2005. Release rates and potential fates of nitrogen and phosphorus from sediments in a eutrophic reservoir. *Freshwater Biology* 50: 301-322
- Olde Venterink H, van der Vliet RE, Wassen MJ. 2001. Nutrient limitation along a productivity gradient in wet meadows. *Plant and Soil* 234:171-179
- Paerl HW, Pinckney JL. 1996. A mini-review of microbial consortia: their roles in aquatic production and biogeochemical cycling. *Microbial Ecology* 31:225-247
- Petterson K. 1980. Alkaline phosphatase activity and algal surplus phosphorus as phosphorus-deficiency indicators in Lake Erken. *Archiv für Hydrobiologie* 89: 54-87
- Poe AC, Piehler MF, Thompson SP, and Paerl HW. 2003. Denitrification in a constructed wetland receiving agricultural runoff. *Wetlands*. 23(4):817-826
- Reddy KR, Kadlec RH, Flaig E., Gale PM. 1999. Phosphorus retention in streams and wetlands: a review. *Critical Reviews in Environmental Science and Technology* 29(1):83-146
- Rejmánková E, and Komárková J. 2000. A function of cyanobacterial mats in phosphorus-limited tropical wetlands. *Hydrobiologia* 431: 135-153
- Rejmánková E, Komárková J, and Rejmánek M. 2004. $\delta^{15}\text{N}$ as an indicator of N_2 -fixation by cyanobacterial mats in tropical marshes. *Biogeochemistry*. 67: 353-368
- Rejmánková E, Komárek J, Komárková J. 2004. Cyanobacteria – a neglected component of biodiversity: patterns of species diversity in inland marshes of northern Belize (Central America). *Diversity and Distributions* 10:189-199
- Richardson CJ, Qian SS. 1999. Long-term phosphorus assimilative capacity in freshwater wetlands: A new paradigm for sustaining ecosystem structure and function. *Environmental Science and Technology* 33(10):1545-1551
- Richardson CJ, Ferrell GM, Vaithiyathan P. 1999. Nutrient effects on stand structure, resorption efficiency, and secondary compounds in Everglades sawgrass. *Ecology* 80(7):2182-2192

- Risgaard-Petersen N, Jensen K. 1997. Nitrification and denitrification in the rhizosphere of the aquatic macrophyte *Lobelia dortmanna* L. *Limnology and Oceanography* 42(3):529-537
- Risgaard-Petersen N. 2003. Coupled nitrification-denitrification in autotrophic and heterotrophic estuarine sediments: On the influence of benthic microalgae. *Limnology and Oceanography* 48: 93-105
- Rodusky AJ, Steinmann AD, East TL, Sharfstein B, Meeker RM. 2001. Periphyton nutrient limitation and other potential growth-controlling factors in Lake Okeechobee, USA. *Hydrobiologia* 448:27-39
- Round FE, Crawford RM, Mann DG. 1990. The Diatoms: Biology and Morphology on the Genera. Cambridge University Press, Cambridge, UK
- SAS Institute Inc. 1999. SAS / STAT® User's Guide, Version 8. Cary, NC, USA.
- Saunders DL, Kalff J. 2001. Nitrogen retention in wetlands, lakes and rivers. *Hydrobiologia* 443:205-212
- Scinto LJ, Reddy KR 2003. Biotic and abiotic uptake of phosphorus by periphyton in a subtropical freshwater wetland. *Aquatic Botany* 77:203-222
- Schindler DW. 1977. Evolution of phosphorus limitation in lakes. *Science*. 195: 260-267
- Seitzinger SP. 1988. Denitrification in freshwater and coastal marine ecosystems: Ecological and geochemical significance. *Limnology and Oceanography* 33: 702-724
- Sharma K, Inglett PW, Reddy KR, Ogram AV. 2005. Microscopic examination of photoautotrophic and phosphatase-producing organisms in phosphorus-limited Everglades periphyton mats. *Limnology and Oceanography* 50:2057-2062
- SigmaPlot (2004) SigmaPlot® 9.0 User's Manual. Systat Software Inc. Point Richmond, CA
- Spieles, D. J., and W. J. Mitsch. 2000. The effects of season and hydrologic and chemical loading on nitrate retention in constructed wetlands: a comparison of low- and high-nutrient riverine systems. *Ecological Engineering* 14:77-91
- Stanley EH, Johnson MD, Ward AK. 2003. Evaluating the influence of macrophytes on algal and bacterial production in multiple habitats of a freshwater wetland. *Limnology and Oceanography* 48:1101-1111
- Sterner RW, Elser JJ. 2002. Ecological stoichiometry: The biology of elements from molecules to the biosphere. Princeton University Press, Princeton, NJ

- Stevenson RJ. 1996. An introduction to algal ecology in freshwater benthic habitats. p. 1-27. In: Stevenson RJ, Bothwell ML, Lowe RL (Eds) *Algal ecology – freshwater benthic ecosystems*, Academic Press, New York, NY, USA
- Tank JL, Dodds WK. 2003. Nutrient limitation of epilithic and epixylic biofilms in 10 North American streams. *Freshwater Biology* 48:1031-1049
- Thomaz SM, Wetzel RG. 1995. ³H-leucine incorporation methodology to estimate epiphytic bacterial biomass production. *Microbial Ecology* 29:63-70
- Toetz D. 1995. Water chemistry and periphyton in an alpine wetland. *Hydrobiologia* 312:93-105
- Tomaszek JA, Gardner WS, Johengen TH. 1997. Denitrification in sediments of a Lake Erie coastal wetland (Old Woman Creek, Huron, Ohio, USA). *Journal of Great Lakes Research* 23: 403-415
- Turner AM, Trexler JC, Jordan CF, Slack SJ, Geddes P, Chick JH, Lotus WF. 1999. Targeting ecosystem features for conservation: standing crops in the Florida Everglades. *Conservation Biology* 13:898-911
- Tyler AC, Mastronicola TA, McGlathery KJ. 2003. Nitrogen fixation and nitrogen limitation of primary production along a natural marsh chronosequence. *Oecologia* 136:431-438
- Tyrell T. 1999. The relative influences of nitrogen and phosphorus on oceanic primary production. *Nature* 400: 525-531
- Vadeboncoeur Y, Vander Zanden MJ, Lodge DM. 2002. Putting the lake back together: reintegrating benthic pathways into lake food web models. *BioScience* 52:44-54
- Vaithiyanathan P, Richardson CJ. 1997. Nutrient profiles in the everglades: examination along the eutrophication gradient. *The Science of the Total Environment* 205:81-95
- Vaithiyanathan P, Richardson CJ. 1999. Macrophyte species changes in the Everglades: Examination along a eutrophication gradient. *Journal of Environmental Quality* 28(4):1347-1358
- Vitousek PM. 2002. Stoichiometry and flexibility in the Hawaiian model system, p. 117-134. In: Melillo JM, Field CB, Moldan B (Eds), *Interactions of the major biogeochemical cycles*, Island, Washington DC
- Vitousek PM, Cassman K, Cleveland C, Crews T, Field CB, Grimm NB, Howarth RW, Marino R, Martinelli L, Rastetter EB, Sprent JJ. 2002. Towards an ecological understanding of biological nitrogen fixation. *Biogeochemistry* 57/58: 1-45

- Vymazal J. 1995. *Algae and Element Cycling in Wetlands*. CRC Press, Boca Raton, FL, USA
- Vymazal J, Richardson CJ. 1995. Species composition, biomass, and nutrient content of periphyton in the Florida Everglades. *Journal of Phycology* 31:343-354.
- Wehr JD, Sheath RG (Eds.). 2003. *Freshwater Algae of North America: Ecology and Classification*. Academic Press, San Diego, CA, USA
- Wetzel RG. 2001. *Limnology: Lake and River Ecosystems*, 3rd Edition. Academic Press, San Diego, CA, USA
- Wetzel RG. 1996. Benthic algae and nutrient cycling in lentic freshwater ecosystems. In: Stevenson RJ, Bothwell ML, Lowe RL (Eds) *Algal ecology – freshwater benthic ecosystems*, Academic Press, San Diego, CA
- Wetzel RG, Likens GE. 2000. *Limnological Analyses*, 3rd Edition. Springer-Verlag, New York, NY, USA
- White JR, Reddy KR. 1999. Influence of nitrate and phosphorus loading on denitrifying enzyme activity in Everglades wetland soils. *Soil Science Society of America Journal* 63:1945-1954
- Whitmire SL, Hamilton SK. 2005. Rapid removal of nitrate and sulfate in freshwater wetland sediments. *Journal of Environmental Quality* 34: 2062-2070
- Wu X, Mitsch WJ. 1998. Spatial and temporal patterns of algae in newly constructed freshwater wetlands. *Wetlands* 18(1):9-20